Philip Ringrose
Mark Bentley

Reservoir Model Design

A Practitioner's Guide

Springer

The Rock Model

2

Abstract

This topic concerns the difference between a reservoir model and a geological model. *Model representation* is the essential issue – ask yourself whether the coloured cellular graphics we see on the screen truly resemble the reservoir as exposed in outcrop:

WYSIWYG (computing acronym).

Our focus is on achieving a reasonable representation.

Most of the outputs from reservoir modelling are quantitative and derive from property models, so the main purpose of a rock model is to get the properties in the right place – to guide the spatial property distribution in 3D.

For certain model designs, the rock model component is minimal, for others it is essential. In all cases, the rock model should be the guiding framework and should offer predictive capacity to a project.

P. Ringrose and M. Bentley, *Reservoir Model Design*, DOI 10.1007/978-94-007-5497-3_2,

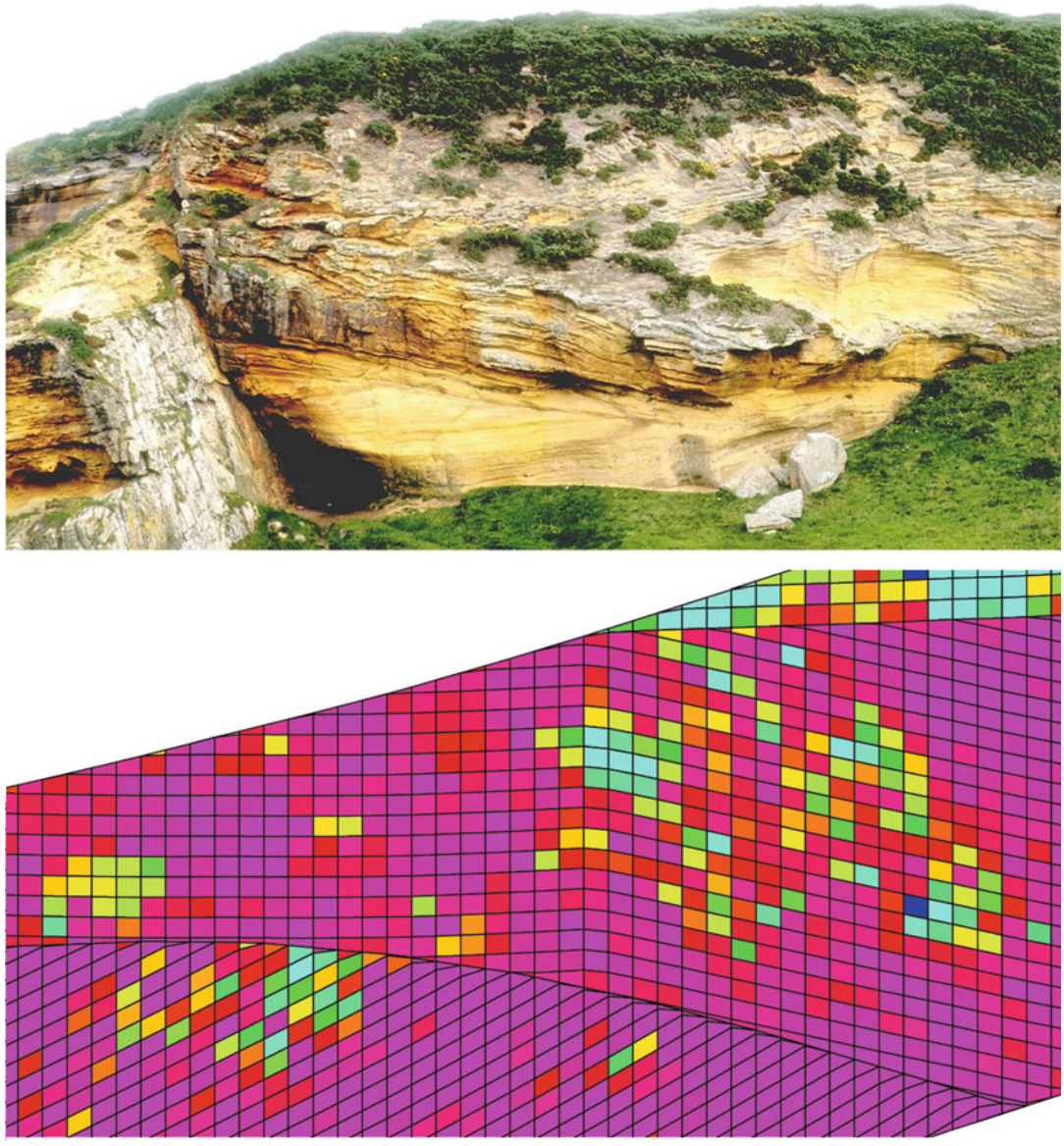

Outcrop view and model representation of the Hopeman Sandstone at Clashach Quarry, Moray Firth, Scotland

2.1 Rock Modelling

In a generic reservoir modelling workflow, the construction of a rock or 'facies' model usually precedes the property modelling. Effort is focussed on capturing contrasting rock types identified from sedimentology and representing these in 3D. This is often seen as the most 'geological' part of the model build along with the fault modelling, and it is generally assumed that a 'good' final model is one which is founded on a thoughtfully-constructed rock model.

However, although the rock model is often essential, it is rarely a model deliverable in itself,

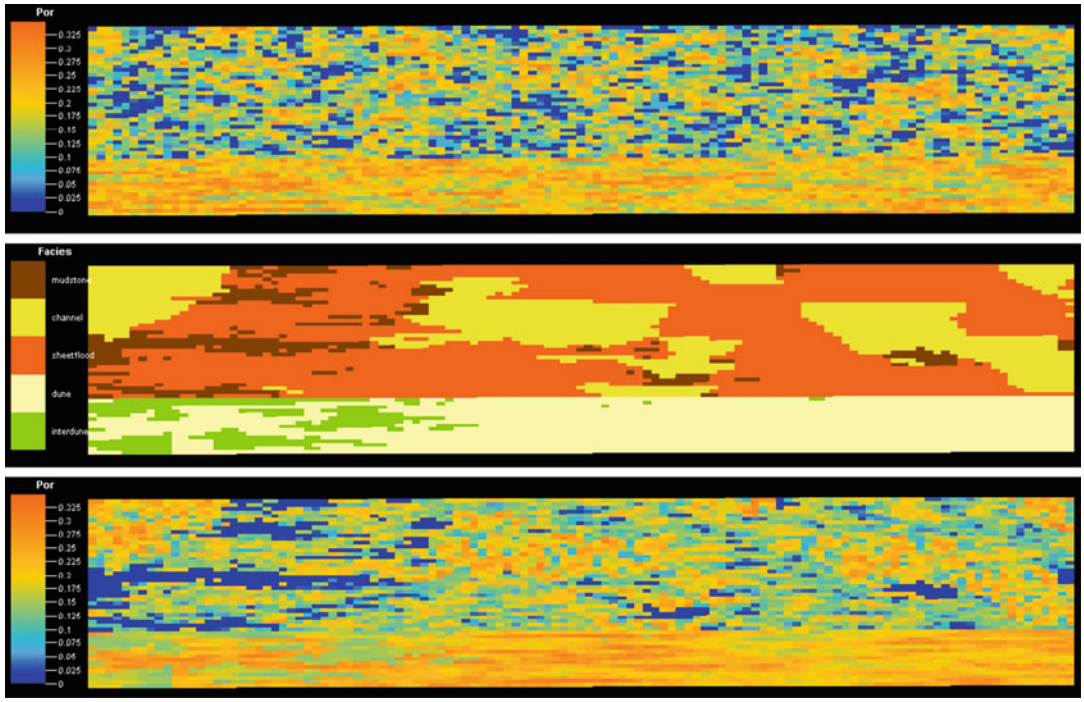

Fig. 2.1 To model rocks, or not to model rocks? *Upper image*: porosity model built directly from logs; *middle image*: a rock model capturing reservoir heterogeneity; *lower image*: the porosity model rebuilt, conditioned to the rock model

and many reservoirs *do not require* rock models. Figure 2.1 shows a porosity model which has been built with and without a rock model. If the upper porosity model is deemed a reasonable representation of the field, a rock model is not required. If, however, the porosity distribution is believed to be significantly influenced by the rock contrasts shown in the middle image, then the lower porosity model is the one to go for. Rock modelling is therefore a means to an end rather than an end in itself, an optional step which is useful if it helps to build an improved property model.

The details of rock model input are software-specific and are not covered here. Typically the model requires specification of variables such as sand body sizes, facies proportions and reference to directional data such as dip-logs. These are part of a standard model build and need consideration, but are not viewed here as critical to the higher level issue of model design. Moreover, many of these variables cannot be specified precisely enough to guide the modelling: rock body databases are generally insufficient and dip-log data too sparse to rely on as a model foundation. Most critical to the design are the issues identified below, mishandling of which is a common source of a poor model build:

- **Reservoir concept** – is the architecture understood in a way which readily translates into a reservoir model?
- **Model elements** – from the range of observed structural components and sedimentological facies types, has the correct selection of elements been made on which to base the model?
- **Model Build** – is the conceptual model carried through *intuitively* into the statistical component of the build?
- **Determinism and probability** – is the balance of determinism and probability in the model understood, and is the conceptual model firmly carried in the deterministic model components?

These four questions are used in this chapter to structure the discussion on the rock model, followed by a summary of more specific rock model build choices.

2.2 Model Concept

The best hope of building robust and sensible models is to use conceptual models to guide the model design. We favour this in place of purely data-driven modelling because of the issue of under-sampling (see later). The geologist should have a mental picture of the reservoir and use modelling tools to convert this into a quantitative geocellular representation. Using system defaults or treating the package as a black box that somehow adds value or knowledge to the model will always result in models that make little or no geological sense, and which usually have poor predictive capacity.

The form of the reservoir concept is not complex. It may be an image from a good outcrop analogue or, better, a conceptual sketch, such as those shown in Fig. 2.2.

It should, however, be specific to the case being modelled, and this is best achieved by drawing a simple section through the reservoir showing the key architectural elements – an example of which is shown in Fig. 2.3.

Analogue photos or satellite images are useful and often compelling but also easy to adopt when not representative, particularly if modern dynamic environments are being compared with ancient preserved systems. It is possible to collect a library of analogue images yet still be unclear exactly how these relate to the reservoir in hand, and how they link to the available well data. By contrast, the ability to draw a conceptual sketch section is highly informative and brings clarity to the mental image of the reservoir held by the modeller. If this conceptual sketch is not clear, the process of model building is unlikely to make it any clearer. If there is no clear up-front conceptual model then the model output is effectively a random draw:

If you can sketch it, you can model it

An early question to address is: *"what are the fundamental building blocks for the reservoir concept?"* These are referred to here as the 'model elements' and discussed further below. For the moment, the key thing to appreciate is that:

model elements ≠ facies types

Selection of model elements is discussed in Sect. 2.4.

With the idea of a reservoir concept as an architectural sketch constructed from model elements established, we will look at the issues surrounding the build of the model framework then return to consider how to select elements to place within that framework.

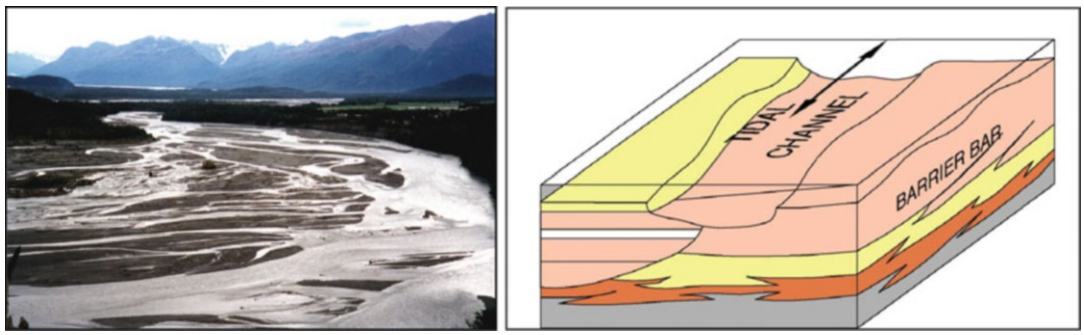

Fig. 2.2 Capturing the reservoir concept in an analogue image or a block diagram sketch

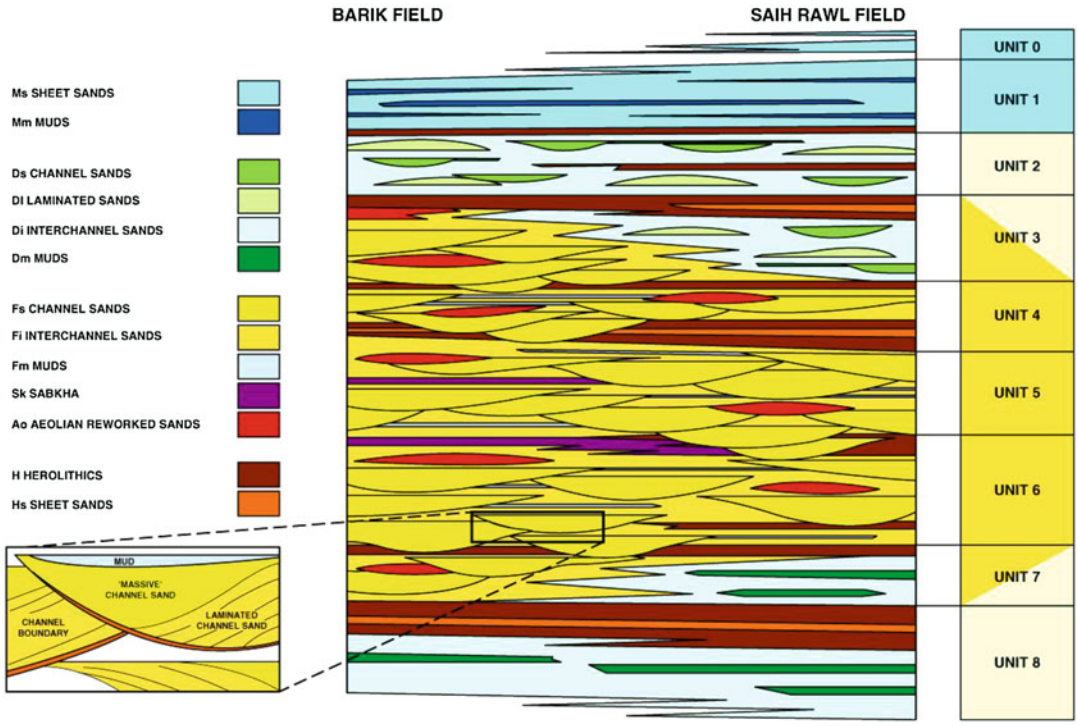

Fig. 2.3 Capturing the reservoir concept in a simple sketch showing shapes and stacking patterns of reservoir sand bodies and shales (From: van de Leemput et al. 1996)

2.3 The Structural and Stratigraphic Framework

The structural framework for all reservoir models is defined by a combination of structural inputs (faults and surfaces from seismic to impart gross geometry) and stratigraphic inputs (to define internal layering).

The main point we wish to consider here is *what are the structural and stratigraphic issues that a modeller should be aware of when thinking through a model design*? These are discussed below.

2.3.1 Structural Data

Building a fault model tends to be one of the more time-consuming and manual steps in a modelling workflow, and is therefore commonly done with each new generation of seismic interpretation. In the absence of new seismic, a fault model may be passed on between users and adopted simply to avoid the inefficiency of repeating the manual fault-building.

Such an inherited fault framework therefore requires quality control (QC). The principal question is whether the fault model reflects the seismic interpretation directly, or whether it has been modified by a conceptual structural interpretation.

A direct expression of a seismic interpretation will tend to be a conservative representation of the fault architecture, because it will directly reflect the resolution of the data. Facets of such data are:

- Fault networks tend to be incomplete, e.g. faults may be missing in areas of poor seismic quality;
- Faults may not be joined (under-linked) due to seismic noise in areas of fault intersections;
- Horizon interpretations may stop short of faults due to seismic noise around the fault zone;

- Horizon interpretations may be extended down fault planes (i.e. the fault is not identified independently on each horizon, or not identified at all)
- Faults may be interpreted on seismic noise (artefacts).

Although models made from such 'raw' seismic interpretations are honest reflections of that data, the structural representations are incomplete and, it is argued here, a structural interpretation should be overlain on the seismic outputs as part of the model design. To achieve this, the workflow similar to that shown in Fig. 2.4 is recommended.

Rather than start with a gridded framework constructed directly from seismic interpretation, the structural build should start with the raw, depth-converted seismic picks and the fault sticks. This is preferable to starting with horizon grids, as these will have been gridded without access to the final 3D fault network. Working with pre-gridded surfaces means the starting inputs are smoothed, not only within-surface but, more importantly, around faults, the latter tending to have systematically reduced fault displacements.

A more rigorous structural model workflow is as follows:

1. Determine the structural concept – are faults expected to die out laterally or to link? Are *en echelon* faults separated by relay ramps? Are there small, possibly sub-seismic connecting faults?
2. Input the fault sticks and grid them as fault planes (Fig. 2.4a)
3. Link faults into a network consistent with the concept (1, above, also Fig. 2.4b)
4. Import depth-converted horizon picks as points and remove spurious points, e.g. those erroneously picked along fault planes rather than stratigraphic surfaces (Fig. 2.4c)
5. Edit the fault network to ensure optimal positioning relative to the raw picks; this may be an iterative process with the geophysicist, particularly if potentially spurious picks are identified
6. Grid surfaces against the fault network (Fig. 2.4d).

2.3.2 Stratigraphic Data

There are two main considerations in the selection of stratigraphic inputs to the geological framework model: *correlation* and *hierarchy*.

2.3.2.1 Correlation

In the subsurface, correlation usually begins with markers picked from well data – *well picks*. Important information also comes from correlation surfaces picked from seismic data. Numerous correlation picks may have been defined in the interpretation of well data and these picks may have their origins in lithological, biostratigraphical or chronostratigraphical correlations – all of these being elements of sequence stratigraphy (see for example Van Wagoner et al. 1990; Van Wagoner and Bertram 1995). If multiple stratigraphic correlations are available these may give surfaces which intersect in space. Moreover, not all these surfaces are needed in reservoir modelling. A selection process is therefore required. As with the structural framework, the selection of surfaces should be made with reference to the conceptual sketch, which is in turn driven by the model purpose.

As a guideline, the 'correct' correlation lines are generally those which most closely govern the fluid-flow gradients during production. An exception would be instances where correlation lines are used to guide the distribution of reservoir volumes in 3D, rather than to capture correct fluid flow units.

The choice of correlation surfaces used hugely influences the resulting model architecture, as illustrated in Fig. 2.5, and in an excellent field example by Ainsworth et al. (1999).

2.3.2.2 Hierarchy

Different correlation schemes have different influences on the key issue of hierarchy, as the stratigraphy of most reservoir systems is inherently hierarchical (Campbell 1967). For example, for a sequence stratigraphic correlation scheme, a low-stand systems tract might have a length-scale of tens of kilometres and might contain within it numerous stacked sand systems

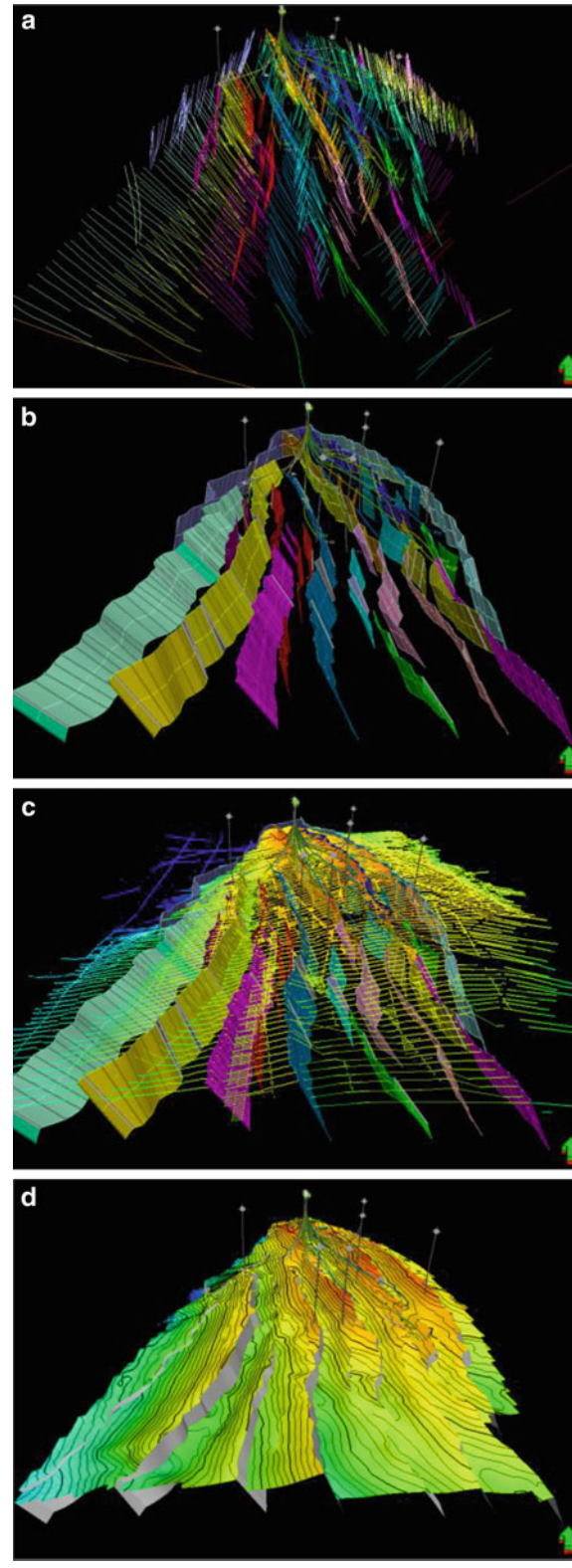

Fig. 2.4 A structural build based on fault sticks from seismic (**a**), converted into a linked fault system (**b**), integrated with depth-converted horizon picks (**c**) to yield a conceptually acceptable structural framework which honours all inputs (**d**). The workflow can equally well be followed using time data, then converting to depth using a 3D velocity model. The key feature of this workflow is the avoidance of intermediate surface gridding steps which are made independently of the final interpreted fault network. Example from the Douglas Field, East Irish Sea (Bentley and Elliott 2008)

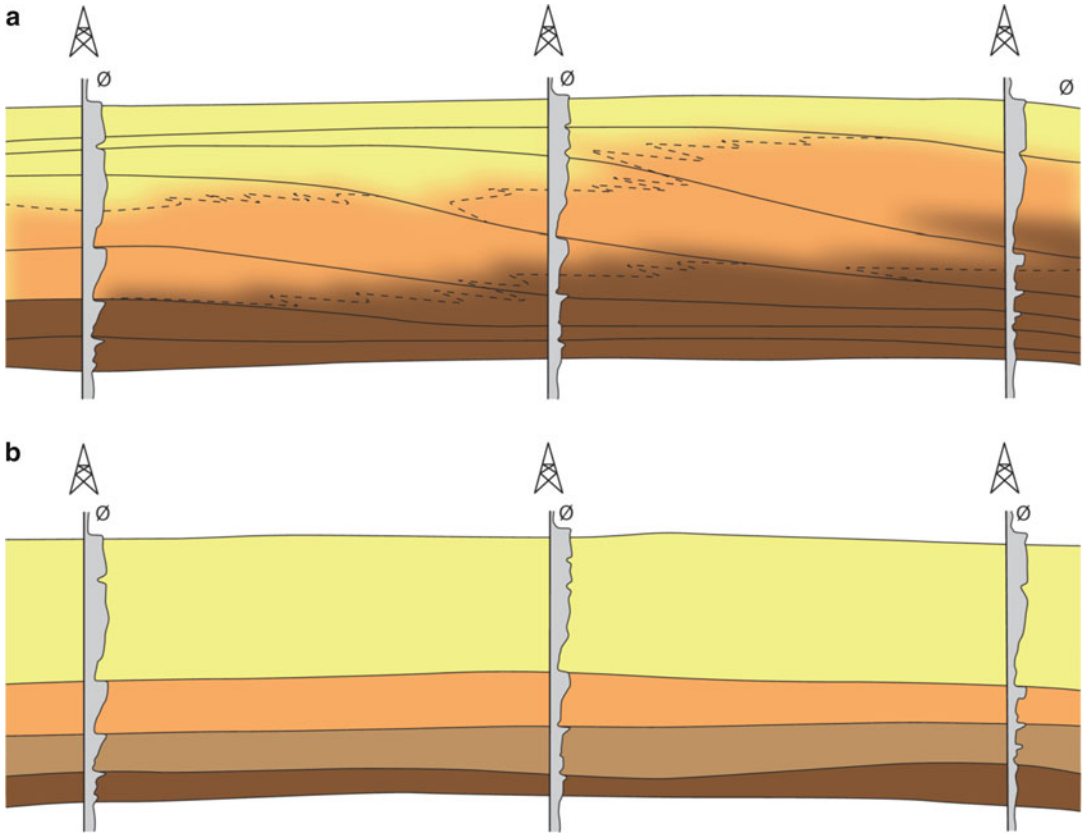

Fig. 2.5 Alternative (**a**) chronostratigraphic and (**b**) lithostratigraphic correlations of the same sand observations in three wells; the chronostratigraphic correlation invokes an additional hierarchical level in the stratigraphy

with a length-scale of kilometres. These sands in turn act as the bounding envelope for individual reservoir elements with dimensions of tens to hundreds of metres.

The reservoir model should aim to capture the levels in the stratigraphic hierarchy which influence the spatial distribution of significant heterogeneities (determining 'significance' will be discussed below). Bounding surfaces within the hierarchy may or may not act as flow barriers – so they may represent important model elements in themselves (e.g. flooding surfaces) or they may merely control the distribution of model elements within that hierarchy. This applies to structural model elements as well as the more familiar sedimentological model elements, as features such as fracture density can be controlled by mechanical stratigraphy – implicitly related to the stratigraphic hierarchy.

So which is the preferred stratigraphic tool to use as a framework for reservoir modelling? The quick answer is that it will be the framework which most readily reflects the conceptual reservoir model. Additional thought is merited, however, particularly if the chronostratigraphic approach is used. This method yields a framework of timelines, often based on picking the most shaly parts of non-reservoir intervals. The intended shale-dominated architecture may not automatically be generated by modelling algorithms, however: a rock model for an interval between two flooding surfaces will contain a shaly portion at both the top and the base of the interval. The probabilistic aspects of the subsequent modelling can easily degrade the correlatable nature of the flooding surfaces, inter-well shales becoming smeared out incorrectly throughout the zone.

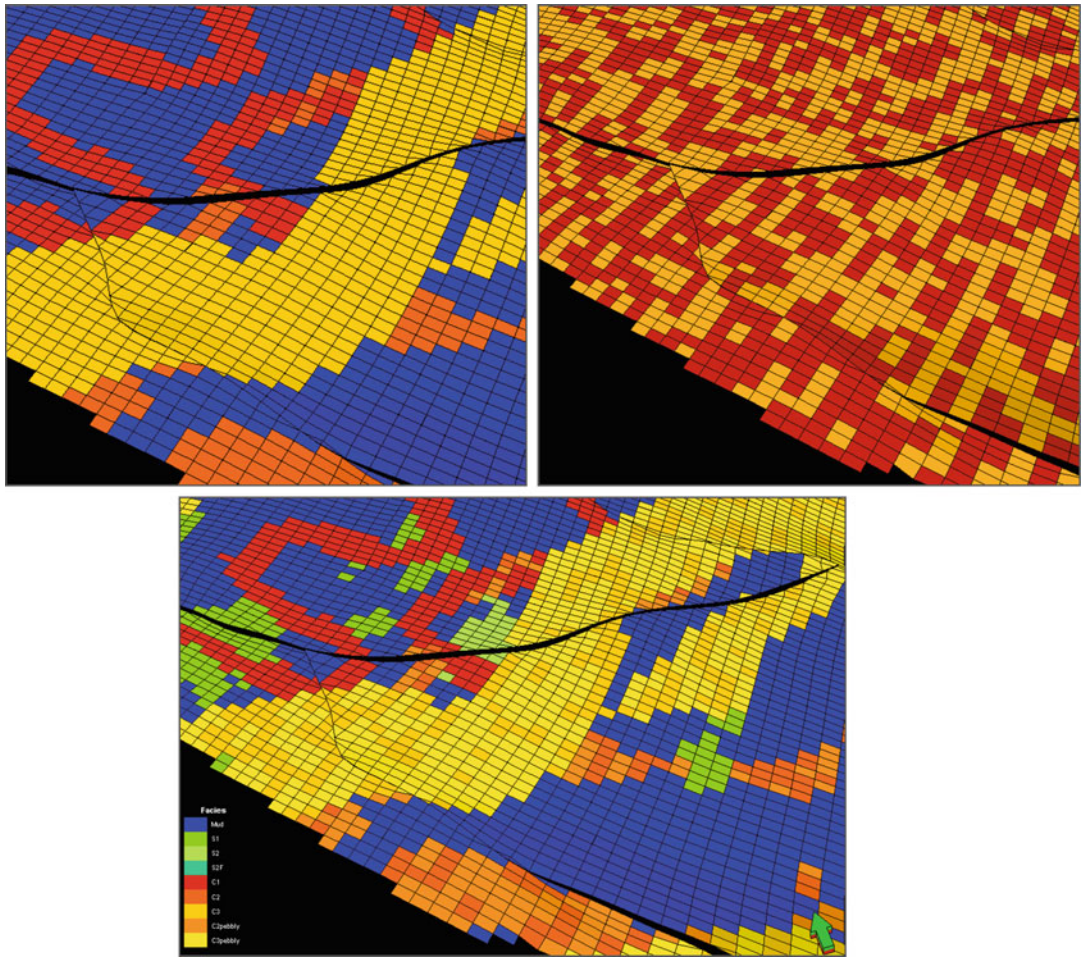

Fig. 2.6 The addition of hierarchy by logical combination: single-hierarchy channel model (*top left*, *blue* = mudstone, *yellow* = main channel) built in parallel with a probabilistic model of lithofacies types (*top right*, *yellow* = better quality reservoir sands), logically combined into the final rock model with lithofacies detail in the main channel only – an additional level of hierarchy

Some degree of hierarchy is implicit in any software package. The modeller is required to work out if the default hierarchy is sufficient to capture the required concept. If not, the workflow should be modified, most commonly by applying logical operations.

An example of this is illustrated in Fig. 2.6, from a reservoir model in which the first two hierarchical levels were captured by the default software workflow: tying layering to seismic horizons (first level) then infilled by sub-seismic stratigraphy (second level). An additional hierarchical level was required because an important permeability heterogeneity existed between lithofacies types *within* a particular model element (the main channels). The chosen solution was to build the channel model using channel objects and creating a separate, in this case probabilistic, model which contained the information about the distribution of the two lithofacies types. The two rock models were then combined using a logical property model operation, which imposed the texture of the fine-scale lithofacies, but only within the relevant channels. Effectively this created a third hierarchical level within the model.

One way or another hierarchy can be represented, but only rarely by using the default model workflow.

2.4 Model Elements

Having established a structural/stratigraphic model framework, we can now return to the model concept and consider how to fill the framework to create an optimal architectural representation.

2.4.1 Reservoir Models Not Geological Models

The rich and detailed geological story that can be extracted from days or weeks of analysis of the rock record from the core store need not be incorporated directly into the reservoir model, and this is a good thing. There is a natural tendency to 'include all the detail' just in case something minor turns out to be important. Models therefore have a tendency to be overcomplex from the outset, particularly for novice modellers. The amount of detail required in the model can, to a large extent, be anticipated.

There is also a tendency for modellers to seize the opportunity to build 'real 3D geological pictures' of the subsurface and to therefore make these as complex as the geology is believed to be. This is a hopeless objective as the subsurface is considerably more complex in detail than we are capable of modelling explicitly and, thankfully, much of that detail is irrelevant to economic or engineering decisions. We are building *reservoir models* – reasonable representations of the detailed geology – *not* geological models.

2.4.2 Building Blocks

Hence the view of the components of a reservoir model as *model elements* – the fundamental building blocks of the 3D architecture. The use of this term distinguishes model elements from geological terms such as 'facies', 'lithofacies', 'facies associations' and 'genetic units'. These geological terms are required to capture the richness of the geological story, but do not necessarily describe the things we need to put into reservoir models. Moreover, key elements of the reservoir model may be small-scale structural or diagenetic features, often (perhaps incorrectly) excluded from descriptions of 'facies'.

Modelling elements are defined here as:

> *three-dimensional rock bodies which are petrophysically and/or geometrically distinct from each other in the specific context of the reservoir fluid system.*

The fluid-fill factor is important as it highlights the fact that different levels of heterogeneity are important for different types of fluid, e.g. gas reservoirs behave more homogeneously than oil reservoirs for a given reservoir type.

The identification of 'model elements' has some parallels with discussions of 'hydraulic units' although such discussions tend to be in the context of layer-based well performance. Our focus is on the building blocks for 3D reservoir architecture, including parts of a field remote from well and production data. It should be spatially predictive.

2.4.3 Model Element Types

Having stepped beyond a traditional use of depositional facies to define rock bodies for modelling, a broader spectrum of elements can be considered for use, i.e. making the sketch of the reservoir as it is intended to be modelled. Six types of model element are considered below.

2.4.3.1 Lithofacies Types

This is sedimentologically-driven and is the traditional way of defining the components of a rock model. Typical lithofacies elements may be coarse sandstones, mudstones or grainstones, and will generally be defined from core and or log data (e.g. Fig. 2.7).

2.4.3.2 Genetic Elements

In reservoir modelling, genetic elements are a component of a sedimentary sequence which are related by a depositional process. These include the rock bodies which typical modelling packages are most readily designed to incorporate, such as channels, sheet sands or heterolithics. These usually comprise several lithofacies, for example, a fluvial channel might

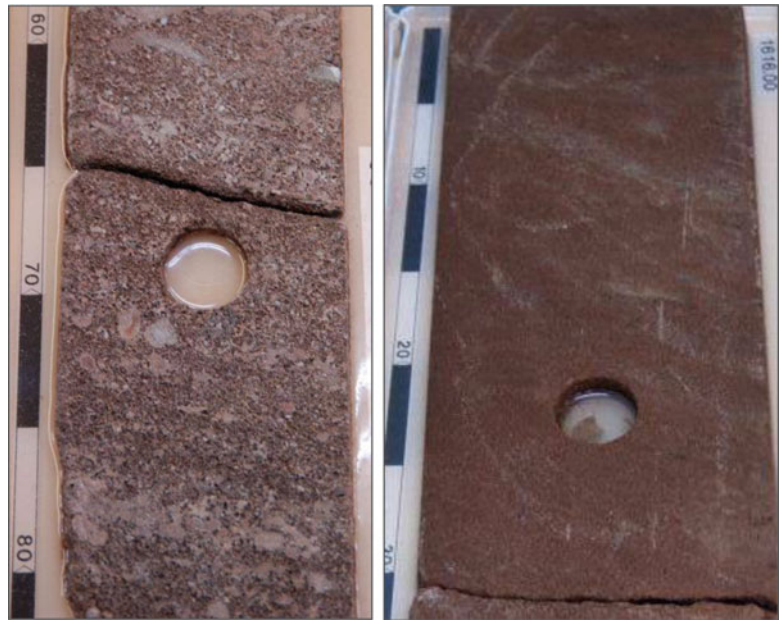

Fig. 2.7 Example lithofacies elements; *left*: coarse, pebbly sandstone; *right*: massively-bedded coarse-grained sandstone

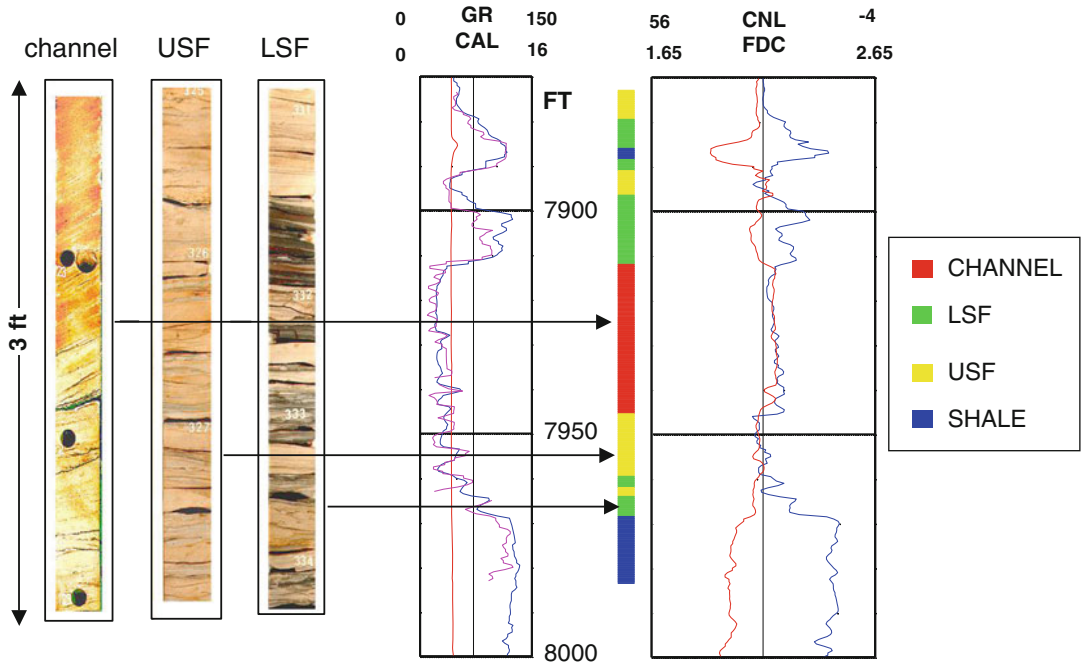

Fig. 2.8 Genetic modelling elements; lithofacies types grouped into channel, upper shoreface and lower shoreface genetic depositional elements (Image courtesy of Simon Smith)

include conglomeratic, cross-bedded sandstone and mudstone lithofacies. Figure 2.8 shows an example of several genetic depositional elements interpreted from core and log observations.

2.4.3.3 Stratigraphic Elements

For models which can be based on a sequence stratigraphic framework, the fine-scale components of the stratigraphic scheme may also be the

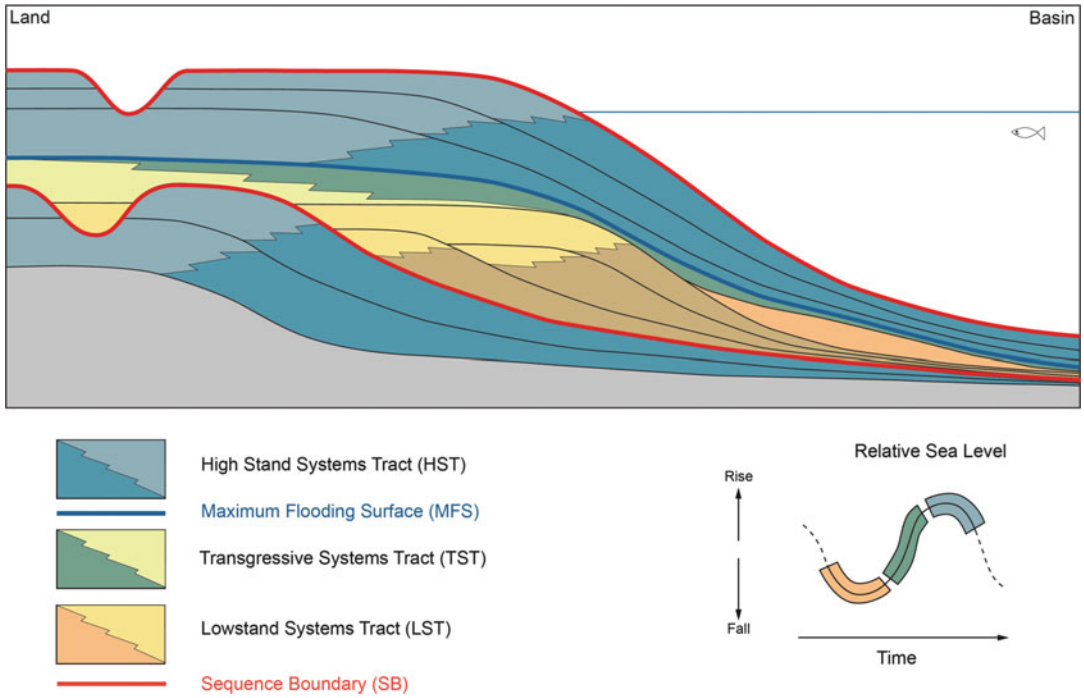

Fig. 2.9 Sequence stratigraphic elements

predominant model elements. These may be parasequences organised within a larger-scale sequence-based stratigraphic framework which defines the main reservoir architecture (e.g. Fig. 2.9).

2.4.3.4 Diagenetic Elements

Diagenetic elements commonly overprint lithofacies types, may cross major stratigraphic boundaries and are often the predominant feature of carbonate reservoir models. Typical diagenetic elements could be zones of meteoric flushing, dolomitisation or de-dolomitisation (Fig. 2.10).

2.4.3.5 Structural Elements

Assuming a definition of model elements as three-dimensional features, structural model elements emerge when the properties of a volume are dominated by structural rather than sedimentological or stratigraphic aspects. Fault damage zones are important volumetric structural elements (e.g. Fig. 2.11) as are mechanical layers (strata-bound fracture sets) with properties driven by small-scale jointing or cementation.

2.4.3.6 Exotic Elements

The list of potential model elements is as diverse as the many different types of reservoir, hence other 'exotic' reservoir types must be mentioned, having their own model elements specific to their geological make-up. Reservoirs in volcanic rocks are a good example (Fig. 2.12), in which the key model elements may be zones of differential cooling and hence differential fracture density.

***

The important point about using the term 'model element' is to stimulate broad thinking about the model concept, a thought process which runs across the reservoir geological sub-disciplines (stratigraphy, sedimentology, structural geology, even volcanology). For avoidance of doubt, the main difference between the model framework and the model elements is that 2D features are used to define the model framework (faults, unconformities, sequence boundaries, simple bounding surfaces) whereas it is 3D model elements which fill the volumes within that framework.

Having defined the framework and identified the elements, the next question is how much information to carry explicitly into the modelling process. Everything that can be identified need not be modelled.

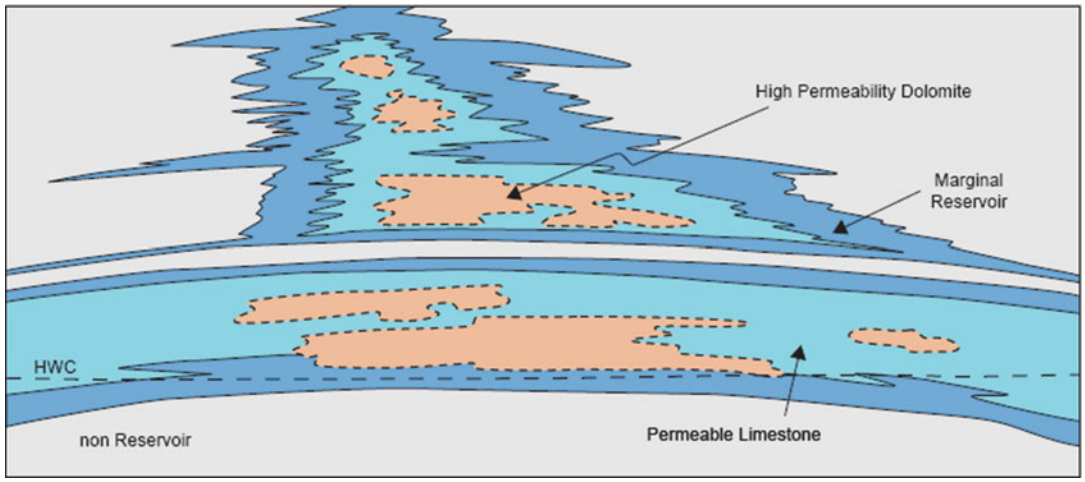

Fig. 2.10 Diagenetic elements in a carbonate build-up; where reservoir property contrasts are driven by differential development of dolomitisation

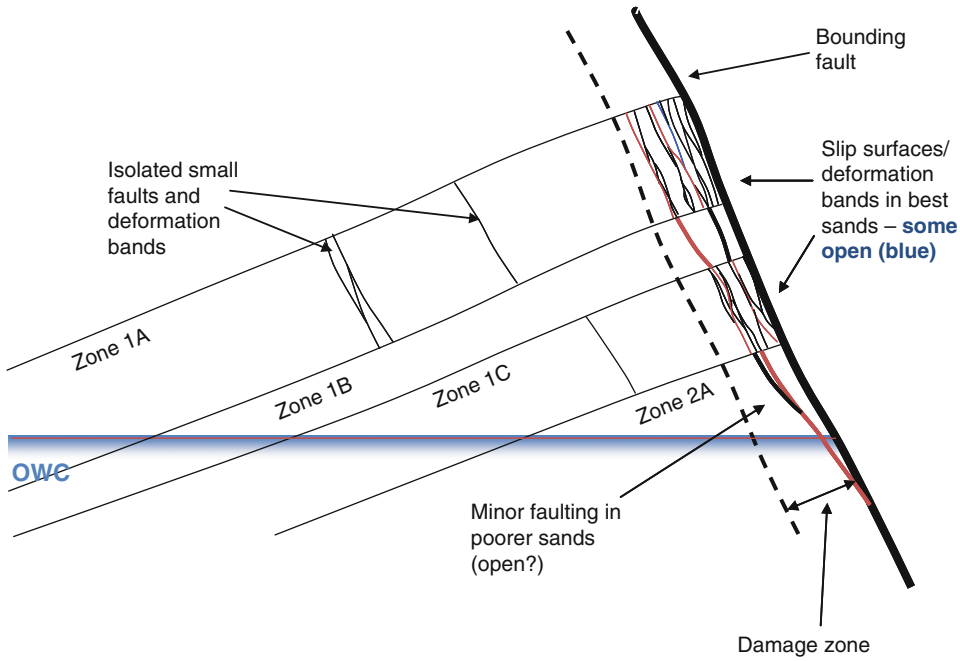

Fig. 2.11 Structural elements: volumes dominated by minor fracturing in a fault damage zone next to a major block-bounding fault (Bentley and Elliot 2008)

2.4.4 How Much Heterogeneity to Include?

The ultimate answer to this fundamental question depends on a combined understanding of geology and flow physics. To be more specific, the key criteria for distinguishing which model elements are required for the model build are:

1. The identification of potential model elements – a large number may initially be selected as 'candidates' for inclusion;

The Property Model

3

Abstract

Now let's say you have a beautiful fit-for-purpose rock model of your reservoir – let's open the box and find out what's inside? All too often the properties used within the geo-model are woefully inadequate.

The aim of this chapter is too ensure the properties of your model are also fit-for-purpose and not, like Pandora's box, full of "all the evils of mankind."

Eros warned her not to open the box once Persephone's beauty was inside[. . .] but as she opened the box Psyche fell unconscious upon the ground. (From The Golden Ass by Apuleius.)

P. Ringrose and M. Bentley, *Reservoir Model Design*, DOI 10.1007/978-94-007-5497-3_3,

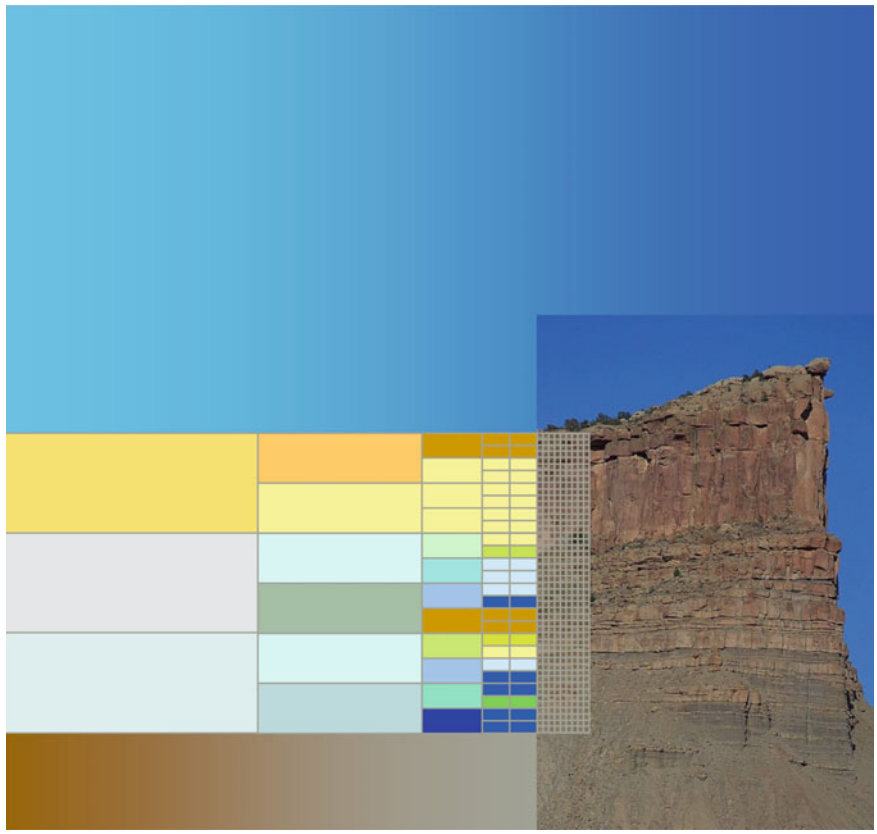

Pixelated rocks

3.1 Which Properties?

First let us recall the purpose of building a reservoir model in the first place. We propose that the overall aim in reservoir model design is:

> *To capture knowledge of the subsurface in a quantitative form in order to evaluate and engineer the reservoir.*

This definition combines knowledge capture, the process of collecting all relevant information, with the engineering objective – the practical outcome of the model (Fig. 3.1). Deciding how to do this is the job of the geo-engineer – a geoscientist with sufficient knowledge of the Earth and the ability to quantify that knowledge in a way that is useful for the engineering decision at hand. A mathematician, physicist or engineer with sufficient knowledge Earth science can make an equally good geo-engineer (Fig. 3.2).

A geological model of a petroleum reservoir is the basis for most reservoir evaluation and engineering decisions. These include (roughly in order of complexity and detail):

- Making estimates of fluid volumes in place,
- Scoping reservoir development plans,
- Defining well targets,
- Designing detailed well plans,
- Optimising fluid recovery (usually for IOR/EOR schemes).

The type of decision involved affects the property modelling approach used. Simple averaging or mapping of properties is more likely to be appropriate for initial volume estimates while advanced modelling with explicit upscaling is mostly employed when designing well plans (Fig. 3.3) or as part of improved reservoir displacement plans or enhanced oil recovery (EOR) strategies.

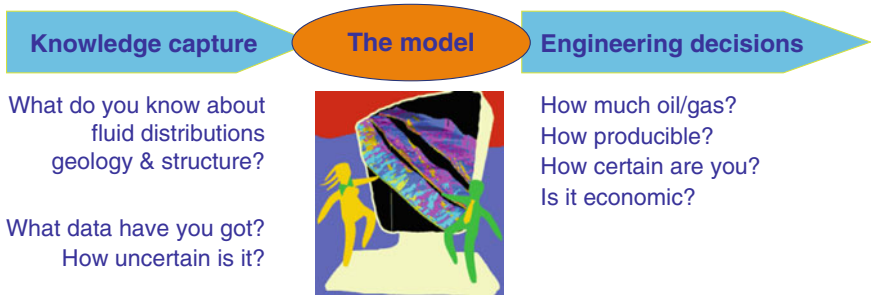

Fig. 3.1 Knowledge capture and the engineering decision

Fig. 3.2 The geo-engineer (Photo, Statoil image archive, © Statoil ASA, reproduced with permission)

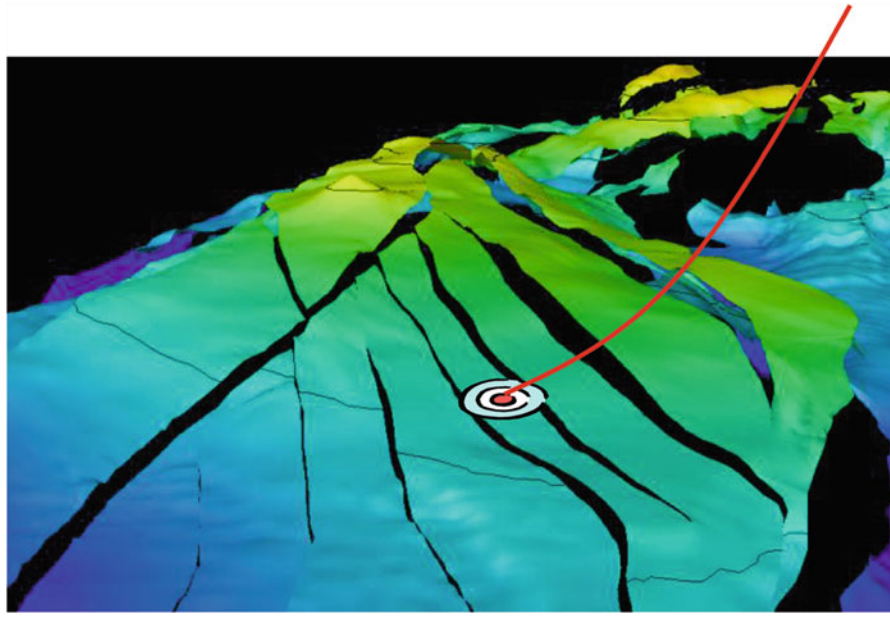

Fig. 3.3 Defining the well target

The next question is which petrophysical properties do we want to model? The focus in this chapter will be on modelling porosity (ϕ) and permeability (k) as these are the essential parameters in the flow equation (Darcy's law). The methods discussed here for handling ϕ and k can also be applied to other properties, such as formation bulk density (ρ_b) or sonic p-wave velocity (v_p), Volume fraction of shale (V_{shale}) or fracture density (F_d), to name but a few. Table 3.1 lists the most commonly modelled rock properties, but the choice should not be limited to these, and indeed a key element of the design should be careful consideration of which properties should or can be usefully represented. Integration of dynamic data with seismic and well data will generally require modelling of several petrophysical properties and their cross correlations.

Permeability is generally the most challenging property to define because it is highly variable in nature and is a tensor property dependent on flow boundary conditions. Permeability is also, in general, a non-additive property, that is:

$$k^{\Delta V} \neq \sum_{1}^{n} k_i^{\partial v} \tag{3.1}$$

In contrast porosity is essentially an additive property:

$$\phi^{\Delta V} = \sum_{1}^{n} \phi_i^{\partial v} \tag{3.2}$$

where ΔV is a large scale volume, δv[n] is the exhaustive set of small scale volumes filling the large-scale volume.

Put in practical terms, if you have defined all the cell porosity values in your reservoir model then the total reservoir porosity is precisely equal to the sum of the cell porosities divided by the number cells (i.e. the average), whereas for permeability this is not the case. We will discuss appropriate use of various permeability averages in following section.

Exercise 3.1

Which methods to use?

Think through the following decision matrix for an oilfield development to decide which approaches are appropriate for which decisions?

Method (for a given reservoir interval)	Choice	Purpose
Conceptual geological sketch of proposed reservoir analogue		Initial fluids-in-place volume estimate
Simple average of porosity, ϕ, permeability, k, and fluid saturation, S_w		Preliminary reserves estimates
2D map of ϕ, k and S_w (e.g. interpolation or kriging between wells)		Reserve estimates for designing top-side facilities (number of wells, platform type)
3D model of ϕ, k and S_w in the reservoir unit (from well data)		Definition of appraisal well drilling plan
3D model of ϕ, k and S_w for each of several model elements (from well data)		Definition of infill or development well drilling plan
3D model of ϕ, k and S_w conditioned to seismic inversion cube (seismic facies)		Submitting detailed well design for final approval
3D model of ϕ, k, S_w and facies conditioned to dynamic data (production pressures and flow rates)		Designing improved oil recovery (IOR) strategy and additional well targets
3D model of ϕ, k, S_w and facies integrating multi-scale static and dynamic data		Implementing enhanced oil recovery (EOR) strategy using an injection blend (e.g. water alternating gas)

Table 3.1 List of properties typically included in geological reservoir models

	Symbol	Property	Units [typical range]
All reservoirs	ϕ	Porosity	Fraction [0, 0.4]
	ϕ_m, ϕ_f	Matrix porosity, Fracture porosity	Fraction [0, 0.4]
	k_h, k_v	Horizontal permeability, vertical permeability	millidarcy, mD [0.001, 10000]
	k_v/k_h	Ratio of vertical to horizontal permeability	millidarcy, mD [10^{-5}, 1]
	V_{shale}, V_{sand}, V_{cement}	Volume fraction (shale, sandstone, cement)	Fraction [0, 1]
	N/G_{sand}, N/G_{res}	Net to gross ratio (sandstone, reservoir)	Fraction [0, 1]
	S_w, S_o, S_g	Fluid Saturation (water, oil, gas)	Fraction [0, 1]
	SAT_{num}	Relative permeability saturation function index	Integer [1, N]
Fractured reservoirs	ϕ_m, ϕ_f	Matrix porosity, Fracture porosity	Fraction [0, 0.4]
	k_f, k_m	Fracture permeability, Matrix permeability	millidarcy, mD [10^{-3}, 10^5]
	F_d	Fracture density	Number per metre, m^{-1} [0.1, 10]
	F_a	Fracture aperture	m [10^{-6}, 10^{-3}]
	C_{mean}	Mean Surface Curvature	2nd derivative [-x>0<+x]
Seismic inversion	ρ_b	Bulk density	g/cc (kg/m^3) [1-2]
	V_p	Seismic velocity (p-wave)	m/s [1400-5000]
	V_p/V_s	Ratio of compression-wave to shear-wave velocity	m/s [700-3000]
	AI_p, AI_s	Acoustic (seismic) Impedance (p-wave, s-wave)	m/s.g/cc (Pa.s/m^3) [6000,14000]
	ϕ_{AVO}	Porosity from AVO inversion	Fraction [0, 0.4]

The final important question to address is: Which reservoir or rock unit do we want to average? There are many related concepts used to define flowing rock intervals – flow units, hydraulic units, geological units or simply "the reservoir". The most succinct term for defining the rock units in reservoir studies is the Hydraulic Flow Unit (HFU), which is defined as representative rock volume with consistent petrophysical properties distinctly different from other rock units. There is thus a direct relationship between flow units and the 'model elements' introduced in the preceding chapter.

Exercise 3.2

Additive properties

Additivity involves a mathematical function in which a property can be expressed as a weighted sum of some independent variable(s). The concept is important to a wide range of statistical methods used in many science disciplines. Additivity has many deeper facets and definitions that are discussed in mathematics and statistical literature.

It is useful to consider a wider selection of petrophysical properties and think through whether they are essentially additive or non-additive (i.e. multiplicative) properties.

What would you conclude about these terms?

- Net-to-gross ratio
- Fluid saturation
- Permeability
- Porosity
- Bulk density
- Formation resistivity
- Seismic velocity, V_p or V_s
- Acoustic Impedance, AI

Abbaszadeh et al. (1996) define the HFU in terms of the Kozeny-Carmen equation to extract Flow Zone Indicators which can be used quantitatively to define specific HFUs from well data. We will return the definition of representative volumes and flow units in Chap. 4 when we look at upscaling, but first we need to understand permeability.

3.2 Understanding Permeability

3.2.1 Darcy's Law

The basic permeability equation is based on the observations and field experience of Henri Darcy (1803–1858) while engineering a pressurized water distribution system in the town of Dijon, France. His equation relates flow rate to the head of water draining through a pile of sand (Fig. 3.4):

$$Q = KA(\Delta H/L) \tag{3.3}$$

where

Q = volume flux of water
K = constant of hydraulic conductivity or coefficient of permeability
A = cross sectional area
ΔH = height of water column
L = length of sand column

From this we can derive the familiar Darcy's Law – a fundamental equation for flow in porous media, based on dimensional analysis and the Navier-Stokes equations for flow in cylindrical pores:

$$u = \frac{-k}{\mu}\nabla(P + \rho g z) \tag{3.4}$$

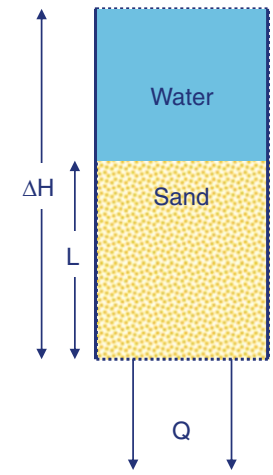

Fig. 3.4 Darcy's experiment

where
u = intrinsic fluid velocity
k = intrinsic permeability
μ = fluid viscosity
∇P = applied pressure gradient
ρgz = pressure gradient due to gravity
∇P (grad P) is the pressure gradient, which can be solved in a cartesian coordinate system as:

$$\nabla P = \frac{dP}{dx} + \frac{dP}{dy} + \frac{dP}{dz} \tag{3.5}$$

The pressure gradient due to gravity is then ρg∇z. For a homogeneous, uniform medium k has a single value, which represents the medium's ability to permit flow (independent of the fluid type). For the general case of a heterogeneous rock medium, k is a tensor property.

Exercise 3.3
Dimensions of permeability

What are the dimensions of permeability? Do a dimensional analysis for Darcy's Law.

For the volumetric flux equation

$$Q = KA(\Delta H/L)$$

The dimensions are

$$\left[L^3T^{-1}\right] = \left[LT^{-1}\right]\ \left[L^2\right]$$

Therefore the SI unit for K is:

$$ms^{-1}$$

Do the same for Darcy's Law:

$$u = -(k/\mu).\nabla(P + \rho gz)$$

The dimensions are

$$[\ \ ] = ([\ \ ]/[\ \ ]).[\ \ ]$$

Therefore the SI unit for k is

$$\_\_\_\_$$

3.2.2 Upscaled Permeability

In general terms, *upscaled permeability* refers to the permeability of a larger volume given some fine scale observations or measurements. The concept is widely used, and abused, and requires some care in its use and application. It is also rather fundamental – if it was a simple thing to estimate the correctly upscaled permeability for a reservoir unit, there would be little value in reservoir modelling (apart from simple volume estimates).

The upscaled (or block) permeability, k_b, is defined as the permeability of an homogeneous block, which under the same pressure boundary conditions will give the same average flows as the heterogeneous region the block is representing (Fig. 3.5). The upscaled block permeability could be estimated, given a fine set of values in a permeability field or model, or it could be measured at the larger scale (e.g. in a well test or core analysis), in which case the fine-scale permeabilities need not be known.

The *effective permeability* is defined strictly in terms of effective medium theory and is an intrinsic large-scale property which is independent of the boundary conditions. The main theoretical conditions for estimation of the effective permeability, k_{eff}, are:

- That the flow is linear and steady state;
- That the medium is statistically homogeneous at the large scale.

When the upscaled domain is large enough, such that these conditions are nearly satisfied, then k_b approaches k_{eff}. The term *equivalent permeability*, is also used (Renard and de Marsily 1997) and refers to a general large-scale permeability which can be applied to a wide range of boundary conditions, to some extent encompassing both k_b and k_{eff}. These terms are often confused or misused, and in this treatment we will refer to the permeability upscaled from a model as the *block permeability*, k_b, and use *effective permeability* as the ideal upscaled permeability we would generally wish to estimate if we could satisfy the necessary conditions. In reservoir modelling we are usually estimating k_b in practice, because we rarely fully satisfy the demands of effective medium theory. However, k_{eff} is an important concept with many constraints that we try to satisfy when estimating the upscaled (block) permeability.

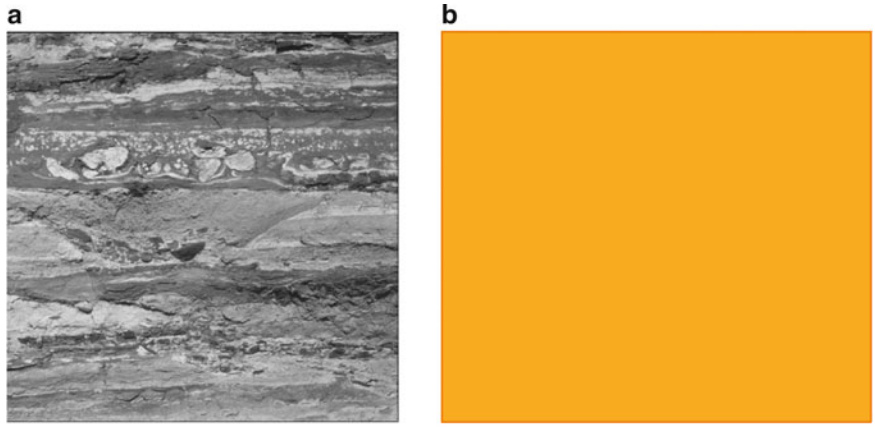

Fig. 3.5 Effective permeability and upscaled block permeability (**a**) Real rock medium has some (unknown) effective permeability. (**b**) Modelled rock medium has an estimated block permeability with the same average flow as the real thing

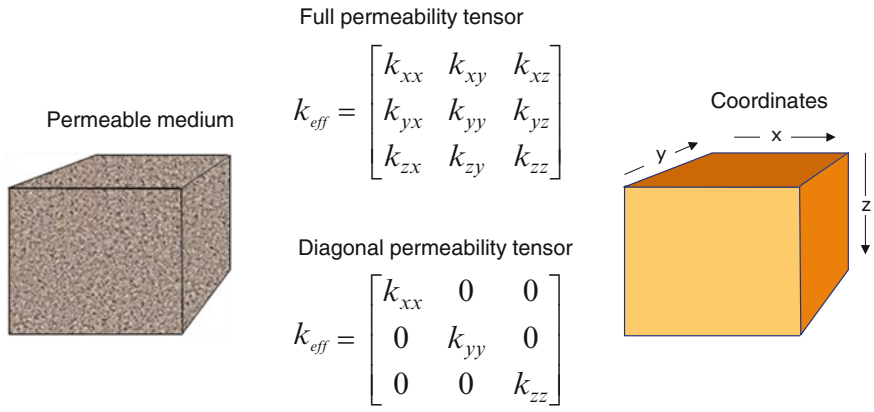

Fig. 3.6 The permeability tensor

Note that in petrophysical analysis, the term 'effective porosity' refers to the porosity of moveable fluids excluding micro-porosity and chemically bound water, while total porosity encompasses all pore types. Although effective porosity and effective permeability both represent properties relevant to, and controlling, macroscopic flow, they are defined on different bases. Effective permeability is essentially a larger scale property requiring statistical homogeneity in the medium, whereas effective porosity is essentially a pore-scale physical attribute. Of course, if both properties are estimated at, or rescaled to, the same appropriate volume, they may correspond and are correctly used together in flow modelling. They should not, however, be automatically associated. For example, in an upscaled heterogeneous volume there could be effective porosity elements (e.g. vuggy pores) which do not contribute to the flow and therefore do not influence the effective permeability.

In general, k_b is a tensor property (Fig. 3.6) where, for example, k_{xy} represents flow in the x direction due to a pressure gradient in the y direction. In practice k_b is commonly assumed to be a diagonal tensor where off-diagonal terms are neglected. A further simplification in many reservoir modelling studies is the assumption that $k_h = k_{xx} = k_{yy}$ and that $k_v = k_{zz}$.

The calculation or estimation of k_b is dependent on the boundary conditions (Fig. 3.7). Note that the assumption of a no-flow or sealed

side boundary condition, forces the result to be a diagonal tensor. This is useful, but may not of course represent reality. Renard and de Marsily (1997) give an excellent review of effective permeability, and Pickup et al. (1994, 1995) give examples of the permeability tensor estimated for a range of realistic sedimentary media.

3.2.3 Permeability Variation in the Subsurface

There is an extensive literature on the measurement of permeability (e.g. Goggin et al. 1988; Hurst and Rosvoll 1991; Ringrose et al. 1999) and its application for reservoir modelling (e.g. Begg et al. 1989; Weber and van Geuns 1990; Corbett et al. 1992). All too often, rather idealised permeability distributions have been assumed in reservoir models, such as a constant value or the average of a few core plug measurements.

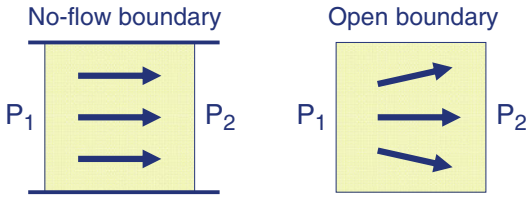

Fig. 3.7 Simple illustration of flow boundary conditions: P1 and P2 are fluid pressures applied at the *left* and *right hand sides* and *arrows* illustrate flow vectors

In reality, the permeability in a rock medium is a highly variable property. In sedimentary basins as a whole we expect variations of at least 10 orders of magnitude (Fig. 3.8), with a general decrease for surface to depth due to compaction and diagenesis. Good sandstone units may have permeabilities typically in the 10–1,000 mD range, but the silt and clay rich units pull the permeability down to around 10^{-3} mD or lower. Deeply buried mudstones forming cap-rocks and seals have permeabilities in the microdarcy to nanodarcy range. Even within a single reservoir unit (not including the shales), permeability may range by at least 5 orders of magnitude. In the example shown in Fig. 3.9 the wide range in observed permeabilities is due both to lithofacies (heterolithic facies tend to be lower than the sand facies) and due to cementation (each facies is highly variable mainly due to the effects of variable degrees of quartz cementation).

3.2.4 Permeability Averages

Due to its highly variable nature, some form of averaging of permeability is generally needed. The question is which average? There are well-known limits for the estimation of k_{eff} in ideal systems. For flow along continuous parallel layers the arithmetic average gives the correct effective permeability, while for flow perpendicular to

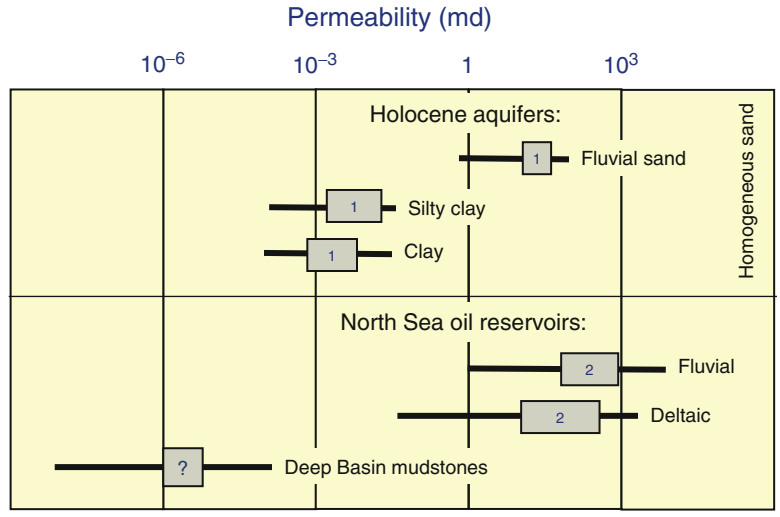

Fig. 3.8 Typical ranges of permeability for near-surface aquifers and North Sea oil reservoirs: *1* = Holocene aquifers (From Bierkins 1996), *2* = Example North Sea datasets (anonymous)

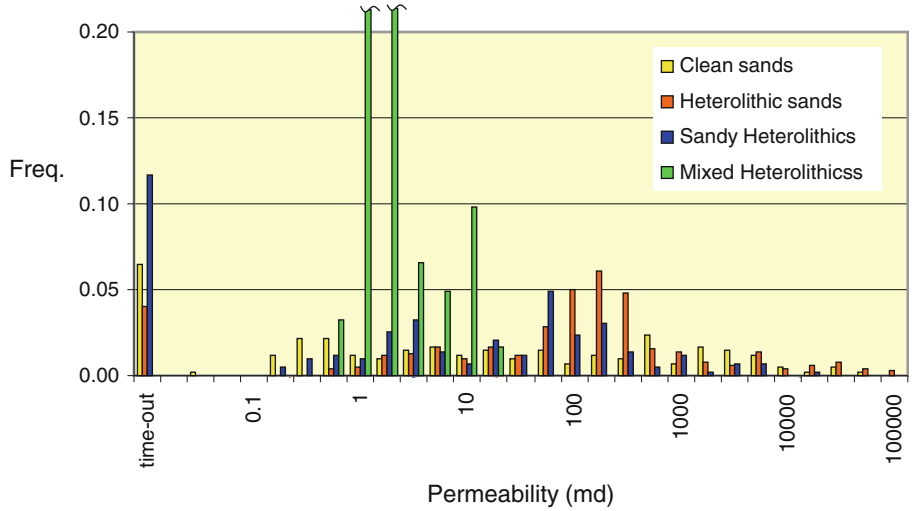

Fig. 3.9 Probe permeameter measurements from a highly variable, deeply-buried, tidal-deltaic reservoir interval (3 m of core) from offshore Norway

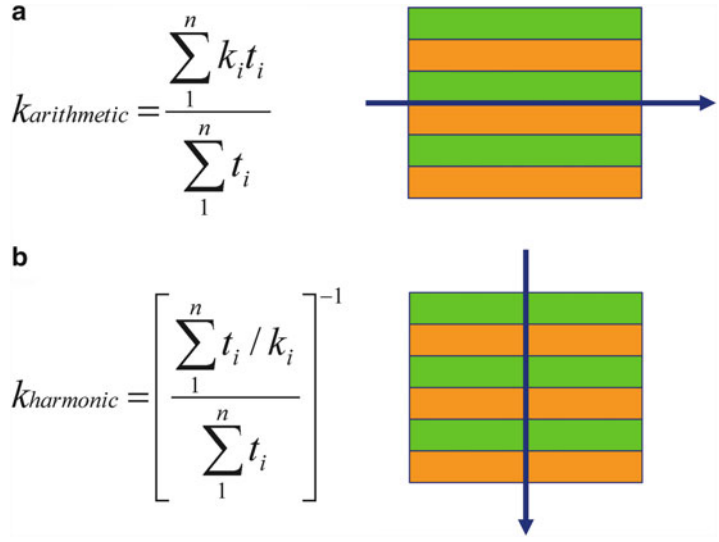

Fig. 3.10 Calculation of effective permeability using averages for ideal layered systems: (**a**) The arithmetic average for flow along continuous parallel layers; (**b**) The harmonic average for flow perpendicular to continuous parallel layers (k_i and t_i are the permeability and thickness of layer i)

continuous parallel layers the harmonic average is the correct solution (Fig. 3.10).

If the layers are in any way discontinuous or variable or the flow is not perfectly parallel or perpendicular to the layers then the true effective permeability will lie in between these averages. This gives us the outer bounds to effective permeability:

$$k_{harmonic} \leq k_{eff} \leq k_{arithmetic}$$

More precise limits to k_{eff} have also been proposed, such as the arithmetic mean of harmonic means of each row of cells parallel to flow (lower bound) and *vice versa* for the upper bound (Cardwell and Parsons 1945). However, for most practical purposes the arithmetic and harmonic means are quite adequate limiting values, especially given that we seldom have an exhaustive set of values to average (the sample problem, discussed in Sect. 3.3 below).

The geometric average is often proposed as a useful or more correct average to use for more variable rock systems. Indeed for flow in a correlated random 2D permeability field with a log-normal distribution and a low variance the effective permeability is equal to the geometric mean:

$$k_{geometric} = \exp\left[\sum_{1}^{n} \ln k_i / n\right] \qquad (3.6)$$

This can be adapted for 3D as long as account is also taken for the variance of the distribution. Gutjahr et al. (1978) showed that for a log-normally distributed permeability field in 3D:

$$k_{eff} = k_{geometric}\left(1 + \sigma^2/6\right) \qquad (3.7)$$

where σ^2 is the variance of ln(k).

Thus in 3D, the theoretical effective permeability is slightly higher than the geometric average, or indeed significantly higher if the variance is large.

An important condition for $k_{eff} \approx k_{geometric}$ is that correlation length, λ, of the permeability variation must be significantly smaller than the size of the averaging volume, L. That is:

$$\lambda_x \lambda_y \lambda_z \ll L_x L_y L_z$$

This relates to the condition of statistical homogeneity. In practice, we have found that λ needs to be at least 5 times smaller than L for $k_b \rightarrow k_{geometric}$ for a log-lognormal permeability field. This implies that the assumption (sometimes made) that $k_{geometric}$ is the 'right' average for a heterogenous reservoir interval is not generally true. Neither does the existence of a log-normal permeability distribution imply that the geometric average is the right average. This is evident in the case of a perfectly layered system with permeability values drawn from a log normal distribution – in such a case $k_{eff} = k_{arithmetic}$.

Averages between the outer-bound limits to k_{eff} can be generalised in terms of the power average (Kendall and Staurt 1977; Journel et al. 1986):

$$k_{power} = \left[\sum k_i^p / n\right]^{1/p} \qquad (3.8)$$

where $p = -1$ corresponds to the harmonic mean, $p \sim 0$ to the geometric mean and $p = 1$ to the arithmetic mean ($p = 0$ is invalid and the geometric mean is calculated using Eq. (3.6)).

For a specific case with some arbitrary heterogeneity structure, a value for p can be found (e.g. by finding a p value which gives best fit to results of numerical simulations). This can be a very useful form of the permeability average. For example, after some detailed work on estimating the permeability of a particular reservoir unit or facies (based on a key well or near-well model) one can derive plausible values for p for general application in the full field reservoir model (e.g. Ringrose et al. 2005). In general, p for k_h will be positive and p for k_v will be negative.

Note that for the general case, when applying averages to numerical models with varying cell sizes, we use volume weighted averages. Thus, the most general form of the permeability estimate using averages is:

$$k_{estimate} = \left[\int k^p dV \Big/ \int dV\right]^{1/p} \langle -1 < p < 1 | \qquad (3.9)$$

where p is estimated or postulated.

3.2.5 Numerical Estimation of Block Permeability

For the general case, where an average permeability cannot be assumed, *a priori,* numerical methods must be used to calculate the block permeability (k_b). This subject has occupied many minds in the fields of petroleum and groundwater engineering and there is a large literature on this subject. The numerical methods used are based on the assumptions of conservation of mass and energy, and generally assume steady-state conditions. The founding father of the subject in the petroleum field is arguably Muskat (1937), while Matheron (1967) founded much of the theory related to estimation of flow properties. De Marsilly (1986) gives an excellent foundation from a groundwater perspective and Renard and de Marsily (1997) give a more recent review on the calculation of equivalent

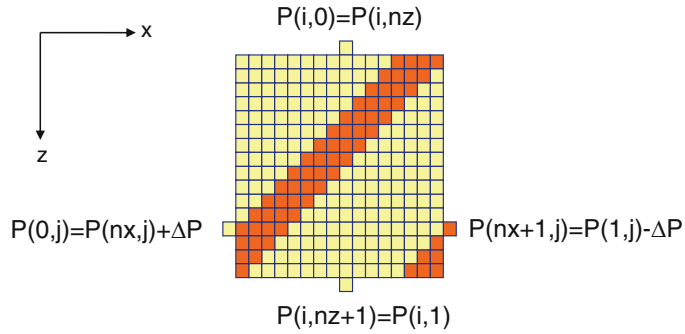

Fig. 3.11 Periodic pressure boundary conditions applied to a periodic permeability field, involving an inclined layer. Example boundary cell pressure conditions are shown

permeability. Some key papers on the calculation of permeability for heterogeneous rock media include White and Horne (1987), Durlofsky (1991) and Pickup et al. (1994).

To illustrate the numerical approach we take an example proposed by Pickup and Sorbie (1996) shown in Fig. 3.11. Assuming a fine-scale grid of permeability values, k_i, we want to calculate the upscaled block permeability tensor, k_b. An assumption on the boundary conditions must be made, and we will assume a period boundary condition (Durlofsky 1991) – where fluids exiting one edge are assumed to enter the opposite edge – and apply this to a periodic permeability field (where the model geometry repeats in all directions). This arrangement of geometry and boundary conditions gives us an exact solution.

First a pressure gradient ΔP is applied to the boundaries in the x direction. For the boundaries parallel to the applied pressure gradient, the periodic condition means that P in cell (i, 0) is set as equal to P in cell (i, nz), where n is the number of cells. A steady-state flow simulation is carried out on the fine-scale grid, and as all the permeabilities are known, it is possible to find the cell pressures and flow values (using matrix computational methods).

We then solve Darcy's Law for each fine-scale block:

$$\vec{u} = -(1/\mu)\underline{\underline{k}}.\nabla P \tag{3.10}$$

where

$\vec{u}$ is the local flow vector

μ is the fluid viscosity

$\underline{\underline{k}}$ is the permeability tensor

ΔP is the pressure gradient

Usually, at the fine scale we assume the local permeability is not a tensor so that only one value of k is required per cell.

We then wish to know the upscaled block permeability for the whole system. This is a relatively simple step once all small scale Darcy equations are known, and involves the following steps:

1. Solve the fine-scale equations to give pressures, P_{ij} for each block.
2. Calculate inter-block flows in the x-direction, using Darcy's Law.
3. Calculate total flow, Q, by summing individual flows between any two planes.
4. Calculate k_b using Darcy's Law applied to the upscaled block.
5. Repeat for the y and z directions.

For the upscaled block this results in a set of terms governing flow in each direction, such that:

$$\begin{aligned} u_x &= -\frac{1}{\mu}\left(k_{xx}\frac{\partial P}{\partial x} + k_{xy}\frac{\partial P}{\partial y} + k_{xz}\frac{\partial P}{\partial z}\right) \\ u_y &= -\frac{1}{\mu}\left(k_{yx}\frac{\partial P}{\partial x} + k_{yy}\frac{\partial P}{\partial y} + k_{yz}\frac{\partial P}{\partial z}\right) \\ u_z &= -\frac{1}{\mu}\left(k_{zx}\frac{\partial P}{\partial x} + k_{zy}\frac{\partial P}{\partial y} + k_{zz}\frac{\partial P}{\partial z}\right) \end{aligned} \tag{3.11}$$

For example, the term k_{zx} is the permeability in the z direction corresponding to the pressure gradient in the x direction. These off-diagonal terms are intuitive when one looks at the permeability field. Take the vertical (x, z) geological model section shown in Fig. 3.12. If the inclined orange layers have lower permeability, then flow applied in the +x direction (to the right) will tend to generate a flux in the –z direction (i.e. upwards). This results

Note to graphics – Ensure grid edges align – redraft if necessary?

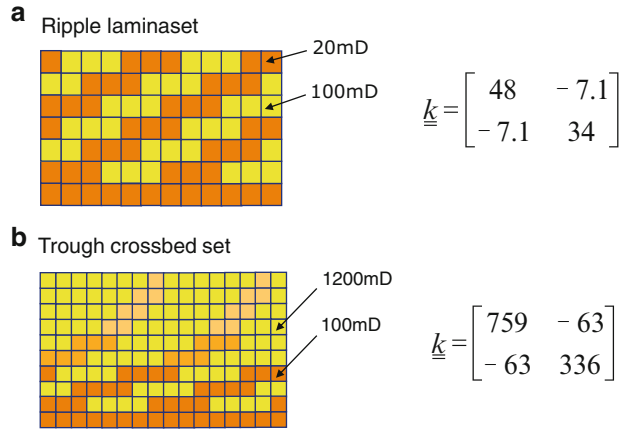

Fig. 3.12 Example tensor permeability matrices calculated for simple 2D models of common sedimentary structures

in a vertical flow and requires a k_{zx} permeability term in the Darcy equation (for a 2D tensor).

Example solutions of permeability tensors for simple geological models are given by Pickup et al. (1994) and illustrated in Fig. 3.12. Ripple laminasets and trough cross-beds are two widespread bedding architectures found in deltaic and fluvial depositional settings – ripple laminasets tend to be 2–4 cm in height while trough cross-bed sets are typically 10–50 cm in height. These simple models are two dimensional and capture typical geometry and permeability variation (measured on outcrop samples) in a section parallel to the depositional current. In both cases, the tensor permeability matrices have relatively large off-diagonal terms, 15 and 8 % of the k_{xx} value, respectively. The negative off-diagonal terms reflect the chosen coordinate system with respect to flow direction (flow left to right with z increasing downwards). Vertical permeability is also significantly lower than the horizontal permeability due to the effects of the continuous low permeability bottomset.

Geological elements like these will tend to fill the volume within a particular reservoir unit, imparting their flow anisotropy and cross-flow tendencies on the overall reservoir unit. Of course, real rock systems will have natural variability in both architecture and petrophysical properties, and our aim is therefore to represent the expected flow behaviour. The effects of geological architecture on flow are frequently neglected – for example, it may be assumed that a Gaussian random field represents the inter-well porosity and permeability architecture. More advanced, geologically-based, flow modelling will, however, allow us to assess the potential effects of geological architecture on flow, and attempt to capture these effects as a set of upscaled block permeability values. Structural architecture in the form of fractures or small faults may also generate pervasive tendencies for strongly tensorial permeability within a rock unit. By aligning grid cells to geological features (faults, dominant fracture orientations, or major bed-set boundaries) the cross-flow terms can be kept to a minimum. However, typically one aligns the grid to the largest-scale geological architecture (e.g. major fault blocks) and so other smaller-scale features inevitably generate some cross-flow.

3.2.6 Permeability in Fractures

Understanding permeability in fractured reservoirs requires some different flow physics – Darcy's law does not apply. Flow within a fracture (Fig. 3.13) is described by Poiseuille's

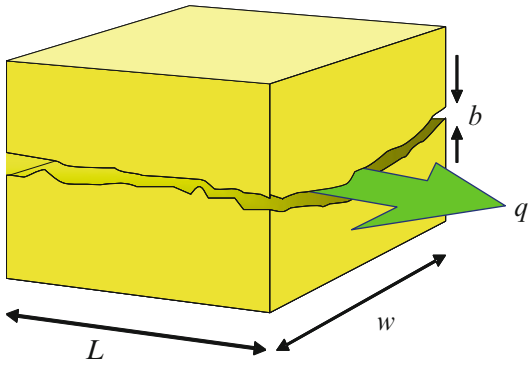

Fig. 3.13 Flow in a fracture

law, which for a parallel-plate geometry gives (Mourzenko et al. 1995):

$$q = \frac{w b^3}{12\mu} \frac{\Delta P}{L} \tag{3.12}$$

where
q is the volumetric flow rate,
w is the fracture width,
b is the fracture aperture,
μ is the fluid viscosity,
ΔP/L is the pressure gradient.

Note that the flow rate is proportional to b^3, and thus highly dependent on fracture aperture. In practice, the flow strongly depends on the stress state and the fracture roughness (Witherspoon et al. 1980), but the underlying concept still holds. To put some values into this simple equation – a 1 mm wide fracture in an impermeable rock matrix would have an effective permeability of around 100 Darcys.

Unfortunately, fracture aperture is not easily measured, and generally has to be inferred from pressure data. This makes fracture systems much harder to model than conventional non-fractured reservoirs.

In practice, there are two general approaches for modelling fracture permeability:

- Implicitly, where we model the overall rock permeability (matrix and fractures) and assume we have captured the "effect of fractures" as an effective permeability.
- Explicitly, where we represent the fractures in a model.

For the explicit case, there are then several options for how this may be done:

1. *Discrete Fracture Network (DFN) models,* where individual fractures with explicit geometry are modelled in a complex network.
2. *Dual permeability models,* where the fracture and matrix permeability are explicitly represented (but fracture geometry is implicitly represented by a shape factor).
3. *Dual porosity models,* where the fracture and matrix porosity are explicitly represented, but the permeability is assumed to occur only in the fractures (and the fracture geometry is implicitly represented by a shape factor).

Fractured reservoir modelling is discussed in detail by Nelson (2001) and covered in most reservoir engineering textbooks, and in Chap. 6 we describe approaches for handling fractured reservoir models. The important thing to keep in mind in the context of understanding permeability, is that fractures behave quite differently (and follow different laws) from the general Darcy-flow concept for flow in permeable (granular) rock media.

3.3 Handling Statistical Data

3.3.1 Introduction

Many misunderstandings about upscaled permeability, or any other reservoir property, are caused by incorrect understanding or use of probability distributions. The treatment of probability distributions is an extensive subject covered in a number of textbooks. Any of the following are suitable for geoscientists and engineers wanting to gain deeper appreciation of statistics and the Earth sciences: Size 1987; Isaaks and Srivastava 1989; Olea 1991; Jensen et al. 2000, and Davis 2003. Here we will identify some of the most important issues related to property modelling, namely:

- Understanding sample versus population statistics;
- Using log-normal and other transforms;
- Use and implications of applying cut-off values.

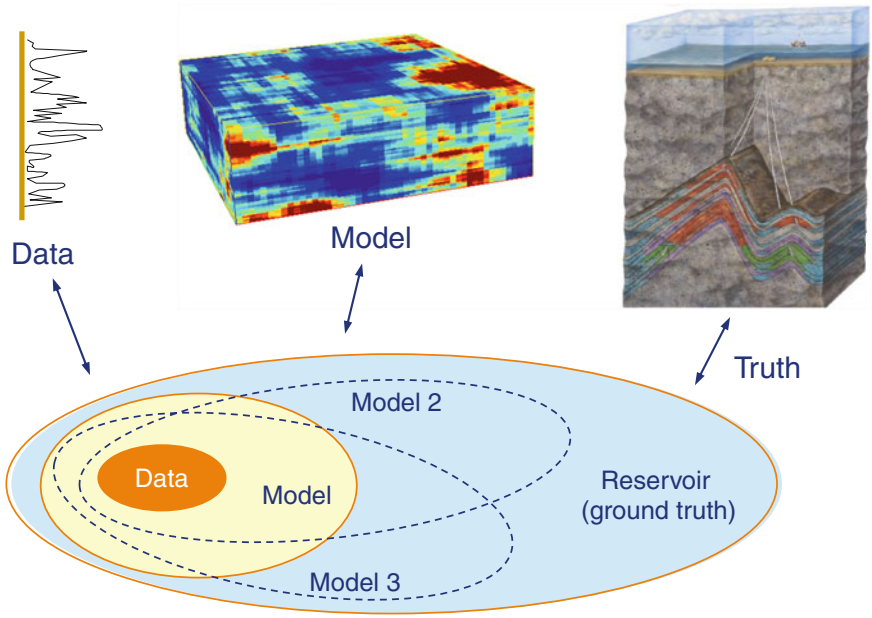

Fig. 3.14 Illustration of the axiom: Data ≠ Model ≠ Truth (Redrawn from Corbett and Jensen 1992, ©EAGE reproduced with kind permission of EAGE Publications B.V., The Netherlands)

Our overall aim in reservoir modelling is to estimate and compare distributions for:

1. The well data (observations);
2. The reservoir model (a hypothesis or postulate);
3. The population (the unknown "true" reservoir properties).

We must always remember not to confuse observations (data) with the model (a hypothesis) and both of these with the "ground truth" (an unknown). This leads us to one of the most important axioms of reservoir modelling:

$$Data \neq Model \neq Truth$$

Of course, we want our models to be consistent with the available data (from wells, seismic, and dynamic data) and we hope they will give us a good approximation of the truth, but too often the reservoir design engineer tries to force an artificial match which leads inevitably to great disappointment. A common mistake is to try to manipulate the data statistics to obtain an apparent match between the model and data. You may have heard versions of the following statements:

- 'We matched the well test permeability (k_h) to the log-derived permeability data by applying a cut-off and using a geometric average.'
- 'The previous models were all wrong, but this one must be right because it matches all the data we have.'

Now statement A sounds good but begs the questions what cut-off was applied and is the geometric average indeed the appropriate average to use? Statement B is clearly arrogant but in fact captures the psychology of every reservoir model builder – we try to do our best with the available data but are reluctant to admit to the errors that must be present. Versions of these statements that would be more consistent with the inequality above might be:

- 'We were able to match the well test permeability (k_h) to within 10 % of the log-derived permeability data by applying the agreed cut-off and using a geometric average, and a power average with $p = 0.3$ gave us an even better match to within 1 %.'
- 'The previous models had several serious errors and weaknesses, but this latest set of three models incorporates the latest data and captures the likely range of subsurface behaviour.'

Figure 3.14 illustrates what the statistical objective of modelling should be. The available

Table 3.2 Statistics for a simple example of estimation of the sand volume fraction, V_s, in a reservoir unit at different stages of well data support

	With 2 wells	With 5 wells	With 30 wells
Mean	38.5	36.2	37.4
σ	4.9	6.6	7.7
SE	3.5	3.0	1.4
C_v	–	0.18	0.21
N_0	–	3	4
N	2	5	30

data is some limited subset of the true subsurface, and the model should extend from the data in order to make estimates of the true subsurface. In terms of set theory:

$$Data \in Model \in Truth$$

Our models should be consistent with that data (in that they encompass it) but should aim to capture a wider range, approaching reality, using both geological concepts and statistical methods. In fact, as we shall see later (in this section and in Sect. 3.4) bias in the data sample and upscaling transforms further complicate this picture whereby the data itself can be misleading.

Table 3.2 illustrates this principle using the simple case of estimating the sand volume fraction, V_s (or N/G_{sand}), at different stages in a field development. We might quickly infer that the 30 well case gives us the most correct estimate and that the earlier 2 and 5 well cases are in error due to limited sample size. In fact, by applying the N-zero statistic (explained below) we can conclude that the 5-well estimate is accurate to within 20 % of the true mean, and that by the 30-well stage we still lie within the range estimated at the 5-well stage. In other words, it is better to proceed with a realistic estimate of the range in V_s from the available data than to assume that the data you have gives the "correct" value. In this case, $V_s = 36\ \% \pm 7\ \%$ constitutes a good model at the 5-well stage in this field development.

3.3.2 Variance and Uncertainty

There are a number of useful measures that can guide the reservoir model practitioner in gaining a realistic impression of the uncertainty involved in using the available data. To put it simply, *variance* refers to the spread of the data you have (in front of you), while *uncertainty* refers to some unknown variability beyond the information at hand. From probability theory we can establish that 'most' values lie close to the mean. What we want to know is 'how close' – or how sure we are about the mean value. The fundamental difficulty here is that the true (population) mean is unknown and we have to employ the theory of confidence intervals to give us an estimate. Confidence limit theory is treated well in most books on statistics; Size (1987) has a good introduction.

Chebyshev's inequality gives us the theoretical basis (and mathematical proof) for quantifying how many values lie within certain limits. For example, for a Gaussian distribution 75 % of the values are within the range of two standard deviations from the mean. Stated simply Chebyshev's theory gives:

$$P(|x - \mu| \geq \kappa\sigma) \leq \frac{1}{\kappa^2} \tag{3.13}$$

where κ is the number of standard deviations.

The *standard error* provides a simple measure of uncertainty. If we have a sample from a population (assuming a normal distribution and statistically independent values), then the standard error of the mean value, $\bar{x}$, is the standard deviation of the sample divided by the square root of the sample size:

$$SE_{\bar{x}} = \frac{\sigma_s}{\sqrt{n}} \tag{3.14}$$

where σ_s is the standard deviation of the sample and n is the sample size.

The standard error can also be used to calculate confidence intervals. For example, the 95 % confidence interval is given by $(\bar{x} \pm SE_{\bar{x}} * 1.96)$.

The *Coefficient of Variation*, C_v, is a normalized measure of the dispersion of a probability distribution, or put simply a normalised standard deviation:

$$C_V = \frac{\sqrt{Var(p)}}{E(p)} \tag{3.15}$$

where Var(p) and E(p) are the variance and expectation of the variable, p.

and k_h throughout the procedure, and also gives a sound basis for estimation of upscaled k_h and k_v. The upscaled k_h (170 mD for the whole interval) is significantly lower than the arithmetic average k_h because of the effects of sandstone connectivity and the presence of shales and mudstone layers. A degree of validation that we have derived a "reasonable estimate" for k_h is found in the observation that k_h lies in the range $k_{geometric}$ to $k_{arithmetic}$ (Fig. 3.36b).

The main challenges of the Total Property Modelling approach are:

1. The approach requires some form of explicit upscaling, and upscaling always has some associated errors;
2. Where only log data are available (i.e. in the absence of fine-scale core data) some form of indirect estimate of the fine-scale sand/mud ratios and rock properties is needed, and this inevitably introduces additional random error in the estimation of N/G_{res}.

However, for challenging, heterogeneous or low-permeability reservoirs, these (generally minor) errors are preferable to the errors associated with the inappropriate simplifications of the N/G approach.

In summary then, the widely used N/G approach is simpler to apply and can be justified for relatively good-quality reservoirs or situations where quick estimates are warranted. The method tends to embed errors in the process of re-scaling from well data to reservoir model, and care should be taken to minimise and record these errors. The TPM approach is generally more demanding but aims to minimize the (inherent) upscaling errors by making estimates of the effective flow properties of the rock units concerned. N/G ratios can be calculated at any stage in the TPM modelling workflow.

3.6 Vertical Permeability and Barriers

3.6.1 Introduction to k_v/k_h

The ratio of vertical to horizontal permeability, k_v/k_h, is an important, but often neglected, reservoir modelling property. Too often, especially when using the net-sand modelling method, a value for the k_v/k_h ratio is assumed at the last minute with little basis in reality. Figure 3.37 captures a typical "history" for this parameter; neglected or assumed = 1 in the early stages then rapidly drops after unexpected barriers are encountered and finally rises again to a more plausible value late in the field life.

The problem of vertical permeability is also further confounded because it is very difficult to measure. Routine core plug analysis usually gives some estimate of core-plug scale k_v/k_h but these data can be misleading due to severe under sampling or biased sampling (discussed by Corbett and Jensen 1992).

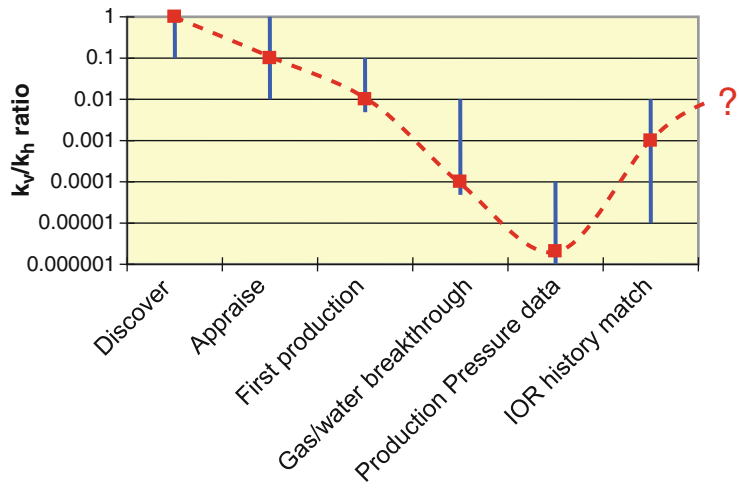

Fig. 3.37 Typical "history" of the k_v/k_h ratio

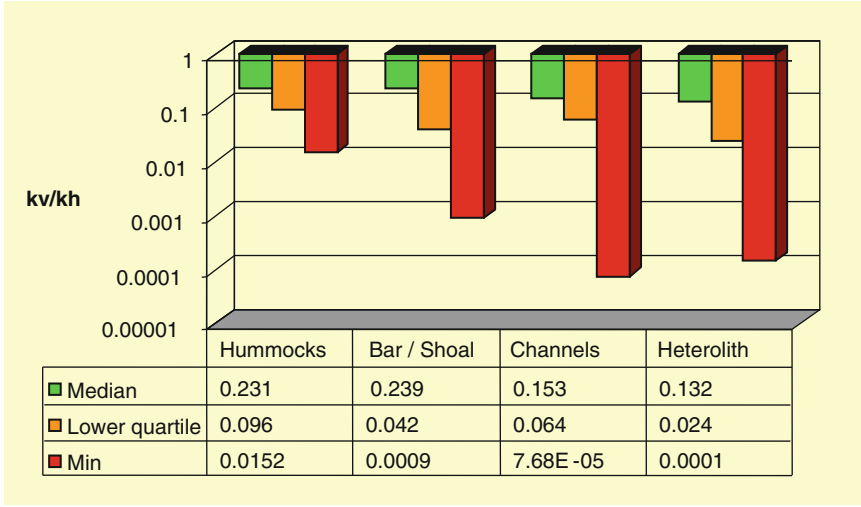

	Hummocks	Bar / Shoal	Channels	Heterolith
Median	0.231	0.239	0.153	0.132
Lower quartile	0.096	0.042	0.064	0.024
Min	0.0152	0.0009	7.68E -05	0.0001

Fig. 3.38 Statistics of measured k_v/k_h ratios from core plug pairs from an example reservoir interval

Figure 3.38 illustrates some typical core-plug anisotropy data. For this example we know from production data that the mean value is far too high (due to under sampling) and in fact the minimum observed plug k_v/k_h ratio gives a more realistic indication of the true values at the reservoir scale.

A frequent problem with modelling or estimating permeability anisotropy is confusion between (or mixing the effects of) thin barriers and rock fabric anisotropy. The following two sections consider these two aspects separately.

3.6.2 Modelling Thin Barriers

Large extensive barriers are best handled explicitly in the geological reservoir model:

- Fault transmissibilities can be mapped onto to cell boundaries;
- Extensive shales and cemented layers can be modelled as objects and then transformed to transmissibility multipliers onto to cell boundaries.

Some packages allow simulation of sub-seismic faults as effective permeability reduction factors within grid cells (see for example Manzocchi et al. 2002, or Lescoffit and Townsend 2005). Some modelling packages offer the option to assign a sealing barrier between specified layers. For the more general situation, the geo-modeller needs to stochastically simulate barriers and ensure they are applied in the simulation model. Pervasive discontinuous thin shales and cements may also be modelled as cell-value reduction factors (an effective k_v/k_h multiplier).

Figure 3.39 shows and example of barrier modelling for calcite cements in an example reservoir. The fine-scale barriers are first modelled as geological objects and then assigned as vertical transmissibility values using single-phase upscaling.

Before plunging into stochastic barrier modelling, it is important to consider using well established empirical relationships that may save a lot of time. Several previous studies have considered the effects of random shales on a sandstone reservoir. Begg et al. (1989) proposed a general estimator for the effective vertical permeability, k_{ve}, for a sandstone medium containing thin, discontinuous, impermeable mudstones, based on effective medium theory and geometry of ideal streamlines. They proposed:

$$k_{VE} = \frac{k_x(1 - V_m)}{(a_z + fd)^2} \tag{3.30}$$

where

V_m is the volume fraction of mudstone

a_z is given by $(k_{sv}/k_{sh})^{1/2}$

k_{sh} and k_{sv} are the horizontal and vertical permeability of the sandstone

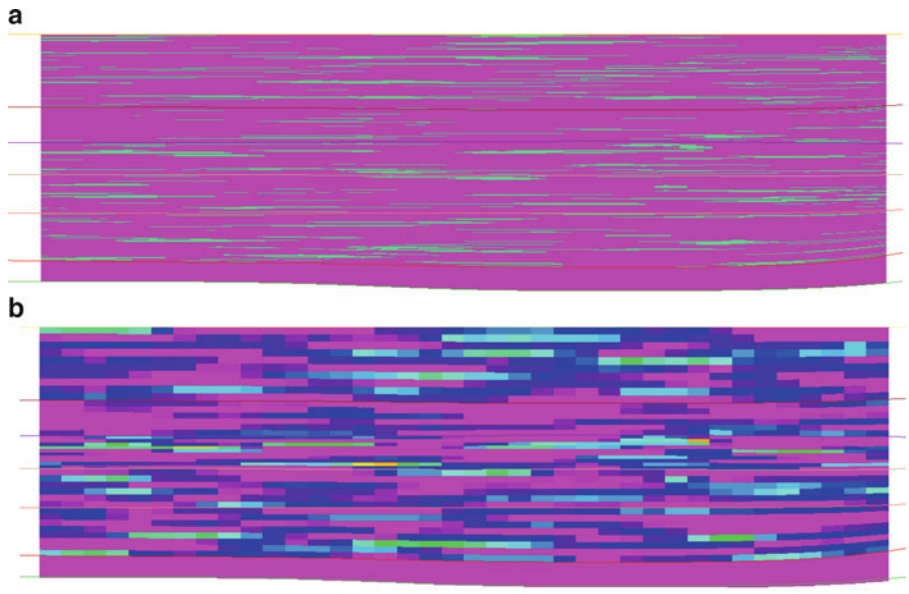

Fig. 3.39 Example modelling of randomly distributed calcite cement barriers in an example reservoir (Reservoir is c. 80 m thick) (**a**) Fine-scale model of calcite barriers. (**b**) Upscaled k_v as vertical transmissibility multipliers (Modified from Ringrose et al. 2005, Petrol Geoscience, Volume 11, © Geological Society of London [2005])

f is the barrier frequency
d is a mudstone dimension
(d = $L_m/2$ for a 2D system with mean mudstone length, L_m).

This method is valid for low mudstone volume fractions and assumes thin, uncorrelated, impermeable, discontinuous mudstone layers.

Desbarats (1987) estimated effective permeability for a complete range of mudstone volume fractions in 2D and 3D, using statistical models with spatial covariance and a range of anisotropies. For strongly stratified media, the effective horizontal permeability, k_{he}, was found to approach the arithmetic mean, while k_{ve} was found to be closer to the geometric mean. Deutsch (1989) proposed using both power-average and percolation models to approximate k_{he} and k_{ve} for a binary permeability sandstone–mudstone model on a regular 3D grid, and showed how both the averaging power and the percolation exponents vary with the anisotropy ratio.

Whatever the chosen method, it is important to separate out the effects of thin barriers (or faults) from the more general rock permeability anisotropy (discussed below).

3.6.3 Modelling of Permeability Anisotropy

Using advances in small-scale geological modelling, it is now possible to accurately estimate k_v/k_h ratios for sandstone units. Ringrose et al (2003, 2005) and Nordahl et al (2005) have developed this approach for some common bedding types found in tidal deltaic sandstone reservoirs (i.e. flaser, wavy and lenticular bedding). Their method gives a basis for general estimation for facies-specific k_v/k_h ratios. Example results are shown in Figs. 3.40 and 3.41.

The method takes the following steps:

1. Perform a large number of bedding simulations to understand the relationship between k_{sand}, k_{mud} and V_{mud} (simulations are unconditioned to well data and can be done rapidly).
2. Input values for the small-scale models are the typical values derived from measured core permeabilities.
3. A curve is fitted to the simulations to estimate the k_v or k_v/k_h ratio as a function of other modelled parameters: e.g. k_h, V_{mud}, or ø.

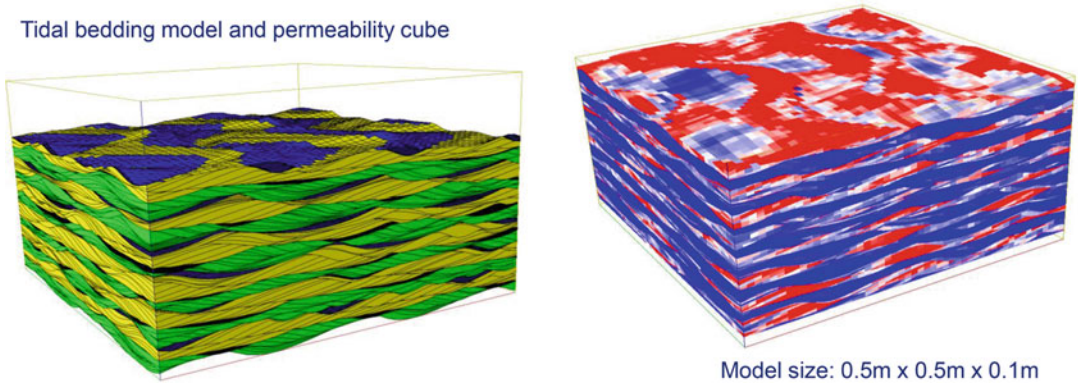

Fig. 3.40 Example model of heterolithic flaser bedding (*left*) with corresponding permeability model (*right*). Note the bi-directional sand lamina sets (*green* and *yellow* laminae) and the partially preserved mud drapes (*dark tones*). Higher permeabilities indicated by *hot colours* (Modified from Ringrose et al. 2005 Petrol Geoscience, Volume 11, © Geological Society of London [2005])

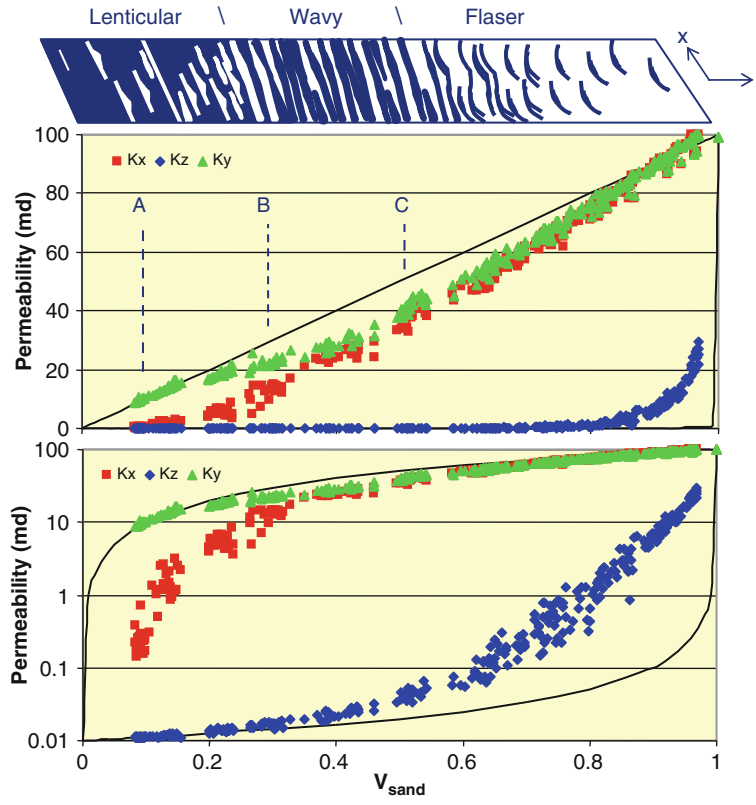

Fig. 3.41 Results of sub-metre-scale simulation of heterolithic bedding in tidal deltaic reservoirs. Effective permeability simulation results are for the constant petrophysical properties case (i.e. sandstone and mudstone have constant permeability). Observed effective permeability is compared to bedding styles and the critical points *A*, *B* and *C*. *A* is the percolation threshold for k_x, and *C* is the percolation threshold for k_z, while *B* is the theoretical percolation threshold for a simple 3D system. Thin lines are the arithmetic and harmonic averages

The following function was found to capture the characteristic vertical permeability of this system (Ringrose et al. 2003):

$$k_v = k_{sand}\left(\frac{k_{mud}}{k_{sand}}\right)^{\frac{V_m}{V_{mc}}} \tag{3.31}$$

where V_{mc} is the critical mudstone volume fraction (or percolation threshold).

This formula is essentially a re-scaled geometric average constrained by the percolation threshold. This is consistent with the previous findings by Desberats (1987) and Deutsch (1989) who observed that the geometric average was close to simulated k_v for random shale systems, and also noted percolation behaviour in such systems. This equation captures the percolation behaviour (the percolation threshold is estimated for the geometry of a specific depositional system or facies), while still employing a general average function that can be easily applied in reservoir simulation.

The method has been applied to a full-field study by Elfenbein et al. (2005) and compared to well-test estimates of anisotropy (Table 3.5). The comparison showed a very good match in the Garn 4 Unit but a poorer match in the Garn 1–3 Units. This can be explained by the fact that the lower Garn 1–3 Units have abundant calcite cements (which were modelled in the larger-scale full-field geomodel), illustrating the importance of understanding both the thin large-scale barriers and the inherent sandstone anisotropy (related to the facies and bedding architecture).

3.7 Saturation Modelling

3.7.1 Capillary Pressure

An important interface between the static and dynamic models is the definition of initial water saturation. There are numerous approaches to this problem, and in many challenging situations analysis and modelling of fluid saturations requires specialist knowledge in the petrophysics and reservoir engineering disciplines. Here we introduce the important underlying concepts that will enable the initial saturation model to be linked to the geological model and its uncertainties.

The initial saturation model is usually based on the assumption of capillary equilibrium with saturations defined by the capillary pressure curve. We recall the basic definition for capillary pressure:

$$\begin{aligned} P_c &= P_{\text{non-wetting phase}} \\ &\quad - P_{\text{wetting-phase}}[P_c = f(S)] \end{aligned} \tag{3.32}$$

The most basic form for this equation is given by:

$$P_c = AS_{wn}{}^{-b}\sqrt{\phi/k} \tag{3.33}$$

That is, capillary pressure is a function of the wetting phase saturation and the rock properties, summarized by ϕ and k. The exponent b is related to the pore size distribution of the rock. Note the use of the normalised water saturation:

$$S_{wn} = (S_w - S_{wi})/(S_{wor} - S_{wi}) \tag{3.34}$$

Table 3.5 Comparison of simulated kv/kh ratios with well test estimates from the case study by Elfenbein et al. (2005)

Reservoir unit	Modelled k_v/k_h: Geometric average of simulation model	Modelled k_v/k_h: Geometric average of well test volume	Well test k_v/k_h: Analytical estimate	Comments
			Tyrihans South, well test in well 6407/1-2	
Garn 4	0.031	0.043	<0.05	Test of Garn 4 interval
Garn 3	0.11			Producing interval uncertain
Garn 2	0.22			Complex two-phase flow
Garn 1	0.11			
			Tyrihans North, well test in well 6407/1-3	
Garn 4	0.025			
Garn 3	0.123	0.19	0.055	Test of Garn 1 to 3 interval
Garn 2	0.24			Analytical gas cap
Garn 1	0.12			Partial penetration model

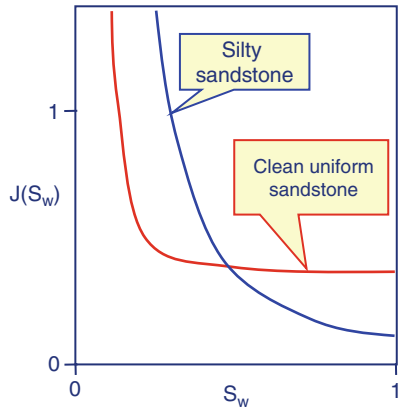

Fig. 3.42 Example capillary pressure J-functions

We can expand the P_c equation to include the fluid properties:

$$P_c(S_w) = \sigma \cos\theta J(S_w)\sqrt{\phi/k} \qquad (3.35)$$

where
σ = interfacial tension
θ = interfacial contact angle
$J(S_w)$ = Leverett J-junction.

Rearranging this we obtain the J-function:

$$J(S_w) = \frac{P_c(S_w)}{\sigma \cos\theta}\left(\frac{k}{\phi}\right)^{1/2} \qquad (3.36)$$

Figure 3.42 shows two example J-functions for contrasting rock types.

To put this more simply, we could measure and model any number of capillary pressure curves, $P_c = f(S)$. However, the J-function method allows a number of similar functions to be normalized with respect to the rock and fluid properties and plotted with a single common curve.

3.7.2 Saturation Height Functions

There are a number of ways of plotting the $P_c = f(S)$ function to indicate how saturation varies with height in the reservoir. The following equation is a general form of the P_c equation, including all the key rock and fluid terms.

$$S_{wn}{}^{-b} = \frac{(\rho_w - \rho_o)gh}{\sigma \cos\theta}\left(\frac{k}{\phi}\right)^{1/2} \qquad (3.37)$$

Here P_c is defined by the fluid buoyancy term, $\Delta(\rho)gh$, where h is the height above the free water level. This equation gives a useful basis for forward modelling water saturation, given some known rock and fluid properties.

For practical purposes we often want to estimate the S_w function from well log data. There are again several approaches to this (Worthington 2001 gives a review), but the simplest is the power law function which has the same form as the J-function:

$$S_w = C.h^d \qquad (3.38)$$

A significant issue in reservoir modelling is how the apparent (and true) saturation height function is affected by averaging of well data and/or upscaling of the fine-scale geological model data.

To illustrate these effects in the reservoir model, we take a simple case. We must first define the *free water level* (FWL) – the fluid water interface in the absence of rock pores, i.e. resulting only from fluid forces (buoyancy and hydrodynamic pressure gradients). The effect of rock pores is to introduce another factor (capillary forces) on the oil-water distribution, so that the oil-water contact is different from the free water level.

A simple model for this behaviour is given by the following saturation-height function:

$$S_w = S_{wi} + (1 - S_{wi})\left[0.1h\sqrt{k/\phi}\right]^{-2/3} \qquad (3.39)$$

Figure 3.43 shows example curves, based on this function, and illustrates how at least 10 m variation in oil-water contact can occur due to changes in pore throat size. In general, for a high porosity/permeability rock OWC $\approx$ FWL. However, for low permeability or heterogeneous reservoirs the fluid contact will vary considerably as a function of rock properties, and OWC $\neq$ FWL.

Further difficulties in interpretation of these functions come with upscaling or averaging saturations from heterogeneous systems. For example, suppose you had a thinly-bedded reservoir comprising alternating rock types 2 and 4 (Fig. 3.43), then the average saturation-height

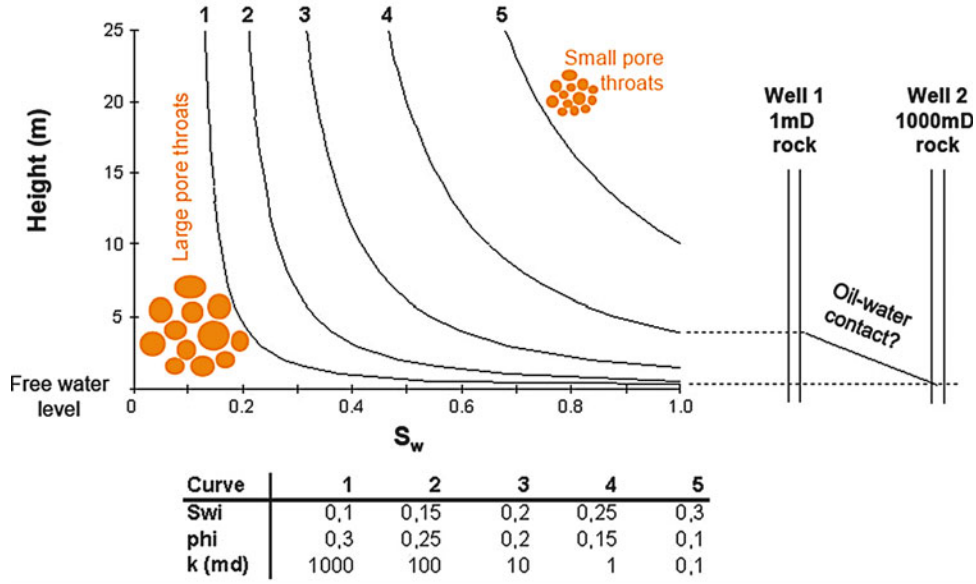

Fig. 3.43 Example saturation-height functions for the listed input parameters, illustrating how an apparent change in oil-water contact may be caused by rock property variations between wells

Table 3.6 Selected examples of tilted oil-water contacts

Field, Location	Tilt of OWC (m/km)	References
South Glenrock, Wy. USA	<95	Dahlberg (1995)
Norman Wells, NWT, Canada	75	Dahlberg (1995)
Tin-Fouye, Algeria	10	Dahlberg (1995)
Weyburn, Sask., Canada	10	Dahlberg (1995)
Kraka, North Sea (Denmark)	10	Thomasen and Jacobsen (1994)
Billings Nose, N.Da., USA	5	Berg et al. (1994)
Knutson, N.Da., USA	3	Berg et al. (1994)

function (detected by a logging tool) would be close to curve 3. That is, the average S_w corresponds to the average k/ϕ. However, if the thin beds were composed of an unknown random mix of rocks types 1, 2, 3, 4 and 5 then it would clearly be very difficult to infer the correct relationship between S_w, k and ϕ.

3.7.3 Tilted Oil-Water Contacts

Depending on which part of the world the petroleum geologist is working, tilted oil-water contacts are either part of accepted or disputed folk law. In parts of the Middle East, North Africa and North America, there are numerous well-documented examples. These represent continental basins with appreciable levels of topographically driven groundwater flow, or hydrodynamic gradients. Dahlberg (1995) provides a fairly comprehensive study of the evidence for, and interpretation of, tilted oil water contacts. Berg et al. (1994) give good documentation of some examples from Dakota, USA. In the offshore continental shelf petroleum provinces, such as offshore NW Europe the cases are fewer, but still evident. Table 3.6 lists a range of examples.

Here, we are concerned with the implications that tilted hydrocarbon-water contacts might

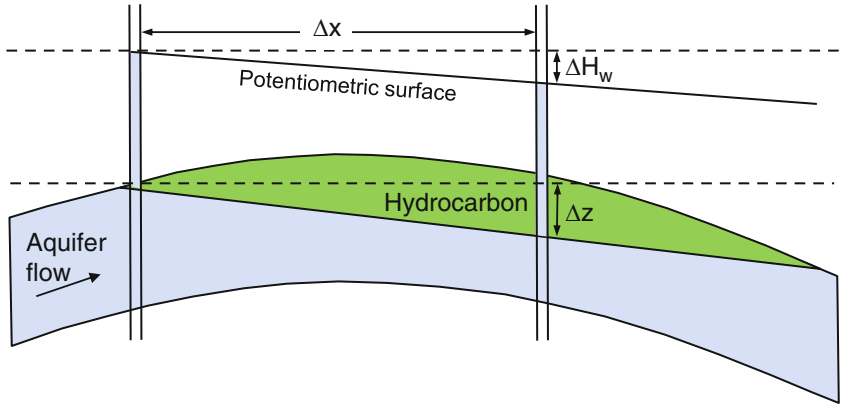

Fig. 3.44 Terms defining a tilted oil-water contact (Redrawn from Dahlberg 1995 (Fig. 12.5), Springer-Verlag, New York, with kind permission from Springer Science and Business Media B.V.)

have for a dynamic modelling of petroleum accumulations. For simplicity we mainly consider oil-water contacts, but the theory applies to any hydrocarbon: gas, condensate or oil. The main principle governing this phenomenon is potentiometric head. If an aquifer contains flowing water driven by some pressure gradient (Fig. 3.44), then this pressure gradient causes a slope in the petroleum-water interface of any accumulation within that aquifer, defined by Hubbert (1953) as:

$$\Delta z/\Delta x \approx (\rho_w/\rho_w - \rho_o).(\Delta H_w/\Delta x) \quad (3.40)$$

where

$\rho_w - \rho_o$ = density of water and petroleum

$\Delta z/\Delta x$ = slope of the hydrocarbon-water interface

$\Delta H_w/\Delta x$ = potentiometric surface in aquifer

The greater the difference in fluid density (i.e. the lighter the petroleum), the smaller the tilt of the fluid contact. It is important to differentiate the free-water level (FWL) from the oil-water contact (OWC). Where the capillary pressures are significant (due to small pores), the difference between FWL and OWC can be significant (Fig. 3.43). In Eq. (3.40), the $\Delta z/\Delta x$ term relates to the FWL (and only approximately to the OWC). A more comprehensive treatment of this topic is given by Muggeridge and Mahmode (2012), who include the terms for the effective permeability in the aquifer, k_{aq}, and reservoir, k_{res}, to derive a relationship between the hydrocarbon-water interface and the hydrodynamic pressure gradient in terms of steady-state flow:

$$(\Delta z/\Delta x) = \left(k_{res}/k_{aq}\Delta\rho g\right).(\Delta H_w/\Delta x) \quad (3.41)$$

As can be seen from Table 3.6, the actual value of the tilted oil-water contact can be quite small (most documented examples are around 10 m/km), so that uncertainties in detection become important. There are many situations which can give an apparent tilt in oil-water contact, including:

- Undetected faults (usually the first explanation to be proposed) or stratigraphic boundaries;
- Variations in reservoir properties – systematic changes in pore throat size across a field can lead to a variation in the oil-water contact of 5 m or more (Fig. 3.43);
- Misinterpretation of paleo-oil-water contacts (marked by residual oil stains or tar mats) as present-day contacts;
- Errors in deviation data for well trajectories.

Thus, proof of the presence of a tilted oil-water contact requires either multiple well data explained by a common inclined surface (Fig. 3.45) or multiple data types explained

coherently in terms of a common hydrodynamic model (as in the Kraka field example discussed below). Possible hydrodynamic aquifer influence on a static (i.e. passive) petroleum accumulation must also be considered alongside the concepts of a dynamic petroleum accumulation (e.g. ongoing migration or leakage) or pressure transients in the aquifer.

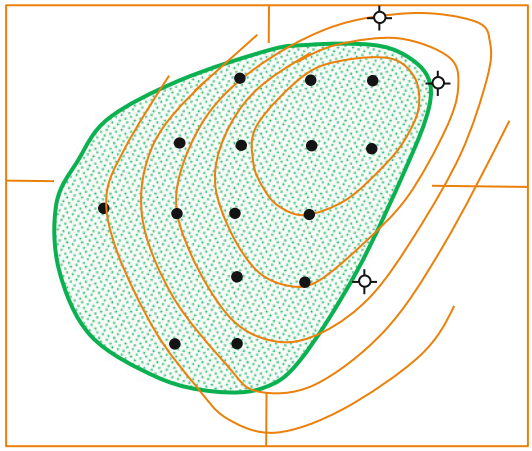

Fig. 3.45 Map of the Cairo Pool oilfield, Arkansas showing a hydrodynamic offset of an oil accumulation (After Dahlberg 1995). Contours are 20 foot intervals; *black dots* = wells with oil in the reservoir interval, *open circles* = wells with water in the reservoir interval (Redrawn from Dahlberg 1995 (Fig. 12.5), Springer-Verlag, New York, with kind permission from Springer Science and Business Media B.V.)

3.7.3.1 Kraka Field Example

This small chalk reservoir in the Danish sector of the North Sea provides an interesting account of the phenomenon of tilted oil-water contacts and their interpretation. The subtle nature of the tilt and the use of multiple data sources to confirm an initially doubtful interpretation are very informative. A study of the field by Jørgensen and Andersen (1991) included some initial observations on a tilted oil-water contact, and a tentative argument that it was due to tectonic tilting during the Tertiary. A subsequent study by Thomasen and Jacobsen (1994), give a detailed description and a more thorough basis for interpretation a 0.6° dip in both free water level and oil-water contact (Fig. 3.46).

Their main observations were:

- Repeat Formation Tester (RFT) data from three wells indicated a free-water level (interpreted from the change in slope of water and oil zones) falling by about 70 m over a 2 km distance (Fig. 3.47).
- Due to the heterogeneous and fractured nature of the chalk reservoir zone, logs from seven wells show highly variable saturations (Fig. 3.48). These were interpreted by best-fit capillary pressure saturation functions. Difficulties in fitting a function assuming a horizontal free-water level were resolved by fitting functions to individual wells and then identifying the implied tilt in free water level.

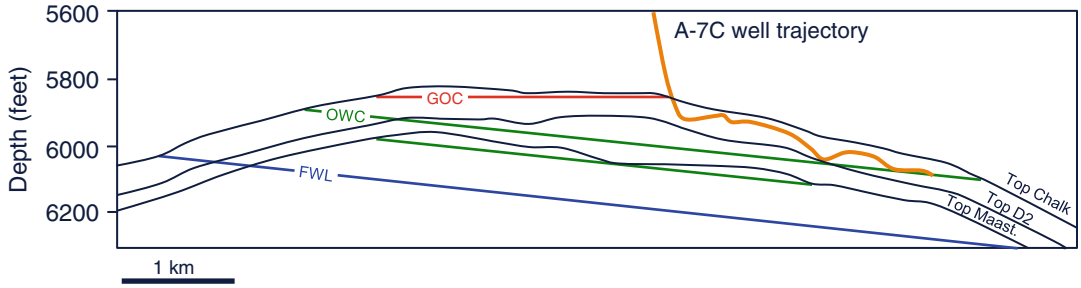

Fig. 3.46 Cross-section through the Kraka field (From Thomasen and Jacobsen 1994) showing interpreted fluid contacts and horizontal well to exploit down-dip reserves (Redrawn from Thomasen and Jacobsen 1994, ©1994, Society of Petroleum Engineers Inc., reproduced with permission of SPE. Further reproduction prohibited without permission)

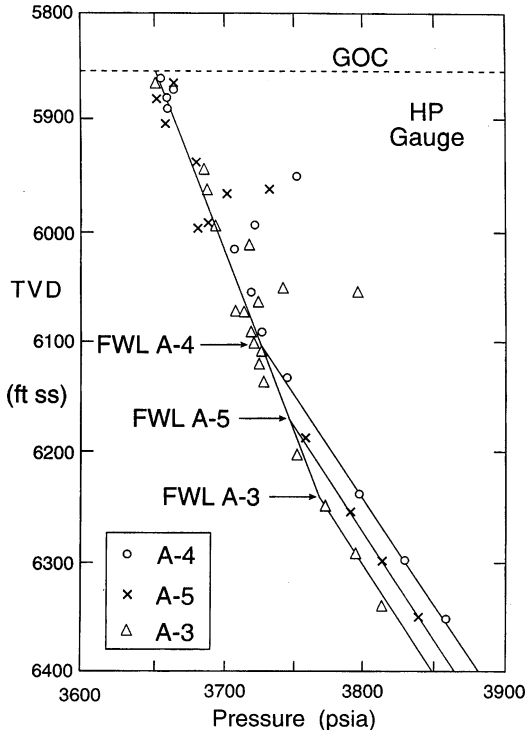

Fig. 3.47 RFT data for three wells for the Kraka field (From Thomasen and Jacobsen 1994) (Redrawn from Thomasen and Jacobsen 1994, ©1994, Society of Petroleum Engineers Inc., reproduced with permission of SPE. Further reproduction prohibited without permission)

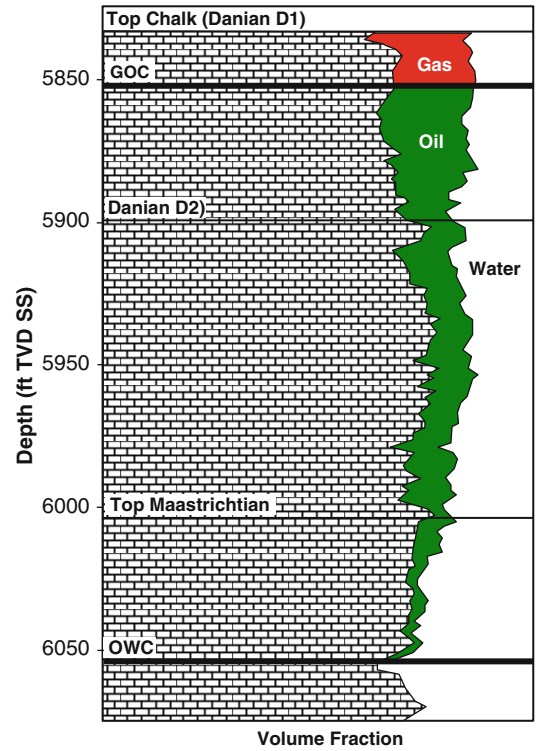

Fig. 3.48 Type log for the Kraka field illustrating the variable oil saturations and the thick transition zone (Redrawn from Thomasen and Jacobsen 1994, ©1994, Society of Petroleum Engineers Inc., reproduced with permission of SPE. Further reproduction prohibited without permission)

The slope of the free-water level inferred from this was found to be close to the RFT pressure data model.

- An intra-reservoir seismic reflection interpreted as the matrix oil-water contact was mapped around the field and extrapolated to its intersection with top reservoir, and was again found to be in good agreement with the saturation model.
- The orientation of the inferred hydrodynamic gradient (towards the SE) was found to be in agreement with regional gradients from inter-field pressure variations.

This integrated interpretation had a significant economic benefit in terms of the appropriate placement of horizontal wells in the thicker part of the accumulation, and in the estimation of inter-well permeability in this fairly marginal field development.

3.8 Summary

We have covered a range of issues related to petrophysical property modelling of oil and gas reservoirs. The theoretical principles that underlie the modelling "buttons" and workflows in geological reservoir modelling packages have been discussed along with many of the practical issues that govern the choice of parameters.

To summarise this chapter, we offer a check list of key questions to ask before proceeding with your property modelling task:

1. Have you agreed with your colleagues across disciplines (geoscience, petrophysics and reservoir engineering):
   - The key geological issues you need to address – rock heterogeneity, sedimentary barriers, faults, etc.

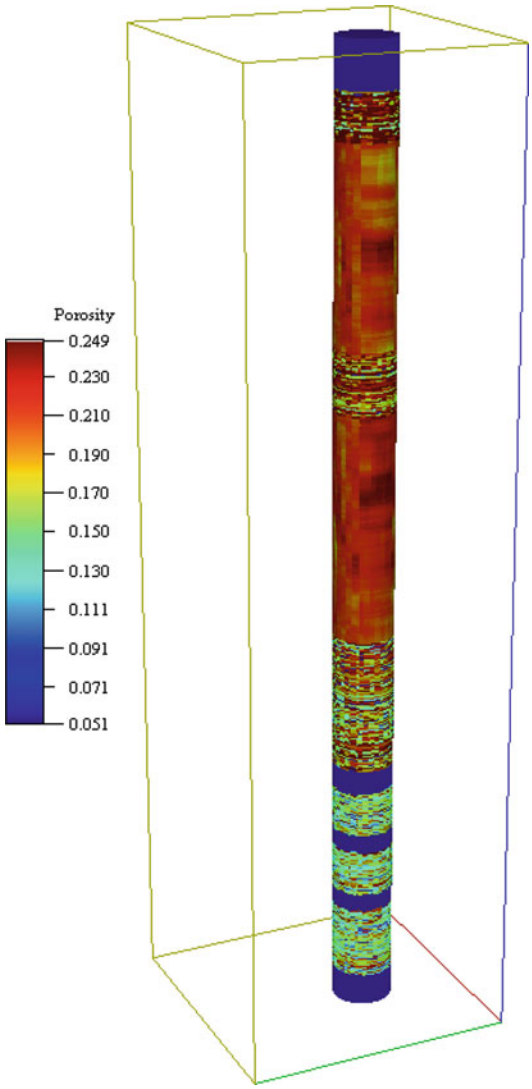

Fig. 3.49 Near-wellbore porosity model (1 m^2 × 10 m)

- A consistent method for handling net-to-gross (N/G) and cut-off values?

2. Is your petrophysical data representative of the rock unit (sampling problems, tails of distributions), and if not how will you address that uncertainty?
3. Have you used appropriate averaging and/or upscaling methods?
4. Is the model output consistent with data input? Compare the statistics of input and output distributions. The variance may be as important as the mean.
5. Have you run sensitivities to check important assumptions?
6. Have you considered the effects of possible un-detected flow barriers in the system?

A final word about the future of property modelling – if we are looking for fit-for-purpose models for interpreting petrophysical well data, then we are probably talking about high-resolution near-wellbore models (Fig. 3.49). These models could be very detailed or could be just a simple equation. Either way they need to be focussed on the scale of rock property variation – the subject of the next chapter.

References

Abbaszadeh M, Fujii H, Fujimoto F (1996) Permeability prediction by hydraulic flow units – theory and applications. SPE Form Eval 11(4):263–271

Begg SH, Carter RR, Dranfield P (1989) Assigning effective values to simulator gridblock parameters for heterogeneous reservoirs. SPE Reserv Eng 1989:455–463

Berg RR, DeMis WD, Mitsdarffer AR (1994) Hydrodynamic effects on Mission Canyon (Mississippian) oil accumulations, Billings Nose area, North Dakota. AAPG Bull 78(4):501–518

Bierkins MFP (1996) Modeling hydraulic conductivity of a complex confining layer at various spatial scales. Water Resour Res 32(8):2369–2382

Bourbie T, Zinszner B (1985) Hydraulic and acoustic properties as a function of porosity in Fontainebleau sandstone. J Geophys Res 90(B13):11524–11532

Box GEP, Cox DR (1964) An analysis of transformations. J R Stat Soc Series B: 211–243, discussion 244–252

Brandsæter I, McIlroy D, Lia O, Ringrose PS (2005) Reservoir modelling of the Lajas outcrop (Argentina) to constrain tidal reservoirs of the Haltenbanken (Norway). Petrol Geosci 11:37–46

Bryant S, Blunt MJ (1992) Prediction of relative permeability in simple porous media. Phys Rev A 46:2004–2011

Buland A, Kolbjornsen O, Omre H (2003) Rapid spatially coupled AVO inversion in the fourier domain. Geophysics 68(1):824–836

Cardwell WT, Parsons RL (1945) Average permeabilities of heterogeneous oil sands. Trans Am Inst Mining Met Pet Eng 160:34–42

Corbett PWM, Jensen JL (1992) Estimating the mean permeability: how many measurements do you need? First Break 10:89–94

Corbett PWM, Ringrose PS, Jensen JL, Sorbie KS (1992) Laminated clastic reservoirs: the interplay of capillary pressure and sedimentary architecture. SPE paper 24699, presented at the SPE annual technical conference, Washington, DC

Cosentino L (2001) Integrated reservoir studies. Editions Technip, Paris, 310 pp
Dahlberg EC (1995) Applied hydrodynamics in petroleum exploration, 2nd edn. Springer, New York
Davis JC (2003) Statistics and data analysis in geology, 3rd edn. Wiley, New York, 638 pp
de Marsilly G (1986) Quantitative hydrogeology. Academic, San Diego
Delfiner P (2007) Three statistical pitfalls of phi-k transforms. SPE Reserv Eval Eng 10:609–617
Desberats AJ (1987) Numerical estimation of effective permeability in sand-shale formations. Water Resour Res 23(2):273–286
Deutsch C (1989) Calculating effective absolute permeability in sandstone/shale sequences. SPE Form Eval 4:343–348
Deutsch CV (2002) Geostatistical reservoir modeling. Oxford University Press, Oxford, 376 pp
Deutsch CV, Journel AG (1992) Geostatistical software library and user's guide, vol 1996. Oxford University Press, New York
Doyen PM (2007) Seismic reservoir characterisation. EAGE Publications, Houten
Durlofsky LJ (1991) Numerical calculations of equivalent grid block permeability tensors for heterogeneous porous media. Water Resour Res 27(5):699–708
Elfenbein C, Husby Ø, Ringrose PS (2005) Geologically-based estimation of kv/kh ratios: an example from the Garn Formation, Tyrihans Field, Mid-Norway. In: Dore AG, Vining B (eds) Petroleum geology: North-West Europe and global perspectives. Proceedings of the 6th petroleum geology conference. The Geological Society, London
Goggin DJ, Chandler MA, Kocurek G, Lake LW (1988) Patterns of permeability variation in eolian deposits: page sandstone (Jurassic), N.E. Arizona. SPE Form Eval 3(2):297–306
Gutjahr AL, Gelhar LW, Bakr AA, MacMillan JR (1978) Stochastic analysis of spatial variability in subsurface flows 2. Evaluation and application. Water Resour Res 14(5):953–959
Hohn ME (1999) Geostatistics and petroleum geology, 2nd edn. Kluwer, Dordrecht
Howson C, Urbach P (1991) Bayesian reasoning in science. Nature 350:371–374
Hubbert MK (1953) Entrapment of petroleum under hydrodynamic conditions. AAPG Bull 37(8):1954–2026
Hurst A, Rosvoll KJ (1991) Permeability variations in sandstones and their relationship to sedimentary structures. In: Lake LW, Carroll HB Jr, Wesson TC (eds) Reservoir characterisation II. Academic, San Diego, pp 166–196
Isaaks EH, Srivastava RM (1989) Introduction to applied geostatistics. Oxford University Press, Oxford
Jensen JL, Corbett PWM, Pickup GE, Ringrose PS (1995) Permeability semivariograms, geological structure and flow performance. Math Geol 28(4):419–435
Jensen JL, Lake LW, Corbett PWM, Goggin DJ (2000) Statistics for petroleum engineers and geoscientists, 2nd edn. Elsevier, Amsterdam
Jørgensen LN, Andersen PM (1991) Integrated study of the Kraka Field. SPE paper 23082, presented at the offshore Europe conference, Aberdeen, 3–6 Sept 1991
Journel AG, Alabert FG (1990) New method for reservoir mapping. J Petrol Technol 42.02:212–218
Journel AG, Deutsch CV (1997) Rank order geostatistics: a proposal for a unique coding and common processing of diverse data. Geostat Wollongong 96:174–187
Journel AG, Deutsch CV, Desbarats AJ (1986) Power averaging for block effective permeability. SPE paper 15128, presented at SPE California regional meeting, Oakland, California, 2–4 April
Kendall M, Staurt A (1977) The advanced theory of statistics, vol. 1: distribution theory, 4th edn. Macmillan, New York
Lescoffit G, Townsend C (2005) Quantifying the impact of fault modeling parameters on production forecasting for clastic reservoirs. In: Evaluating fault and cap rock seals, AAPG special volume Hedberg series, no. 2. American Association of Petroleum Geologists, Tulsa, pp 137–149
Leuangthong O, Khan KD, Deutsch CV (2011) Solved problems in geostatistics. Wiley, New York
Manzocchi T, Heath AE, Walsh JJ, Childs C (2002) The representation of two-phase fault-rock properties in flow simulation models. Petrol Geosci 8:119–132
Matheron G (1967) Éléments pour une théorie des milieux poreux. Masson and Cie, Paris
McIlroy D, Flint S, Howell JA, Timms N (2005) Sedimentology of the tide-dominated Jurassic Lajas Formation, Neuquen Basin, Argentina. Geol Soc Lond Spec Publ 252:83–107
Mourzenko VV, Thovert JF, Adler PM (1995) Permeability of a single fracture; validity of the Reynolds equation. J de Phys II 5(3):465–482
Muggeridge A, Mahmode H (2012) Hydrodynamic aquifer or reservoir compartmentalization? AAPG Bull 96 (2):315–336
Muskat M (1937) The flow of homogeneous fluids through porous media. McGraw-Hill, New York (Reprinted by the SPE and Springer 1982)
Nair KN, Kolbjørnsen O, Skorstad A (2012) Seismic inversion and its applications in reservoir characterization. First Break 30:83–86
Nelson RA (2001) Geologic analysis of naturally fractured reservoirs, 2nd edn. Butterworth-Heinemann, Boston
Nordahl K, Ringrose PS, Wen R (2005) Petrophysical characterisation of a heterolithic tidal reservoir interval using a process-based modelling tool. Petrol Geosci 11:17–28
Olea RA (ed) (1991) Geostatistical glossary and multilingual dictionary, IAMG studies in mathematical geology no. 3. Oxford University Press, Oxford
Pickup GE, Sorbie KS (1996) The scaleup of two-phase flow in porous media using phase permeability tensors. SPE J 1:369–381
Pickup GE, Ringrose PS, Jensen JL, Sorbie KS (1994) Permeability tensors for sedimentary structures. Math Geol 26:227–250

Pickup GE, Ringrose PS, Corbett PWM, Jensen JL, Sorbie KS (1995) Geology, geometry and effective flow. Petrol Geosci 1:37–42

Renard P, de Marsily G (1997) Calculating equivalent permeability: a review. Adv Water Resour 20:253–278

Ringrose PS (2008) Total-property modeling: dispelling the net-to-gross myth. SPE Reserv Eval Eng 11:866–873

Ringrose PS, Pickup GE, Jensen JL, Forrester M (1999) The Ardross reservoir gridblock analogue: sedimentology, statistical representivity and flow upscaling. In: Schatzinger R, Jordan J (eds) Reservoir characterization – recent advances, AAPG memoir no. 71., pp 265–276

Ringrose PS, Skjetne E, Elfeinbein C (2003) Permeability estimation functions based on forward modeling of sedimentary heterogeneity. SPE 84275, presented at the SPE annual conference, Denver, CO, USA, 5–8 Oct 2003

Ringrose PS, Nordahl K, Wen R (2005) Vertical permeability estimation in heterolithic tidal deltaic sandstones. Petrol Geosci 11:29–36

Shuey RT (1985) A simplification of the Zoeppritz equations. Geophysics 50(4):609–614

Size WB (ed) (1987) Use and abuse of statistical methods in the earth sciences, IAMG studies in mathematical geology, no. 1. Oxford University Press, Oxford

Soares A (2001) Direct sequential simulation and cosimulation. Math Geol 33(8):911–926

Thomasen JB, Jacobsen NL (1994) Dipping fluid contacts in the Kraka Field, Danish North Sea. SPE paper 28435, presented at the 69th SPE annual technical conference and exhibition, New Orleans, LA, USA, 25–28 Sept 1994

Weber KJ, van Geuns LC (1990) Framework for constructing clastic reservoir simulation models. J Petrol Tech 42:1248–1297

White CD, Horne RN (1987) Computing absolute transmissibility in the presence of fine-scale heterogeneity. SPE paper 16011, presented at the 9th SPE symposium of reservoir simulation, San Antonio, TX, 1–4 Feb 1987

Witherspoon PA, Wang JSY, Iwai K, Gale JE (1980) Validity of cubic law for fluid flow in a deformable rock fracture. Water Resour Res 16(6):1016–1024

Worthington PF (2001) Scale effects on the application of saturation-height functions to reservoir petrofacies units. SPE Reserv Eval Eng 4(5):430–436

Worthington PF, Cosentino L (2005) The role of cut-offs in integrated reservoir studies (SPE paper 84387). SPE Reserv Eval Eng 8(4):276–290

Upscaling Flow Properties

4

Abstract

To upscale flow properties means to estimate large-scale flow behaviour from smaller-scale measurements. Typically, we start with a few measurements of rock samples (lengthscale ~3 cm) and some records of flow rates and pressures in test wells (~100 m). Our challenge is to estimate how the whole reservoir will flow (~1 km).

Flow properties of rocks vary enormously over a wide range of length-scales, and estimating upscaled flow properties can be quite a challenge. Unfortunately, many reservoir modellers choose to overlook this problem and blindly hope that a few measurements will correctly represent the whole reservoir. The aim of this chapter is to help make intelligent estimates of large-scale flow properties. In the words of Albert Einstein:

> *Two things are infinite: the universe and human stupidity; and I'm not sure about the universe.*

P. Ringrose and M. Bentley, *Reservoir Model Design*, DOI 10.1007/978-94-007-5497-3_4,

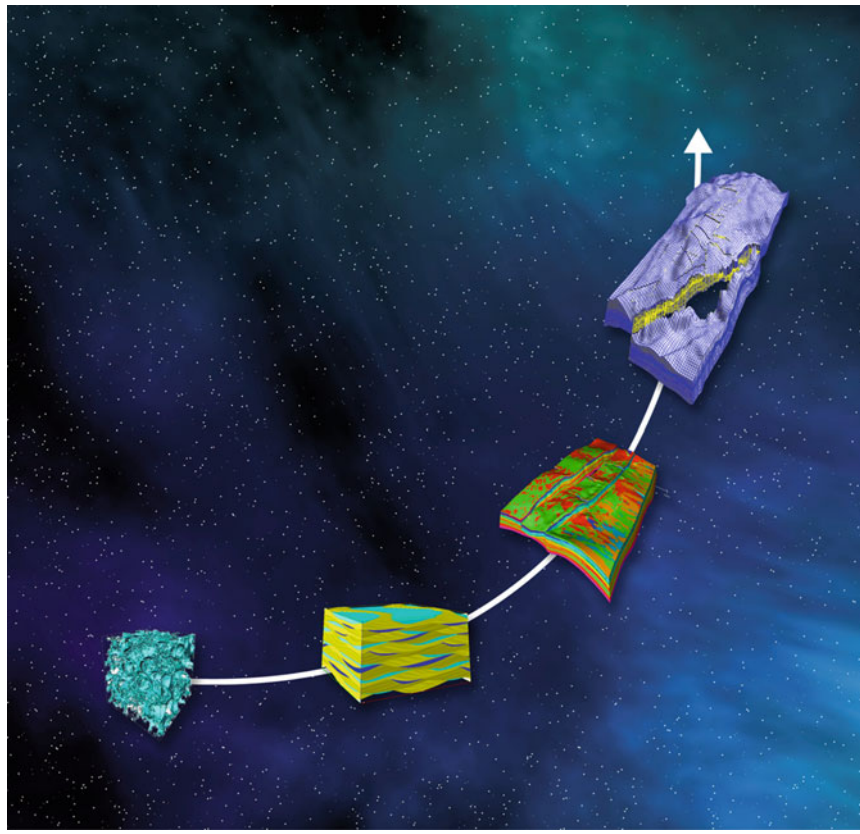

Upscaling – from pore to field, and beyond . . .

4.1 Multi-scale Flow Modelling

This chapter concerns the implementation of multi-scale flow modelling for oil and gas reservoir studies. *Multi-scale flow modelling* is defined here as any method which attempts to explicitly represent the flow properties at more-than-one scale within a reservoir. We may, for example, have (a) an estimate of flow properties around a single well in a specific flow unit (or reservoir interval) and (b) a *rationale* for using this estimate to calculate the flow properties in the whole reservoir. This *rationale* could simply be some multiplication factors transforming the single-well flow property to the reservoir scale, or might involve a 3-dimensional array (or grid) of values drawn from statistical population (which includes the single-well flow property).

In multi-scale geological modelling, the essence is that geological concepts are used to make the transition from smaller-scale measurements to larger-scale estimates (models) of reservoir properties or behaviour (Fig. 4.1). Geological modelling in itself is an art form requiring some intimate knowledge of the geological system – typically involving Picasso-type geologists (Fig. 4.2) with an interest in detail. For upscaling we require representative geological models in which the geological elements (e.g. layers of sandstone, siltstone, mudstone and limestone) are represented as properties relevant for fluid modelling – porosity, permeability, capillary pressure functions, etc.

This process inevitably involves some simplification of the intricate variability of rock architecture, as we aim to group the rock elements into

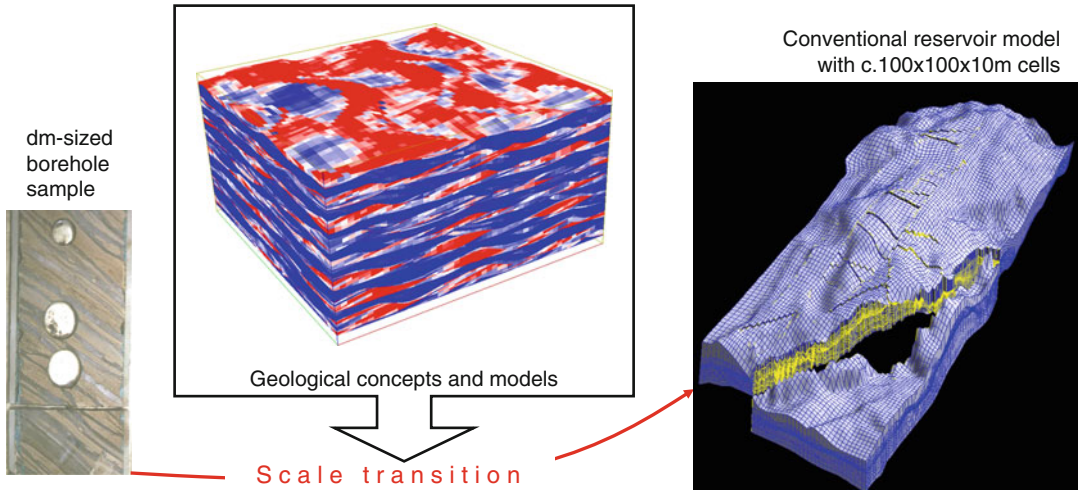

Fig. 4.1 Scale transition in reservoir modelling and the role of geological concepts

Fig. 4.2 The art of geological modelling: "Picasso-type geologists" aim to represent fine detail in their art work while "Rothko-type geologists" aim to capture only the representative flow units as essential colours (Pablo Picasso, Violins and Grapes, oil on canvas (1912) and Mark Rothko, *No. 10,* 1950. Oil on canvas, 229.2 × 146.4 cm, reproduced with permission DIGITAL IMAGE © The Museum of Modern Art/Scala, Florence)

flow units with similar properties. In the art analogy this process is more like the work of Mark Rothko, where broad bands of colour capture the essence of the object or concept being described (Fig. 4.2).

The process of transferring information between scales is referred to as *upscaling* or, more generally, re-scaling. Upscaling involves some form of numerical or analytical method for estimating effective or equivalent flow

properties at a larger scale given some set of finer scale rock properties. Upscaling methods for single and multiphase flow are reviewed in detail by Renard and de Marsily (1997), Barker and Thibeau (1997), Ekran and Aasen (2000) and Pickup et al. (2005). We will review the methods involved and establish the principles which guide the flow upscaling process. The term *downscaling* has also been used (Doyen 2007) to mean the process by which smaller-scale properties are estimated from a larger–scale property. This is most commonly done in the context of seismic data where, for example, a porosity value estimated from seismic impedance is used to constrain the porosity values of thin layers below the resolution of the seismic wavelet. In more general terms, if we know all the fine-scale properties then the upscaled property can be estimated uniquely. Conversely, if we know only the large-scale property value then there are many alternative fine-scale property models that could be consistent with the upscaled property.

We will develop the argument that upscaling is essential in reservoir modelling – whether implicit or explicit. There is no such thing as the *correct* value for the permeability of a given hydraulic flow unit. The relevant permeability value depends on length-scale, the boundary conditions and flow process. Efforts to define the diagnostic characteristics for hydraulic flow units (HFU) (e.g. Abbaszadeh et al. 1996) provide valuable approaches to petrophysical data analysis, but HFUs should always be related to a representative elementary volume (REV). As we will show it is not always simple to define the REV, and when flow process are brought into play different REVs may apply to different flow processes. Hydraulic flow units are themselves multi-scale.

The framework we will use for upscaling involves a series of steps where smaller-scale models are nested within larger scale models. These steps essentially involve models or concepts at the pore-scale, geological concepts and models at the field-scale and reservoir simulations (Fig. 4.3).

The factors involved in these scale transitions are enormous; certainly around 10^9 as we go from the rock pore to the full-field reservoir model (Table 4.1), and important scale markers involved in reservoir modelling are best illustrated on a logarithmic scale (Fig. 4.4). Despite these large scale transitions, most flow processes average out the local variations – so that what we are looking for is the correct average flow behaviour at the larger scales. How we do this is the rationale for this chapter.

Flow simulation of detailed reservoir models is a fairly demanding exercise, involving many mathematical tools for creating and handling flow grids and calculating the flows and pressures between the grid cells. The mathematics of flow simulation is beyond the scope of this book, and will be treated only in an introductory sense. Mallet (2008) gives a recent review of the processes involved in the creation of numerical rock models and their use in flow simulation. King and Mansfield (1999) also give a fairly comprehensive discussion of flow simulation of geological reservoir models, in terms of managing and handling the grid and associated flow terms (transmissibility factors). In this chapter, we will take as our starting point the existence of a numerical rock model, created by some set of recipes in a geological modelling toolkit, and will focus on the methods involved for performing multi-scale upscaling. Before we do that we need to introduce, or recapitulate, some of the basic theory for multiphase fluid flow.

4.2 Multi-phase Flow

4.2.1 Two-Phase Flow Equations

In Chap. 3 we introduced the concept of permeability and the theoretical basis for estimating effective permeability using averages and numerical recipes. This introduced us to upscaling for single-phase flow properties. Here we extend this by looking at two-phase flow and the upscaling of multi-phase flow properties.

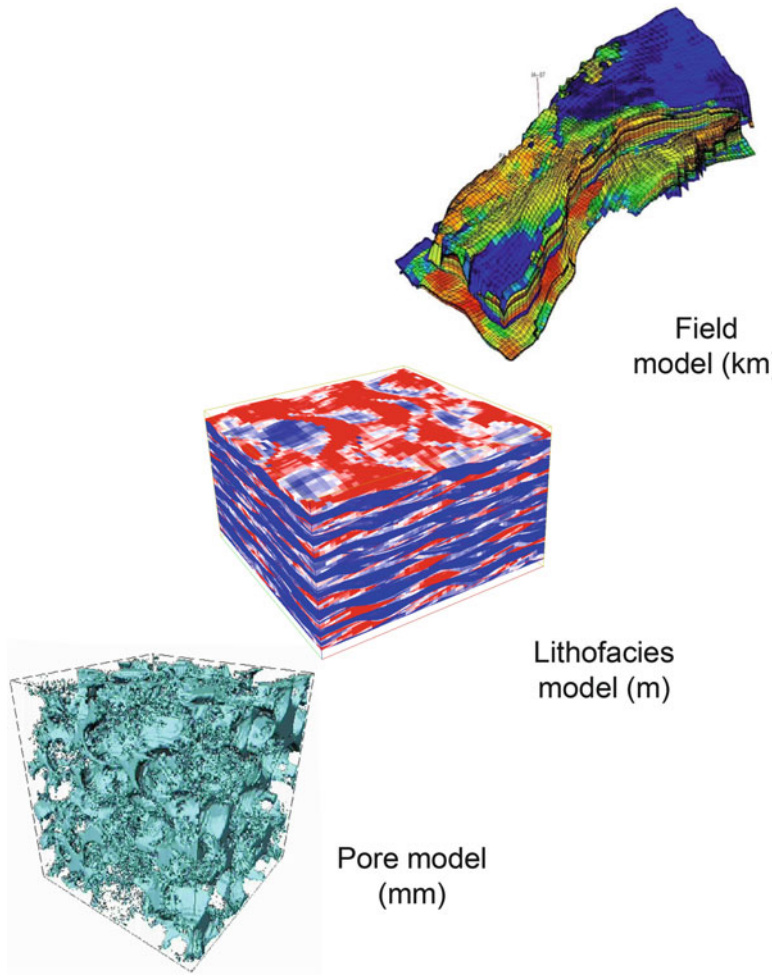

Fig. 4.3 Reservoir models at different scales (Statoil image archives, © Statoil ASA, reproduced with permission)

Table 4.1 Typical dimensions for important volumes used in multi-scale reservoir modelling

	X (m)	Y(m)	Z(m)	Volume (m^3)	Cubic root (m)	Fraction of reservoir volume
Pore-scale model	5×10^{-5}	50×10^{-5}	50×10^{-5}	1.25×10^{-13}	0.00005	0.00000005
Core plug sample	0.025	0.025	0.025	0.000031	0.031	0.00003
Well test volume	400	300	10	1,200,000	106	0.1
Reservoir model	8,000	4,000	40	1,280,000,000	1,086	1

For a fuller treatment of multi-phase flow theory applied to oil and gas reservoir systems refer to reservoir engineering textbooks (e.g. Chierici 1994; Dake 2001; Towler 2002). A more geologically-based introduction to multi-phase flow in structured sedimentary media is given by Ringrose et al. (1993) and Ringrose and Corbett (1994).

The first essential concept in multiphase flow is the principal of mass balance. Any fluid which flows into a grid cell (mass accumulation) over a particular interval of time must be equal to the mass of fluids which have flowed out. This principle may be rather trivial for single phase flow, but becomes more critical for multiphase flow, where different fluids may have different

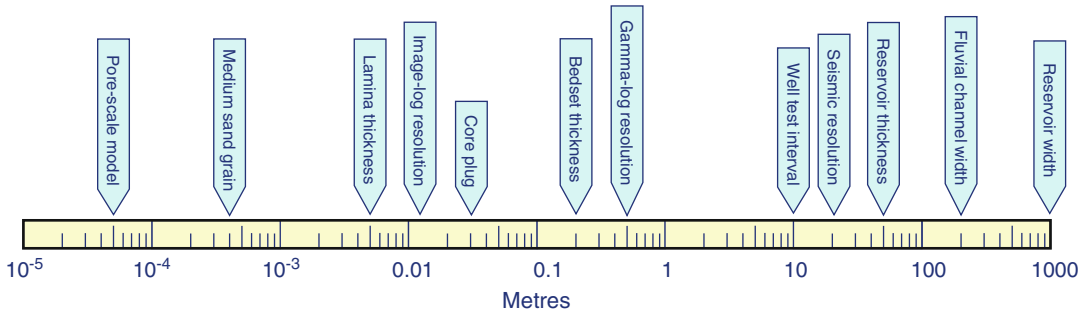

Fig. 4.4 Important length scales involved in reservoir modelling

densities, viscosities, and permeabilities. What goes in must be balanced by what comes out, and for a complex set of flow equations the zero-sum constraint for each grid cell is essential.

Fluid flow in porous media is represented by Darcy's Law (Sect. 4.3.2) which relates the fluid velocity, u, to the pressure gradient and two terms representing the rock and the fluid:

$$u = -\underline{\mathbf{k}}/\mu.\nabla(P + \rho gz) \tag{4.1}$$

The pressure term comprises an imposed pressure gradient, $\nabla(P)$, and a pressure gradient due to gravity, $\nabla(\rho gz)$. In Cartesian coordinates the gradient of pressure, ∇P, is resolved as:

$$\nabla P = \frac{dP}{dx} + \frac{dP}{dy} + \frac{dP}{dz} \tag{4.2}$$

The rock (or the permeable medium) is represented by the permeability tensor, $\underline{\mathbf{k}}$, and fluid by the viscosity, μ.

When two or more fluid phases are flowing, it becomes necessary to introduce terms for the density, viscosity and permeability of each phase and for the interfacial forces (both fluid-fluid and fluid-solid). For two-phase immiscible flow (oil and water), the two-phase Darcy equation and the capillary pressure equation are used:

$$u_o = -\underline{\mathbf{k}}k_{ro}/\mu_o.\nabla(P_o + \rho_o gz) \tag{4.3}$$

$$u_w = -\underline{\mathbf{k}}k_{rw}/\mu_w.\nabla(P_w + \rho_w gz) \tag{4.4}$$

$$P_c = P_o - P_w \tag{4.5}$$

where:

o and w refer to the oil and water phases,

k_{rw} and k_{ro} are the relative permeabilities of each phase,

μ and ρ are fluid viscosity and density,

P_c is the capillary pressure,

∇P_o is the gradient of pressure for the oil phase

This set of equations is non-linear as the k_{rw}, k_{ro} and P_c terms are all functions of phase saturation, S_w, which is itself controlled by the flow rates. Thus, in order to solve these equations for a given set of initial and boundary conditions, numerical codes (reservoir simulators) are used, in which saturation-dependent functions for k_{rw}, k_{ro} and P_c are given as input, and an iterative numerical recipe is used to estimate saturation and pressure. Figure 4.5 shows a typical set of oil-water relative permeability curves with the endpoint terminology.

Note that the total fluid mobility is <1 (mobility is the permeability/viscosity ratio for the flowing phase). That is, the permeability of a rock containing more than one phase is significantly lower than a rock with only one phase. Clearly the fluid viscosity is a key factor but the fluid-fluid interactions also play a role. The functions are drawn between 'endpoints,' which are a mathematical convenience, but are also based on physical phenomena – the point at which the flow rate of one phase becomes insignificant. However, the endpoint values themselves are not physically fixed. For example, there exists a measurable irreducible water saturation, but its precise value depends on many things (e.g. oil phase pressure or temperature). Many of the problems and errors in upscaling

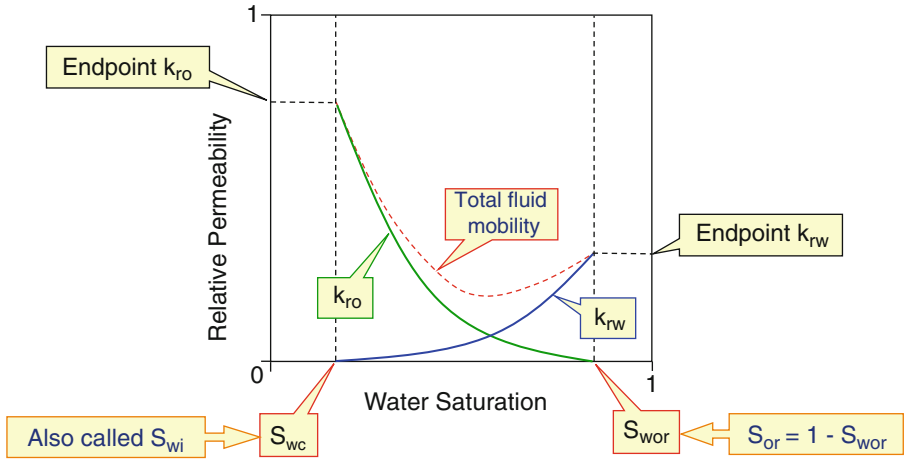

Fig. 4.5 Example oil-water relative permeability functions

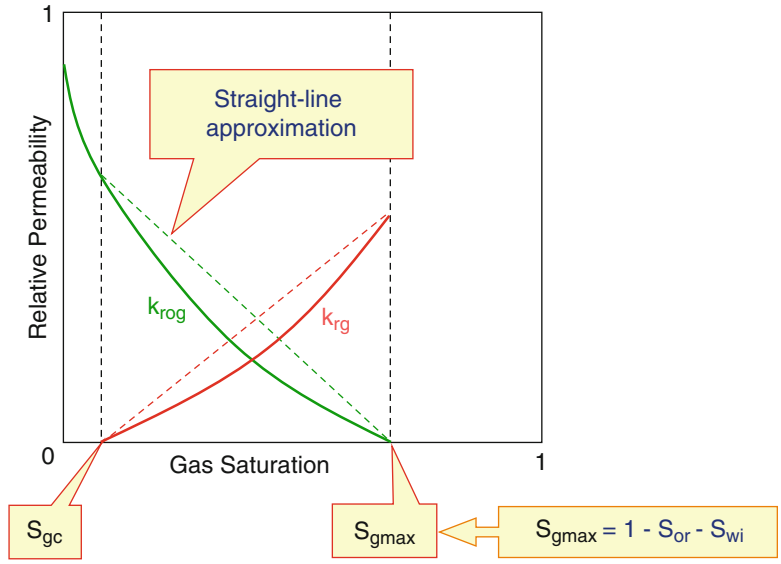

Fig. 4.6 Example gas-oil relative permeability functions

arise from poor treatment or understanding of these endpoints.

The most common functions used for relative permeability are the Corey exponent functions:

$$k_{ro} = A(1 - S_{wn})^x \tag{4.6}$$

$$k_{rw} = B(S_{wn})^y \tag{4.7}$$

where S_{wn} is the normalized saturation:

$$S_{wn} = (S_w - S_{wc})/(S_{wor} - S_{wc}) \tag{4.8}$$

Typical values for a water-wet light oil might be:

$$k_{ro} = 0.85(1 - S_{wn})^3 \text{ and } k_{rw} = 0.3(S_{wn})^3 \tag{4.9}$$

A similar set of functions can be used to describe a gas-oil system (Fig. 4.6), where the functions are bounded by the critical gas saturation, S_{gc}, and the maximum gas saturation, S_{gmax}. However, gas-oil relative permeability curves tend to have less curvature (lower Corey exponents) and sometimes straight-line functions

are assumed, implying perfect mixing or a fully-miscible gas-oil system.

These functions describe the flows and pressures for multi-phase flow. The third equation required to completely define a two-phase flow system is the capillary pressure equation. For the general case (any fluid pair):

$$P_c = P_{\text{non-wetting phase}} - P_{\text{wetting-phase}} \quad [P_c = f(S)] \qquad (4.10)$$

Capillary pressure, P_c, is a function of phase saturation, and must be defined by a set of functions. The capillary pressure curve is a summary of fluid-fluid interactions, and for any element of rock gives the average phase pressures for all the fluid-fluid contacts within the porous medium at a given saturation. For an individual pore, P_c can be related to measurable geometries (curvatures) and forces (interfacial tension), and defined theoretically – but for a real porous medium it is an average property. Figure 4.7 shows some example measured Pc curves, based on mercury intrusion experiments (Neasham 1977).

The slope of the P_c curve is related to the pore size distribution. More uniform pore-size distributions have a fairly flat function (as for the 1,000 mD curve in Fig. 4.7), while highly variable pore size distributions have a gradually rising function (as with the 50 mD curve in Fig. 4.7). The capillary entry pressure is a function of the largest accessible pore. Different P_c curves are followed for drainage (oil invasion) and imbibition (waterflood) processes.

We summarise our introduction by noting that the complexities of multi-phase flow boil down to a set of rules governing how two or more phases interact in the porous medium. Figure 4.8 shows an example micro-model (an artificial etched-glass pore space network) in which fluid phase distributions can be visualised. Even for this comparatively simple pore space, the number and nature of the fluid-fluid and fluid-solid interfaces is bewildering. What determines whether gas, oil or water will invade the next available pore as the pressure in one phase changes?

One response – the modelling approach – is that good answers to this problem are found in mathematical modelling of pore networks (e.g. McDougall and Sorbie 1995; Blunt 1997; Øren and Bakke 2003; Behbahani and Blunt 2005).

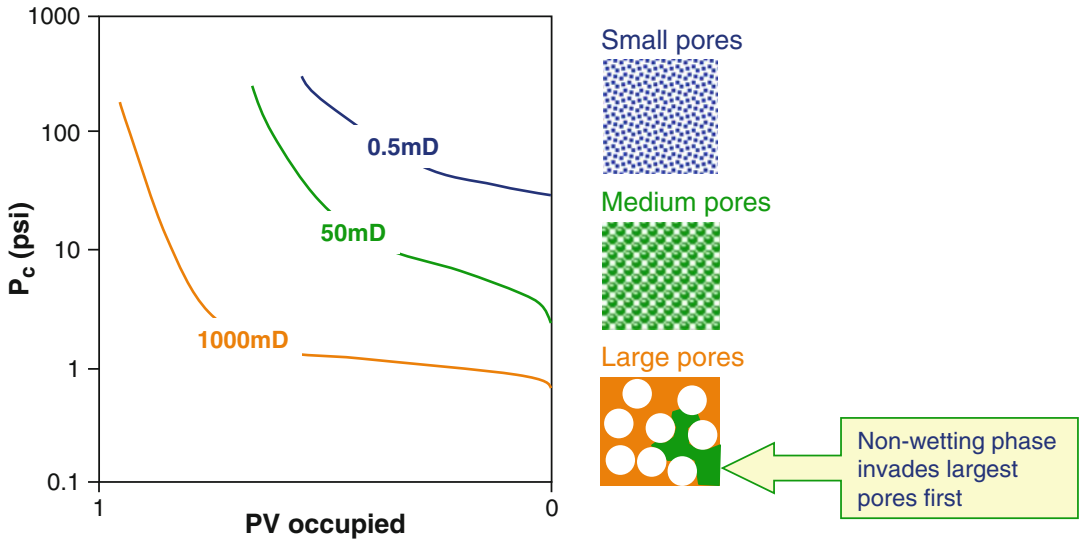

Fig. 4.7 Example capillary pressure functions: capillary drainage curves based on mercury intrusion experiments measuring the non-wetting phase pressure required to invade a certain pore volume (PV)

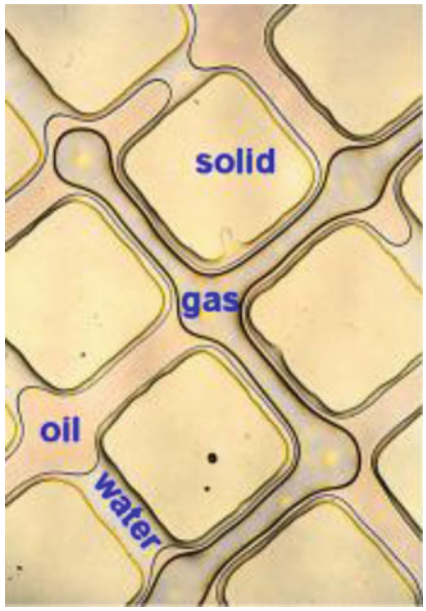

Fig. 4.8 Example micro-model, where fluid distributions are visualised within an artificial laboratory pore-space (Statoil archive image of micromodel experiment conducted at Heriot Watt University)

Another response – the laboratory approach – is that you need to measure the multiphase flow behaviour in real rock samples at true reservoir conditions (pressures and temperatures). In reality, you need both measurements and modelling to obtain a good appreciation of the "rules" governing multiphase flow. Our concern here is to understand how to handle and upscale these functions within the reservoir model.

4.2.2 Two-Phase Steady-State Upscaling Methods

Multiphase flow upscaling, involves the process of calculating the large-scale multiphase flows given a known distribution of the small-scale petrophysical properties and flow functions. There are many methods for doing this, but it is useful to differentiate two:

1. Dynamic methods
2. Steady-state methods

Fuller discussions of these methods are found in, for example, Barker and Thibeau (1997), Ekran and Aasen (2000), Pickup et al. (2005).

Reservoir simulators generally perform *dynamic* multi-phase flow simulations – that is, the pressures and saturations are allowed to vary with position and time in the simulation grid. The Kyte and Berry (1975) upscaling method is the most well-known dynamic two-phase upscaling method, but there have been many alternatives proposed, such as Stone's (1991) method and Todd and Longstaff (1972) for miscible gas. The strength of the dynamic methods is that they attempt to capture the '*true*' flow behaviour for a given set of boundary conditions. Their principle weaknesses are that they can be difficult and time-consuming to calculate and can be plagued by numerical errors.

In contrast, the steady-state methods are easier to calculate and understand and represent ideal multi-phase flow behaviour. There are three steady-state end-member assumptions:

- *Viscous limit* (VL): The assumption that the flow is steady state at a given, constant fractional flow. Capillary pressure is assumed to be zero.
- *Capillary equilibrium* (CE): The assumption that the saturations are completely controlled by capillary pressure. Applied pressure gradients are assumed to be zero or negligible.
- *Gravity-Capillary equilibrium* (GCE): Similar to CE, except that in addition the saturations are also controlled by the effect of gravity on the fluid density difference. Note that GCE is similar to the vertical equilibrium (VE) assumption also applied in reservoir simulation (Coats et al. 1971), except that VE assumes negligible capillary pressure.

The viscous limit assumption is similar to a steady-state core flood experiment which is sometimes used in core analysis of multi-phase flow (referred to as special core analysis, or SCAL). Here, a known and constant fraction of oil and water is injected into the sample (let us say 20 % oil and 80 % water) and the permeability for each phase is calculated from the pressure drop and flow rate for that phase. The procedure

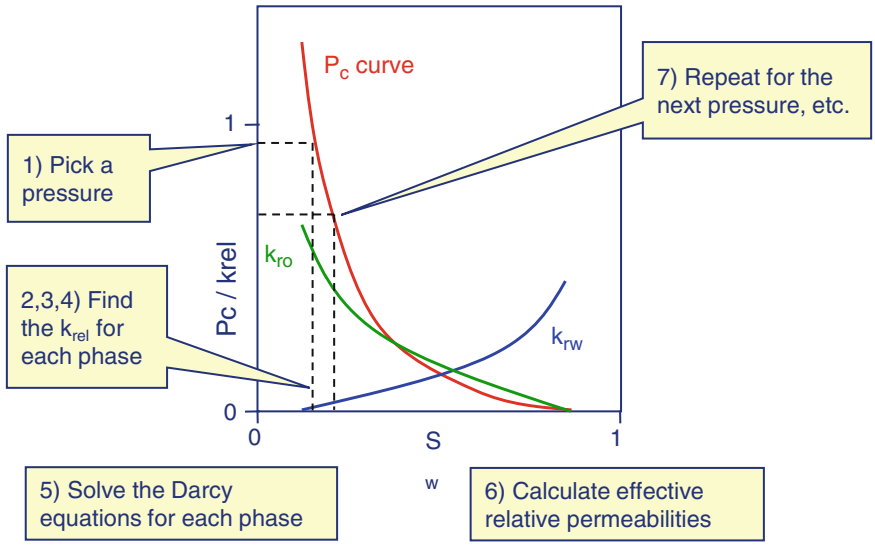

Fig. 4.9 Illustration of the capillary equilibrium steady-state upscaling method

is then repeated for a different fractional flow, and so on. It is assumed that capillary pressure and gravity have no effect. The method can be assumed to apply for a Darcy-flow-dominated two-phase flow system. The method is considered to be valid at larger length-scales, where capillary forces can generally be neglected (e.g. for model grid cell sizes greater than about 1 m vertically).

For the capillary equilibrium steady state assumption it is the Darcy flow effects that are neglected and all fluxes are deemed to be controlled by the capillary pressure curve. For a given pressure, the saturation is known from the P_c curve and the local phase permeability is then determined from the relative permeability curves. The calculation is then repeated for each chosen decrement of pressure until the saturation range is covered (Fig. 4.9). The method is considered to be valid at smaller length-scales, where capillary forces are likely to dominate (e.g. at length-scales less than about 0.2 m). There is also a rate-dependence for viscous and capillary forces – higher flow rates favour viscous forces while lower flow rates favour capillary forces. Note that layering in sedimentary rock media is often at the mm to cm scale

Fig. 4.10 SEM image of laminae in an aeolian sandstone (Image courtesy of British Gas)

(Fig. 4.10), and therefore capillary forces are likely to be important at this length-scale.

The gravity-capillary equilibrium method uses the same principle as the CE method except that vertical pressure gradient is also

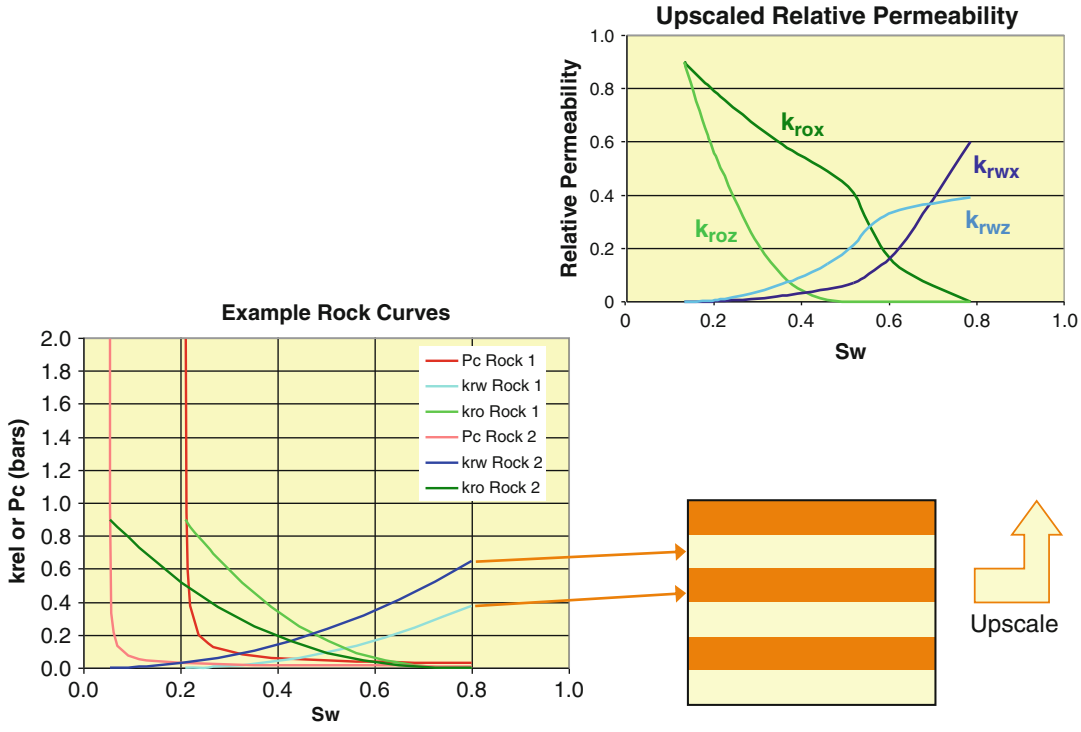

Fig. 4.11 Capillary equilibrium steady-state upscaling method applied to a simple layered model

applied resulting in a vertical trend in the saturation at any chosen pressure reference. The GCE solution should tend towards the CE solution as the length-scale becomes increasingly small.

All three steady-state methods involve a series of independent single-phase flow calculations and therefore can employ a standard single-phase pressure solver algorithm. The methods can therefore be rapidly executed on standard computers.

The capillary equilibrium method can be easily calculated for a simple case, as illustrated in Figure 4.11 by an example set input functions for a regular layered model. Upscaled relative permeability curves for this simple case can be calculated analytically (using a spreadsheet or calculator). The method uses the following steps (refer to Fig. 4.9):

1. Chose a value for pressure, P_{c1};
2. Find the corresponding saturation value, S_{w1};
3. Determine the relative permeability for oil and water for each rock type, k_{ro1}, k_{rw1}, k_{ro2}, k_{rw2};
4. Find the phase permeabilities, e.g. $k_{o1} = k_1 * k_{ro1}$;
5. Calculate the upscaled permeability for each direction and for each phase using the arithmetic and harmonic averages;
6. Invert back to upscaled relative permeability, e.g. $k_{ro1} = k_{o1}/k_{upscaled}$ (once again the arithmetic and harmonic averages are used to obtain the upscaled absolute permeability);
7. Repeat for next value pressure, P_{c2}.

Note that the upscaled curves are highly anisotropic, and in fact sometimes lie outside the range of the input curves. This is because of the effects of capillary forces – specifically capillary trapping when flowing across layers. Capillary forces result in preferential imbibition of water (the wetting phase) into the lower permeability layers, making flow of oil (the non-wetting phase) into these low permeability layers even more difficult.

These somewhat non-intuitive effects of capillary pressure in laminated rocks can be demonstrated experimentally (Fig. 4.12). In the case of two-phase flow across layers in a water-wet

laminated rock – a cross-bedded aeolian sandstone (Fig. 4.10), oil becomes trapped in the high permeability layers upstream of low permeability layers due to water imbibition into the lower permeability layers (Huang et al. 1995).

The chosen flow rate for this experiment was at typical reservoir waterflood rate (around 0.1 m/day). This trapped oil can be mobilised either by reducing the capillary pressure (e.g. by modifying the interfacial tension by use of surfactant chemicals) or by increasing the flow rate, and thereby the viscous forces. Alternatively, a modified flow strategy favouring flow along the rock layers (parallel to bedding) would result in less capillary trapping and a more efficient waterflood. In the more general case, where the rock has variable wettability the effects of capillary/viscous interactions become more complex (e.g. McDougall and Sorbie 1995; Huang et al. 1996; Behbahani and Blunt 2005).

Exercise 4.1

Permeability upscaling for a simple layered model.

The simple repetitive layered model shown in Fig. 4.11 can be used to illustrate single and multi-phase permeability upscaling using the "back of the envelope" maths. We assume the two layers are regular and of equal thickness. Rock type 1 has a permeability of 100md and rock type 2 has a permeability of 1,000md.

(a) Calculate the upscaled horizontal and vertical single-phase permeability using averaging.

(b) Calculate selected values for the upscaled two-phase relative permeability curves, assuming steady-state capillary equilibrium conditions. Use the flow functions shown in Fig. 4.11, as tabulated below, with water saturation, S_w; relative permeability to water, krw; relative permeability to oil, krow; capillary pressure, P_c (bars). Choose P_c values of 0.05 and 0.3 (shown in bold).

Table for rock type 1 (100 mD)				Table for rock type 2 (1,000 mD)			
Sw	krw	krow	Pc	Sw	krw	krow	Pc
0.2092	0.0	0.9	10.0	0.05432	0.0	0.9	10.0
0.209791	0.0000004	0.897752	2.744926	0.055066	0.0	0.897752	0.976926
0.212154	0.000009	0.888792	0.938248	0.058048	0.000016	0.888792	0.333925
0.215108	0.000038	0.877668	0.590923	**0.059**	**0.000023**	**0.887**	**0.3**
0.221016	0.000151	0.855673	0.372172	0.061777	0.000065	0.877668	0.210311
0.226	**0.0003**	**0.839**	**0.3**	0.069234	0.000259	0.855673	0.132457
0.238740	0.000943	0.791683	0.201984	0.091604	0.001618	0.791683	0.071887
0.256464	0.002413	0.730655	0.147628	0.113974	0.004141	0.730655	0.052541
0.26828	0.003771	0.691590	0.127213	**0.119**	**0.005**	**0.718**	**0.05**
0.32736	0.015084	0.515190	0.080120	0.128888	0.006471	0.691590	0.045275
0.38644	0.033939	0.368967	0.061135	0.203456	0.025884	0.515190	0.028515
0.44552	0.060336	0.250969	0.050461	0.278024	0.058239	0.368967	0.021758
0.449	**0.062**	**0.245**	**0.05**	0.352592	0.103536	0.250969	0.017959
0.5046	0.094275	0.159099	0.043483	0.42716	0.161775	0.159099	0.015476
0.56368	0.135756	0.091074	0.038504	0.501728	0.232956	0.091074	0.013704
0.62276	0.184779	0.044366	0.034742	0.576296	0.317079	0.044366	0.012365
0.68184	0.241344	0.016099	0.031781	0.650864	0.414144	0.016100	0.011311
0.74092	0.305451	0.002846	0.029380	0.725432	0.524151	0.002846	0.010456
0.8	0.3771	0.000000	0.027386	0.8	0.6471	0.000000	0.009747

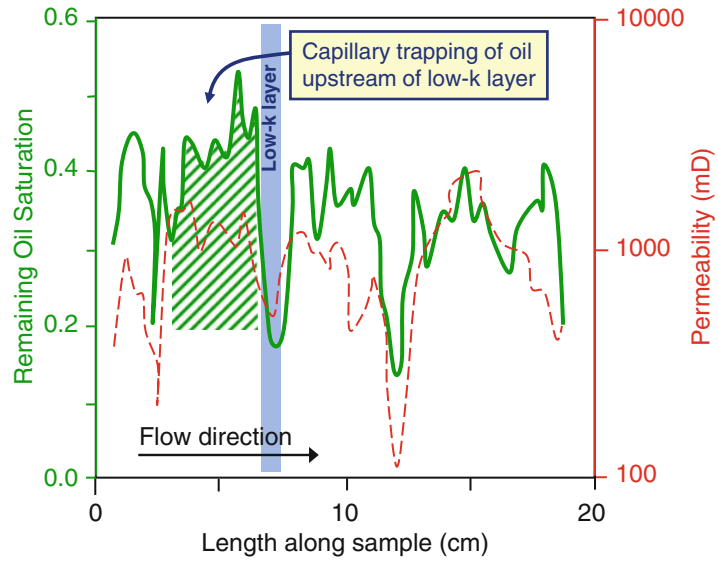

Fig. 4.12 Summary of a waterflood experiment across a laminated water-wet rock sample (Redrawn from Huang et al. 1995, ©1995, Society of Petroleum Engineers Inc., reproduced with permission of SPE. Further reproduction prohibited without permission)

4.2.3 Heterogeneity and Fluid Forces

It is important to relate these multi-phase fluid flow processes to the heterogeneity being modelled. This is a fairly complex issue, and fundamental to what reservoir model design is all about. As a way in to this topic we use the *balance of forces* concept to give us a framework for understanding which scales most affect a particular flow process. For example, we know that capillary forces are likely to be important for rocks with strong permeability variations at the small scale (less than 20 cm scale is a good rule of thumb).

Figure 4.13 shows a simple sketch of the end-members of the fluid force system. We have three end members: gravity-, viscous- and capillary-dominated. Reality will lie somewhere within the triangle, but appreciation of the end-member systems is useful to understand the expected flow-heterogeneity interactions. Note, that for the same rock system the flow behaviour will be completely different for a gravity-dominated, viscous-dominated or capillary-dominated flow regime. The least intuitive is the capillary-dominated case where water (for a water-wet system) imbibes preferentially into the lower permeability layers.

To treat this issue more formally, we use scaling group theory (Rapoport 1955; Li and Lake 1995; Li et al. 1996; Dengen et al. 1997) to understand the balance of forces. The viscous/capillary ratio and the gravity/capillary ratio are two of a number of dimensionless scaling group ratios that can be determined to represent the balance of fluid forces. For example, for an oil-water system we can define the following force ratios:

$$\frac{Viscous}{Capillary} = \frac{u_x \Delta x \mu_o}{k_x (dP_c/dS)} \tag{4.11}$$

$$\frac{Gravity}{Capillary} = \frac{\Delta\rho\, g\, \Delta z}{(dP_c/dS)} \tag{4.12}$$

where,

Δx, Δz are system dimensions,

u_x is fluid velocity,

μ_o is the oil viscosity,

k_x is the permeability in the x direction,

(dP_c/dS) is the slope of the capillary pressure function,

$\Delta\rho$ is the fluid density difference and g is the constant due to gravity.

The viscous/capillary ratio is essentially a ratio of Darcy's law with a capillary pressure

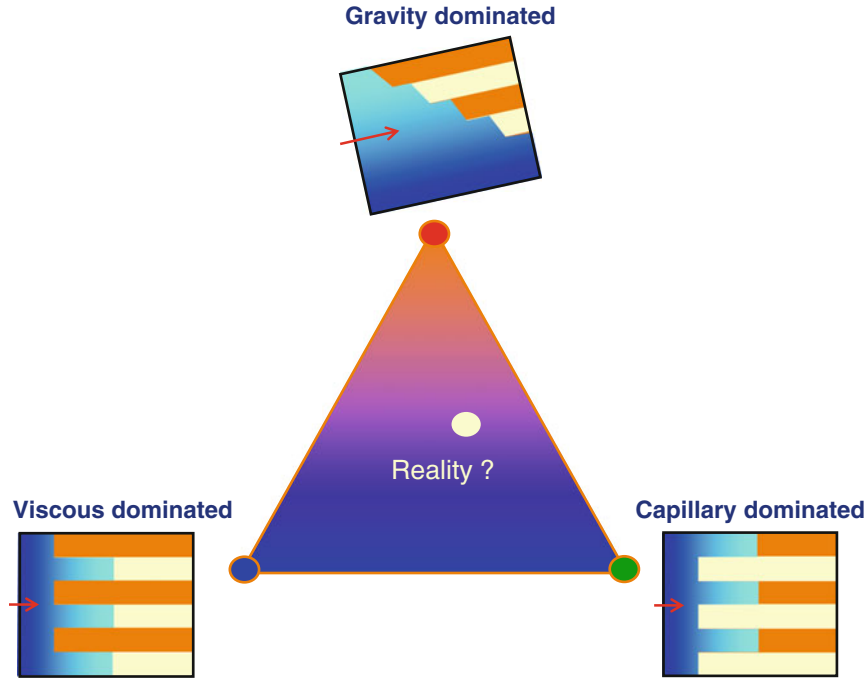

Fig. 4.13 The fluid forces triangle with sketches to illustrate how a water-flood would behave for a layered rock (*yellow* = high permeability layers)

gradient term, while the gravity/capillary ratio is the buoyancy term against the capillary pressure gradient. Δx and Δz represent the physical length scales – essentially the size of the model in the x and z directions. There are several different forms of derivation of these ratios depending on the physical assumptions and the mathematical approach, but the form given above should allow the practitioner to gain an appreciation of the factors involved. It is important that a consistent set of units are used to ensure the ratios remain dimensionless.

For example, a calculation to determine when capillary/heterogeneity interactions are important can be made by studying the ratio of capillary to viscous forces. Figure 4.14 shows a reference well pair assuming 1 km well spacing and a 150 psi pressure drawdown at the producing well. We are interested in the balance of forces and a rock unit within the reservoir, represented by alternating permeability layers with a spacing of Δx. Figure 4.15 shows the result of the analysis of the viscous/capillary

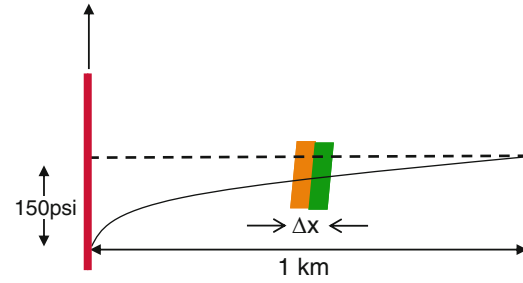

Fig. 4.14 Sketch of pressure drawdown between an injection and production well pair for water-flooding an oil reservoir

ratio for different layer contrasts and heterogeneity length-scales (Ringrose et al. 1996).

If the layering in a reservoir occurs at the >10 m scale then viscous forces tend to dominate (or the Viscous/Capillary ratio must be very low for capillary forces to be significant at this scale). However, if the layers are in the mm-to-cm range then capillary forces are much more likely to be important (or the Viscous/Capillary ratio must be

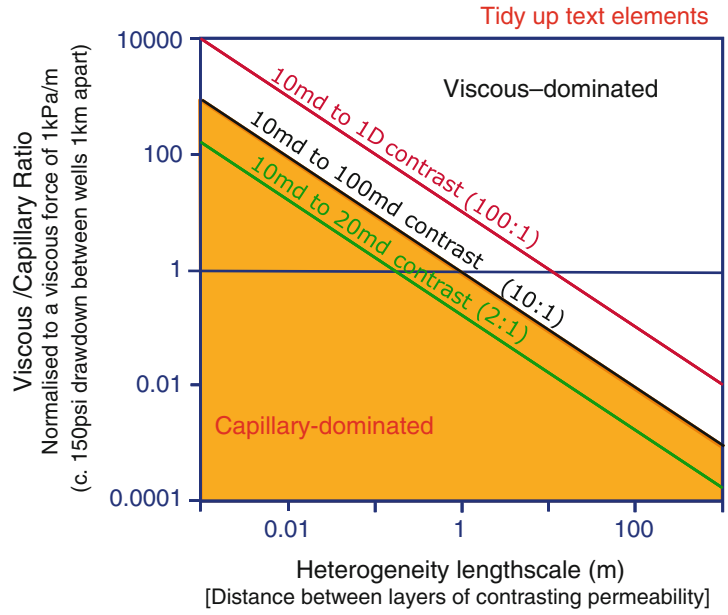

Fig. 4.15 Example calculation of the viscous/capillary ratio for a layered system as a function of length scale, for selected permeability contrasts (Redrawn from Ringrose et al. 1996, ©1996, Society of Petroleum Engineers Inc., reproduced with permission of SPE. Further reproduction prohibited without permission)

very high to override capillary effects). Note, however, that the pressure gradients will vary as a function of spatial position and time and so in fact the Viscous/Capillary ratio will vary – viscous forces will be high close to the wells and lower in the inter-well region.

An important and related concept is the capillary number, most commonly defined as:

$$C_a = \frac{\mu q}{\gamma} \tag{4.13}$$

where μ is the viscosity, q is the flow rate and γ is the interfacial tension.

This is a simpler ratio of the viscous force to the surface tension at the fluid-fluid interface. Capillary numbers around 10^{-4} or lower are generally deemed to be capillary-dominated.

4.3 Multi-scale Geological Modelling Concepts

4.3.1 Geology and Scale

The importance of multiple scales of heterogeneity for petroleum reservoir engineering has been recognised for some time. Haldorsen and Lake (1984) and Haldorsen (1986) proposed four conceptual scales associated with averaging properties in porous rock media:

- Microscopic (pore-scale);
- Macroscopic (representative elementary volume above the pore scale);
- Megascopic (the scale of geological heterogeneity and or reservoir grid blocks);
- Gigascopic (the regional or total reservoir scale).

Weber (1986) showed how common sedimentary structures including lamination, clay drapes and cross-bedding affect reservoir flow properties and Weber and van Geuns (1990) proposed a framework for constructing geologically-based reservoir models for different depositional environments. Corbett et al. (1992) and Ringrose et al. (1993) argued that multi-scale modelling of water-oil flows in sandstones should be based on a hierarchy of sedimentary architectures, with smaller scale heterogeneities being especially important for capillary-dominated flow processes (see Sect. 2.3.2.2 for an introduction to hierarchy). Campbell (1967) established a basic hierarchy of sedimentary features related to fairly universal processes of

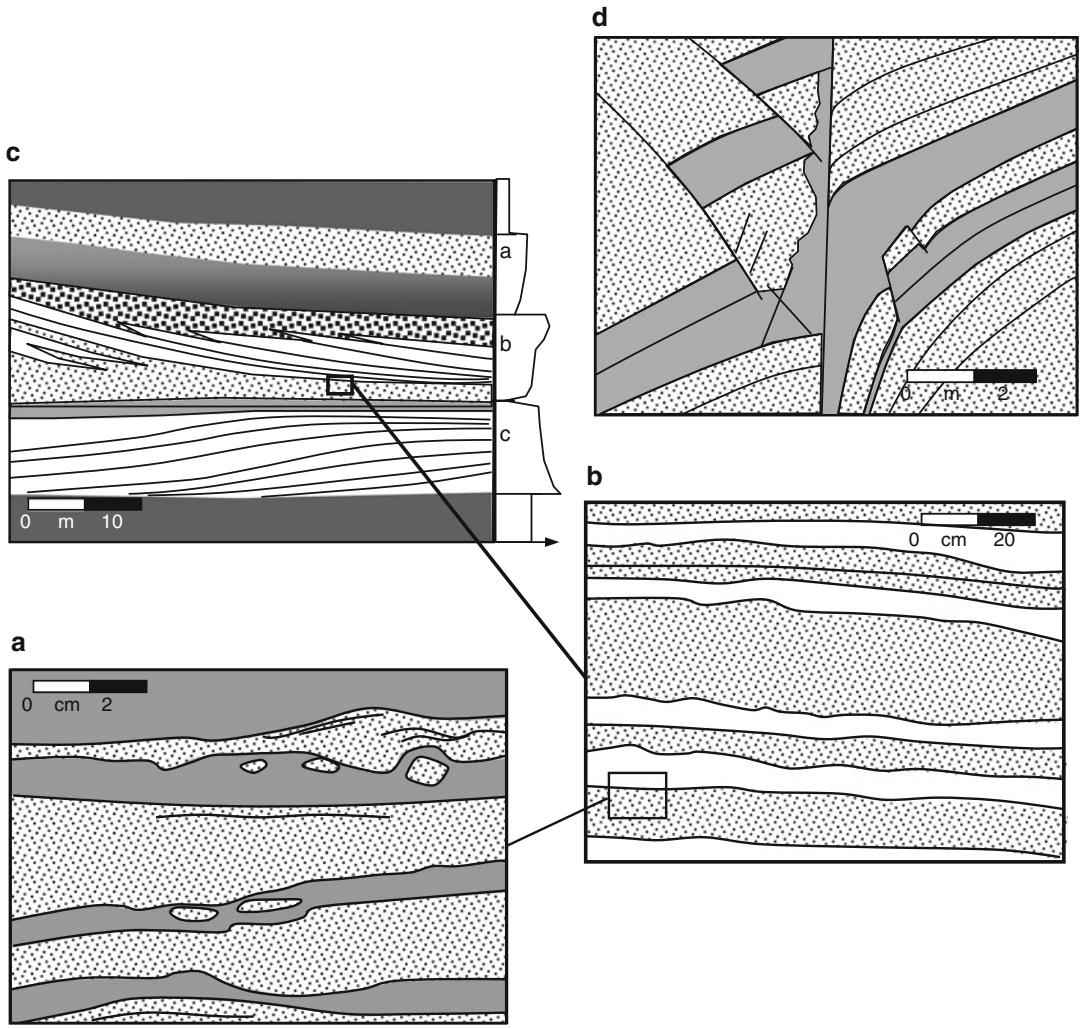

Fig. 4.16 Field outcrop sketches illustrating multi-scale reservoir architecture
(**a**) Sandstone and siltstone lamina-sets from a weakly-bioturbated heterolithic sandstone
(**b**) Sandy and muddy bed-sets in a tidal deltaic lithofacies
(**c**) Prograding sedimentary sequences from a channelized tidal delta
(**d**) Fault deformation fabric around a normal fault through an inter-bedded sandstone and silty clay sequence (Redrawn from Ringrose et al. 2008, The Geological Society, London, Special Publications 309 © Geological Society of London [2008])

deposition, namely lamina, laminasets, beds and bedsets. Miall (1985) showed how the range of sedimentary bedforms can be defined by a series of bounding surfaces from a 1st order surface bounding the laminaset to 4th (and higher) order surfaces bounding, for example, composite point-bars in fluvial systems.

Figure 4.16 illustrates the geological hierarchy for a heterolithic sandstone reservoir. Lamina-scale, lithofacies-scale and sequence-stratigraphic scale elements can be identified. In addition to the importance of correctly describing the sedimentary length scales, structural (Fig. 4.16d) and diagenetic processes act to modify the primary depositional fabric.

At the most elemental level we are interested in the pore scale (Fig. 4.17) – the rock pores that contain fluids and determine the multi-phase flow

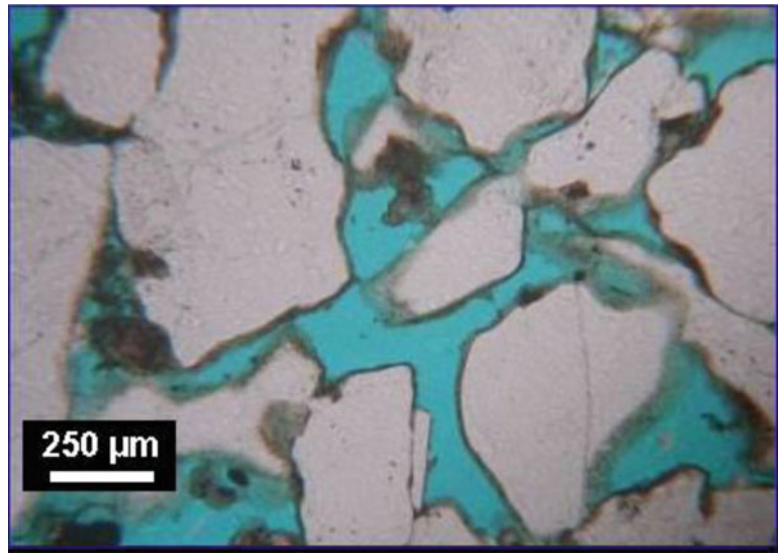

Fig. 4.17 The pore scale – example thin section of pores in a sandstone reservoir (Statoil image archive, © Statoil ASA, reproduced with permission)

behaviour. Numerical modelling at the pore scale has been widely used to better understand permeability, relative permeability and capillary pressure behaviour for representative pore systems (e.g. Bryant and Blunt 1992; Bryant et al. 1993; McDougall and Sorbie 1995; Bakke and Øren 1997; Øren and Bakke 2003). Most laboratory analysis of rock samples is devoted to measuring pore-scale properties – resistivity, acoustic velocity, porosity, permeability, and relative permeability. Pore-scale modelling allows these measured flow properties to be related to fundamental rock properties such as grain size, grain sorting and mineralogy. However, the application of pore-scale measurements and models in larger-scale reservoir models requires *a framework for assigning pore-scale properties* to the geological concept. We do this by assigning flow properties to lamina-scale, lithofacies-scale or stratigraphic-scale models. This can be done quite loosely, with weak assumptions, or systematically within a multi-scale upscaling hierarchy.

Statistical methods for representing the spatial architecture of geological systems were covered in Chap. 2. What concerns us here is how we integrate geological models within a multi-scale hierarchy. This may require a re-evaluation of the scales of models needed to address different scale transitions.

Pixed-based modelling approaches (e.g. SGS, SIS) can be applied at pretty-much any scale, whereas object-based modelling approaches will tend to have very clear associations with pre-defined length scales. In both cases the model grid resolution needs to be fine enough to explicitly capture the heterogeneity being represented in the model. Process-based modelling methods (e.g. Rubin 1987; Wen et al. 1998; Ringrose et al. 2003) are particularly appropriate for capturing the effects of small-scale geological architecture within a multi-scale modelling framework.

In the following sections we look at some key questions the reservoir modelling practitioner will need to address in building multi-scale reservoir models:

1. How many scales to model and upscale?
2. Which scales to focus on?
3. How to best construct model grids?
4. Which heterogeneities matter most?

4.3.2 How Many Scales to Model and Upscale?

Despite the inherent complexities of sedimentary systems, dominant scales and scale transitions can be identified (Fig. 4.18). These dominant scales

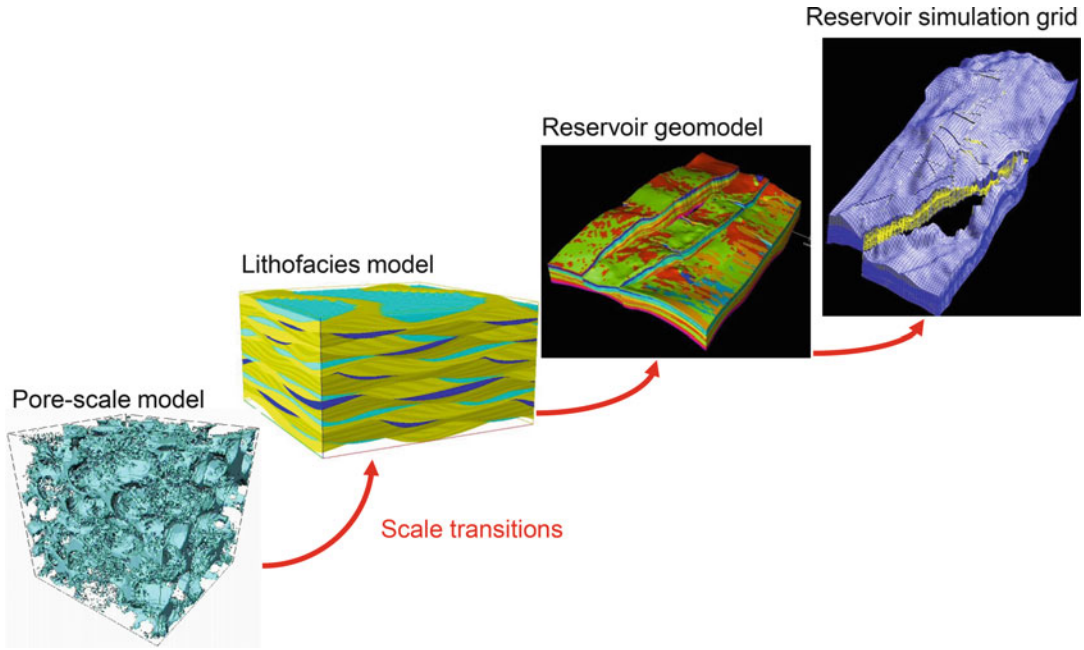

Fig. 4.18 Examples of geologically-based reservoir simulation models at four scales
(**a**) Model of pore space used as the basis for multi-phase pore network models (50 μm cube);
(**b**) Model of lamina-sets within a tidal bedding facies (dimensions 0.05 m × 0.3 m × 0.3 m);
(**c**) Facies architecture model from a sector of the Heidrun field showing patterns of tidal channel and bars (dimensions 80 m × 1 km × 3 km);
(**d**) Reservoir simulation grid for part of the Heidrun field illustrating grid cells displaced by faults in true structural position (dimensions 200 m × 3 km × 5 km)
(Statoil image archives, © Statoil ASA, reproduced with permission)

are based both on the nature of rock heterogeneity and the principles which govern macroscopic flow properties. In this discussion, we assume four scales – pore, lithofacies, geomodel and reservoir. This gives us three scale transitions:

1. *Pore to lithofacies*. Where a set of pore-scale models is applied to models of lithofacies architecture to infer representative or typical flow behaviour for that architectural element. The lithofacies is a basic concept in the description of sedimentary rocks and presumes an entity that can be recognised routinely. The lamina is the smallest sedimentary unit, at which fairly constant grain deposition processes can be associated with a macroscopic porous medium. The lithofacies comprises some recognisable association of laminae and lamina sets. In certain cases, where variation between laminae is small, pore-scale models could be applied directly to the lamina-set or bed-set scales.
2. *Lithofacies to geomodel*. Where a larger-scale geological concept (e.g. a sequence stratigraphic model, a structural model or a diagenetic model) postulates the spatial arrangement of lithofacies elements. Here, the geomodel is taken to mean a geologically-based model of the reservoir, typically resolved at the sequence or zone scale.
3. *Geomodel to reservoir simulator*. This stage may often only be required due to computational limitations, but may also be important to ensure good transformation of a geological model into 3-dimensional grid optimised for flow simulation (e.g. within the constraints of finite-difference multiphase flow simulation). This third step is routinely taken by practitioners, whereas steps 1 and 2 tend to be neglected.

Features related to structural deformation (faults, fractures and folds) occur at a wide range of scales (Walsh et al. 1991; Yielding et al. 1992) and do not naturally fall into a

step-wise upscaling scheme. Structural features are typically incorporated at the geomodel scale. However, effects of smaller scale faults may also be incorporated as effective properties (as transmissibility multipliers) using upscaling approaches. The incorporation of fault transmissibility into reservoir simulators is considered thoroughly by Manzocchi et al (2002). Conductive fractures may also affect sandstone reservoirs, and are often the dominant factor in carbonate reservoirs. Approaches for multi-scale modelling of fractured reservoirs have also been developed (e.g. Bourbiaux et al. 2002) and will be developed further in Chap. 6.

Historical focus over the last few decades has been on including increasingly more detail into the geomodel, with only one upscaling step being explicitly performed. Full-field geomodels are typically in the size range of 1–10 million cells with horizontal cell sizes of 50–100 m and vertical cell sizes of order 1–10 m. Multi-scale modelling allows for better flow unit characterization and improved performance predictions (e.g. Pickup et al. 2000; Scheiling et al. 2002). There are also examples where a large number of grid cells are applied to sector or near-well models reducing cell sizes to the dm-scale. Upscaling of the near-well region requires methods to specifically address radial flow geometry (e.g. Durlofsky et al. 2000).

Recent focus on explicit small-scale lithofacies modelling includes the use of million cell models with mm to cm size cells (e.g. Ringrose et al. 2003; Nordahl et al 2005). Numerical pore-scale modelling employs a similar number of network nodes at the pore scale (e.g. Øren and Bakke 2003). Model resolution is always limited by the available computing power, and although continued efficiencies and memory gains are expected in the future, the use of available numerical discretisation at several scales within a hierarchy is preferred to efforts to apply the highest possible resolution at one of the scales (typically the geomodel). There is also an argument that advances in seismic imaging coupled with computing power will enable direct geological modelling at the seismic resolution scale. However, even when this is possible, seismic-based lithology prediction (using seismic inversion) will require smaller-scale modelling of the petrophysical properties within the seismically resolved element (see Chap. 2).

Upscaling methods impose further limitations on the value and utility of models within a multi-scale framework. In conventional upscaling – from a geological model to a reservoir simulation grid – there are various approaches used. These cover a range which can be classed in terms of the degree of simplification/complexity:

1. *Averaging of well data directly into the flow simulation grid:* This approach essentially ignores explicit upscaling and neglects all aspects of smaller scale structure and flows. The approach is fast and simple and may be useful for quick assessment of expected reservoir flows and mass balance. It may also be adequate for very homogeneous and highly permeable rock sequences.
2. *Single-phase upscaling only in Δz:* This commonly applied approach assumes a simulation grid designed with the same Δx, the Δy as the geological grid. The approach is often used where complex structural architecture provides very tight constraints to design of the flow modelling grid. Upscaling essentially comprises use of averaging methods but ensures a degree of representation of thin layering or barriers. Also, where seismic data gives a good basis for the geological model in the horizontal dimensions, vertical upscaling of fine-scale layering to the reservoir simulator scale is typically required.
3. *Single-phase upscaling in Δx Δy and Δz:* With this approach multi-scale effective flow properties are explicitly estimated and the upscaling tools are widely available (diagonal tensor or full-tensor methods). Multiphase flow effects are however neglected.
4. *Multi-phase upscaling in Δx Δy and Δz:* This approach represents an attempt to calculate effective multiphase flow properties in larger scale models. The approach has been used rather too seldom due to demands of time and resources. However, the development of steady-state solutions to multiphase flow upscaling problems (Smith 1991; Ekran and Aasen 2000; Pickup and Stephen 2000) has led to wider use in field studies (e.g. Pickup et al 2000; Kløv et al 2003).

These four degrees of upscaling complexity help define the number and dimensions of models required. The number of scales modelled is typically related to the complexity and precision of answer sought. Improved oil recovery (IOR) strategies and reservoir drainage optimisation studies are often the reason for starting a multi-scale approach. A minimum requirement for any reservoir model is that the assumptions used for smaller scale processes (pore scale, lithofacies scale) are explicitly stated.

For example, a typical set of assumptions commonly used might be:

> *We assume that two special core analysis measurements represent all pore-scale physical flow processes and that all effects of geological architecture are adequately summarised by the arithmetic average of the well data.*

Assumptions like these are rarely stated (although often implicitly assumed). More ideally, some form of explicit modelling at each scale should be performed using 3D multiphase upscaling methods. At a minimum, it is recommended to explicitly define pore-scale and geological-scale models, and to determine a rationale for associating the pore-scale with the geological scale, as in the example shown in Fig. 4.18.

4.3.3 Which Scales to Focus On? (The REV)

Geological systems present us with variability at nearly every scale (Fig. 4.19). To some extent they are fractal (Turcotte 1992), showing similar variability at all scales. However, geological systems are more accurately described as *multi-fractal* – showing some scale-independent similarities – but dominated by process-controlled scale-dependent features (e.g. Ringrose 1994). However you describe them, geological systems are complex, and we need an approach for simplifying that complexity and focussing on the important features and length-scales.

The Representative Elementary Volume (REV) concept (Bear 1972) provides the essential framework for understanding measurement scales and geological variability. This concept is fundamental to the analysis of flow in permeable media – without a representative pore space we cannot measure a representative flow property

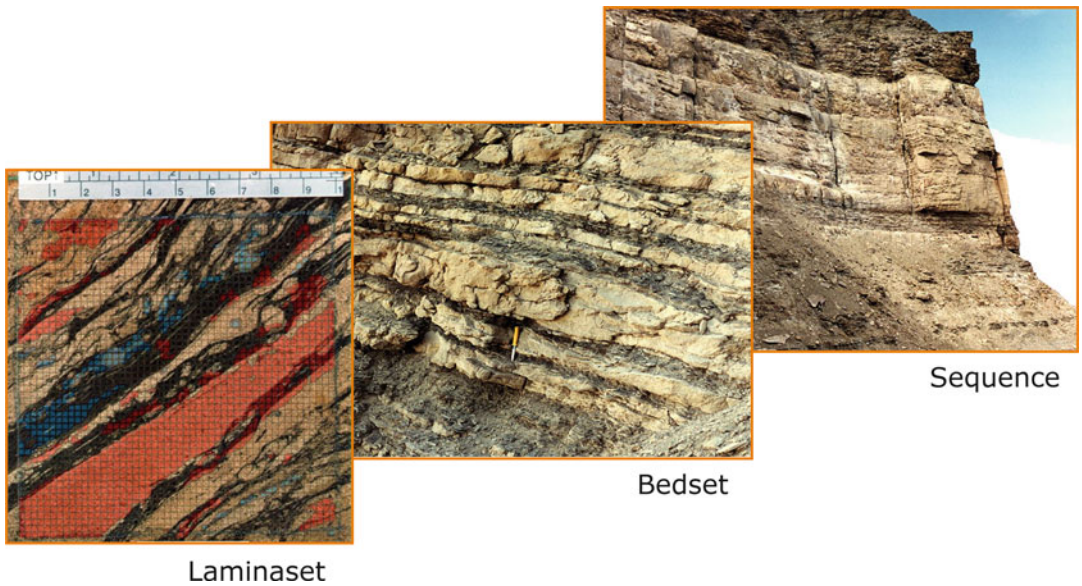

Fig. 4.19 Multi-scale variability in a heterolithic (tidal delta) sandstone system: Laminaset scale: Core photograph with measured permeability (*Red* indicates >1 Darcy); Bedset scale: interbedded sandy and muddy bedsets (hammer for scale); Sequence-stratigraphic scale: Sand-dominated para-sequence between mudstone units (Photos A. Martinius/Statoil © Statoil ASA, reproduced with permission)

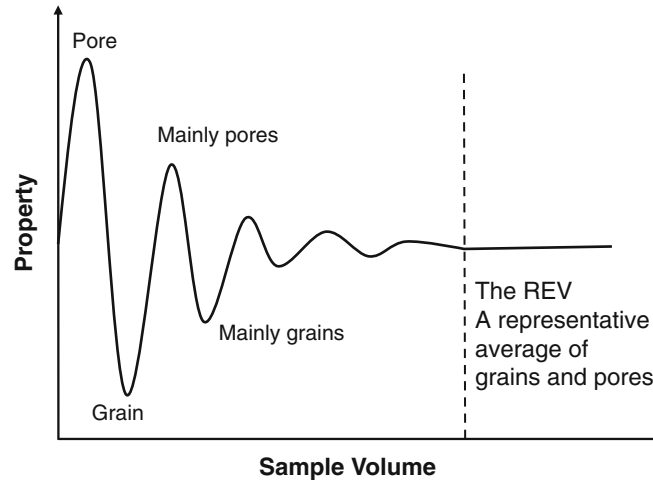

Fig. 4.20 The Representative Elementary Volume (REV) concept, after Bear 1972

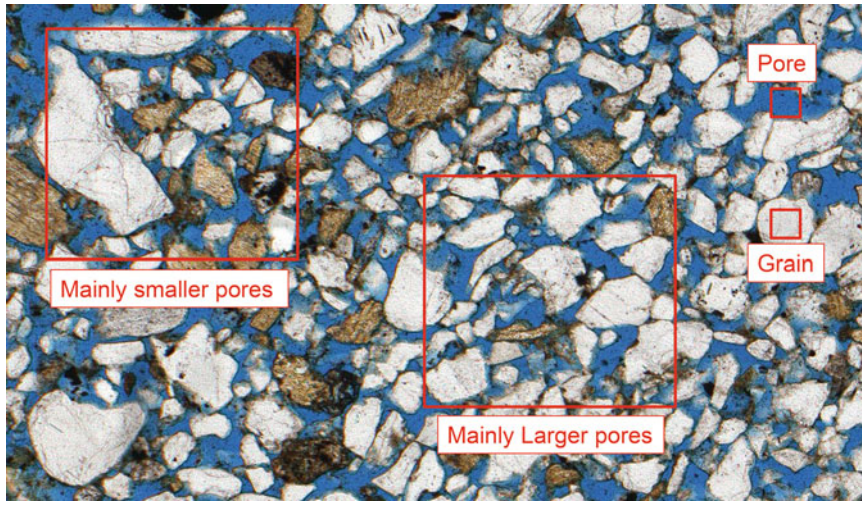

Fig. 4.21 The pore-scale REV illustrated for an example thin section (The whole image is assumed to be the pore-scale REV) (Photo K. Nordahl/Statoil © Statoil ASA, reproduced with permission)

nor treat the medium as a continuum in terms of the physics of flow. The original concept (Fig. 4.20) refers to the scale at which pore-scale fluctuations in flow properties approach a constant value both as a function of changing scale and position in the porous medium, such that a statistically valid macroscopic flow property can be defined, as illustrated in Fig. 4.21.

The pore-scale REV is thus an essential assumption for all reservoir flow properties. However, rock media have several such scales where smaller-scale variations approach a more constant value. It is therefore necessary to develop a multi-scale approach to the REV concept. It is not at first clear how many averaging length-scales exist in a rock medium, or indeed if a REV can be established at the scale necessary for reservoir flow simulation. Despite the challenges, some degree of representativity of estimated flow properties is necessary for flow modelling within geological media, and a multi-scale REV framework is required.

Several workers (e.g. Jackson et al. 2003; Nordahl et al. 2005) have shown that an REV can be established at the lithofacies scale – e.g. at around a length-scale of 0.3 m for tidal

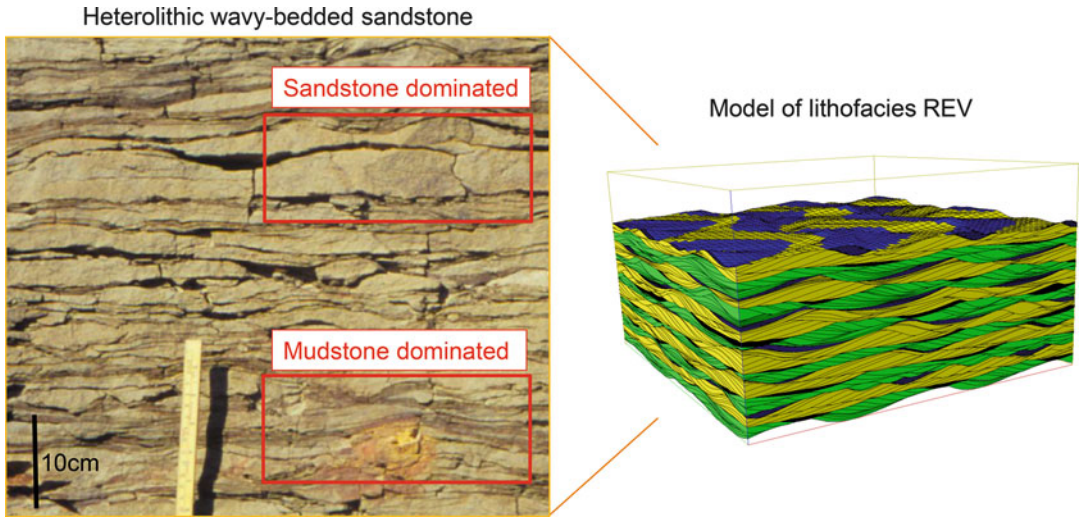

Fig. 4.22 The lithofacies REV illustrated for an example heterolithic sandstone (Photo K. Nordahl/Statoil © Statoil ASA, reproduced with permission)

heterolithic bedding (Fig. 4.22). In fact, the concept of representivity is inherent in the definition of a lithofacies, a recognisable and mappable subdivision of a stratigraphic unit. The same logic follows at larger geological scales, such as the parasequence, the facies association or the sequence stratigraphic unit. Recognisable and continuous geological units are identified and defined by the sedimentologist, and the reservoir modeller then seeks to use these units to define the reservoir modelling elements (*cf* Chap. 2.4).

As a general observation, core plug data is often not sampled at the REV scale and therefore tends to show a wide scatter in measured values, while wire-line log data is often closer to a natural REV in the reservoir system. The true REV – if it can be established – is determined by the geology and not the measurement device. However, wire-line log data usually needs laboratory core data for calibration, which presents us with a dilemma – how should we integrate different scales of measurement?

Nordahl et al. (2005) performed a detailed assessment of the REV for porosity and permeability in a heterolithic sandstone reservoir unit (Fig. 4.23). This example illustrates how apparently conflicting datasets from core plug and wireline measurements can in fact be reconciled within the REV concept. The average and spread of the two datasets differ – the core plugs at a smaller scale record high degree of variability while the wireline data provides a more averaged result at a larger scale. Both sets of data can be integrated into a petrophysical model at the lithofacies REV. Nordahl and Ringrose (2008) extended this concept to propose a multi-scale REV framework (Fig. 4.24), whereby the natural averaging length scales of the geological system can be compared with the various measurement length scales.

Whatever the true nature of rock variability, it is a common mistake to assume that the averaging inherent in any measurement method (e.g. electrical logs or seismic wave inversion) relates directly to the averaging scales in the rock medium. For example, samples from core are often at an inappropriate scale for determining representativity (Corbett and Jensen 1992; Nordahl et al. 2005). At larger scales, inversion of reservoir properties from seismic can be difficult or erroneous due to thin-bed tuning effects. Instead of assuming that any particular measurement gives us an appropriate average, it is much better to relate the measurement to the inherent averaging length scales in the rock system.

So how do we handle the REV concept in practice? The key issue is to find the length-scale (determined by the geology) where the

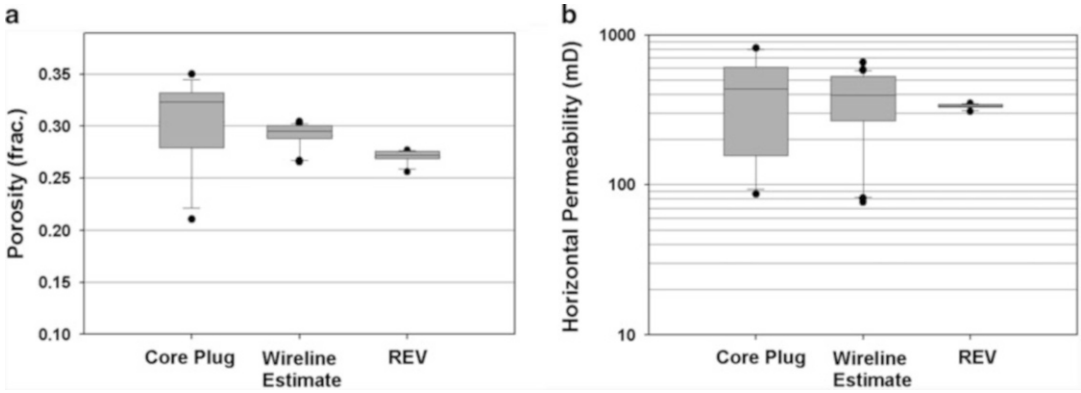

Fig. 4.23 Assessment of the lithofacies REV, from Nordahl et al. (2005). Comparison of porosity (**a**) and horizontal permeability (**b**) estimated or measured from different sources and sample volumes. The lower and upper limits of the box indicate the 25th and the 75th percentile while the whiskers represent the 10th and the 90th percentile. The *solid line* is the median and the *black dots* are the outliers. The values at the REV are measured on the bedding model at a representative scale (With the distribution based on ten realisations) (Redrawn from Nordahl et al. 2005, Petrol Geoscience, v. 11 © Geological Society of London [2005])

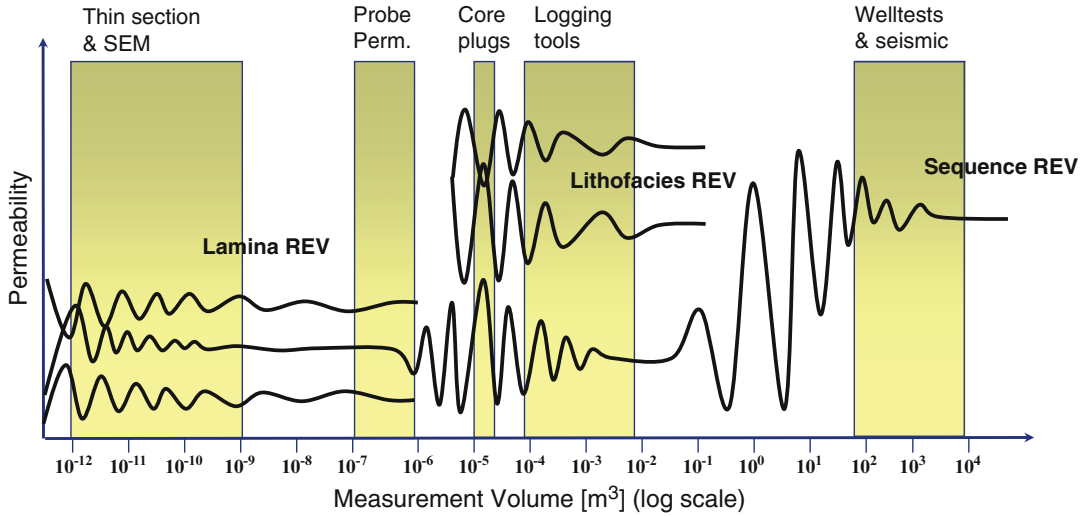

Fig. 4.24 Sketch illustrating multiple scales of REV within a geological framework and the relationship to scales of measurement (Adapted from Nordahl and Ringrose 2008)

measurement or model gives a representative average of the smaller-scale natural variations (Fig. 4.25). At the pore-scale this volume is typically around a few mm^3. For heterogeneous rock systems the REV is of the order of m^3. The challenge is to find the representative volumes for the reservoir system in the subsurface.

4.3.4 Handling Variance as a Function of Scale

Typical practice in petroleum reservoir studies is to assume that an average measured property for any rock unit is valid and that small-scale variability can be ignored. Put more simply, we often assume that the average log-property

Fig. 4.25 Rock sculpture by Andrew Goldsworthy (NW Highlands of Scotland) elegantly capturing the concept of the REV

response for a well through a reservoir interval is the 'right average.' A statistician will know that an arbitrary sample is rarely an accurate representation of the truth. Valid statistical treatment of sample data is an extensive subject treated thoroughly in textbooks on statistics in the Earth Sciences – e.g. Size (1987), Davis (2003), Isaaks and Srivastava (1989) and Jensen et al. (2000).

The challenges involved in correctly inferring permeability from well data are illustrated here using an example well dataset (Fig. 4.26, Table 4.2). This 30 m cored-well interval is from a tidal deltaic reservoir unit with heterolithic lithofacies and moderate to highly variable petrophysical properties (the same well dataset is discussed in detail by Nordahl et al. (2005)).

Table 4.2 compares the permeability statistics for different types of data from this well:

(a) High resolution probe permeameter data;
(b) Core plug data;
(c) A continuous wireline-log based estimator of permeability for the whole interval;
(d) A blocked permeability log as might be typically used in reservoir modelling.

Statistics for ln(k) are shown as the population distributions are approximately log normal. It is well known that the sample variance should reduce as sample scale is increased. Therefore, the reduction in variance between datasets (c) and (d) – core data to reservoir model – is expected. It is, however, a common mistake in multi-scale reservoir modelling for an inappropriate variance to be applied in a larger scale model, e.g. if core plug variance was used directly to represent the upscaled geomodel variance.

Comparison of datasets (a) and (b) reveals another form of variance that is commonly ignored. The probe permeameter grid (2 mm spaced data over a 10 cm × 10 cm core area) shows a variance of 0.38 [ln(k)]. The core plug dataset for the corresponding lithofacies interval (estuarine bar), has σ^2 ln(k) = 0.99, which represents variance at the lithofacies scale. However, blocking of the probe permeameter data at the core plug scale shows a variance reduction factor of 0.79 up to the core plug scale (column 2 in Table 4.2). Thus, in this dataset (where high resolution measurements are available) we know that a significant degree of variance is missing

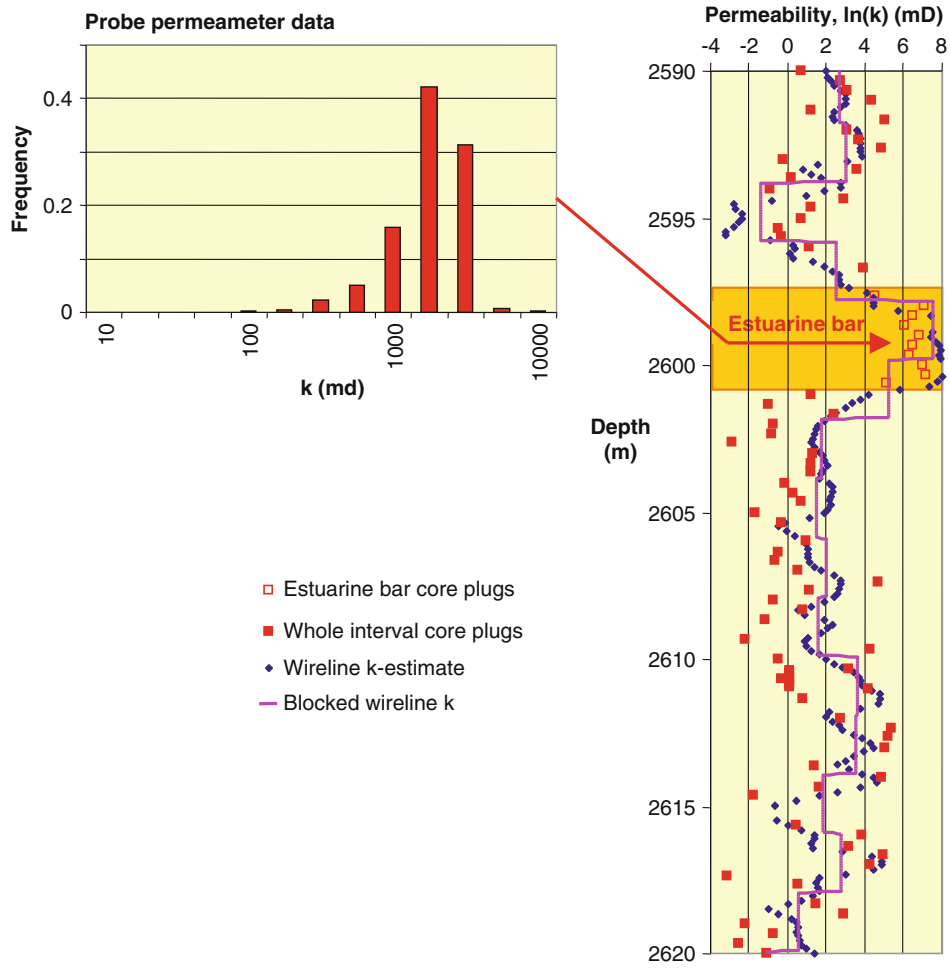

Fig. 4.26 Example dataset from a tidal deltaic flow unit illustrating treatment of permeability data used in reservoir modelling (Redrawn from Ringrose et al. 2008, The Geological Society, London, Special Publications 309 © Geological Society of London [2008])

Table 4.2 Variance analysis of example permeability dataset

	Estuarine bar lithofacies			Whole interval (flow unit)		
	(a) Probe-k data	(b) Probe data upscaled to plug scale	(c) Core plug data	(d) Core plug data	(e) Wireline-k estimate	(f) Blocked well data
Scale of data	10 × 10 cm; 2 mm spaced data	2 × 2 cm squares of 2 mm-spaced data	c.15–30 cm spaced core plugs	c.15–30 cm spaced plugs	15 cm digital log	2 m blocking
N =	2,584	25	11	85	204	16
Mean ln(k)	7.14	7.14	6.39	1.73	2.32	2.17
σ^2 ln(k)	0.38	0.30	0.99	8.44	5.94	4.80
Variance adjustment factor, *f*	–	0.79	–	–	–	0.81

from the datasets conventionally used in reservoir modelling.

Improved treatment of variance in reservoir modelling is clearly needed and presents us with a significant challenge. The statistical basis for treating population variance as a function of sample support volume is well established with the concept of *Dispersion Variance* (Isaaks and Srivastava 1989), where:

$$\underset{\text{Total variance}}{\sigma^2(a,c)} = \underset{\text{Variance within blocks}}{\sigma^2(a,b)} + \underset{\text{Variance between blocks}}{\sigma^2(b,c)} \quad (4.14)$$

where a, b and c represent different sample supports (in this case, a = point values, b = block values and c = total model domain).

The variance adjustment factor, *f*, is defined as the ratio of block variance to point variance and can be used to estimate the correct variance to be applied to a blocked dataset. For the example dataset (Table 4.2, Fig. 4.26) the variance adjustment factor is around 0.8 for both scale adjustment steps.

With additive properties, such as porosity, treatment of variance in multi-scale datasets is relatively straightforward. However, it is much more of a challenge with permeability data as flow boundary conditions are an essential aspect of estimating an upscaled permeability value (see Chap. 3). Multi-scale geological modelling is an attempt to represent smaller scale structure and variability as an upscaled block permeability value. In this process, the principles guiding appropriate flow upscaling are essential. However, improved treatment of variance is also critical. There is, for example, little point rigorously upscaling a core plug sample dataset if it is known that that dataset is a poor representation of the true population variance.

The best approach to this rather complex problem, is to review the available data within a multi-scale REV framework (Fig. 4.24). If the dataset is sampled at a scale close to the corresponding REV, then it can be considered as fairly reliable and representative data. If however, the dataset is clearly not sampled at the REV (and is in fact recording a highly variable property) then care is needed to handle and upscale the data in order to derive an appropriate average. Assuming that we have datasets which can be related to the REV's in the rock system, we can then use the same multi-scale framework to guide the modelling length scales. Reservoir model grid-cell dimensions should ideally be determined by the REV lengthscales. Explicit spatial variations in the model (at scales larger than the grid cell) are then focussed on representing property variations that cannot be captured by averages. To put this concept in its simplest form consider the following modelling steps and assumptions:

1. *From pore scale to lithofacies scale:* Pore-scale models (or measurements) are made at the pore-scale REV and then spatial variation at the lithofacies scale is modelled (using deterministic/probabilistic methods) to estimate rock properties at the lithofacies-scale REV.
2. *From lithofacies scale to geomodel scale.* Lithofacies-scale models (or measurements) are made at the lithofacies-scale REV and then spatial variation at the geological architecture scale is modelled (using deterministic/probabilistic methods) to estimate reservoir properties at the scale of the geological-unit REV (equivalent to geological model elements).
3. *From geomodel to full-field reservoir simulator.* Representative geological model elements are modelled at the full-field reservoir simulator scale to estimate dynamic flow behaviour based on reservoir properties that have been correctly upscaled and are (arguably) representative.

There is no doubt that multi-scale modelling within a multi-scale REV framework is a challenging process, but it is nevertheless much preferred to 'throwing in' some weakly-correlated random noise into an arbitrary reservoir grid and hoping for a reasonable outcome. The essence of good reservoir model design is that it is based on some sound geological concepts, an appreciation of flow physics, and a multi-scale approach to determining statistically representative properties.

Every reservoir system is somewhat unique, so the best way to apply this approach method is try it out on real cases. Some of these are illustrated in the following sections, but consider trying Exercise 4.2 for your own case study.

Exercise 4.2
Find the REVs for your reservoir?

Use your own knowledge a particular geological reservoir system or outcrop to sketch on the most likely scales of high variability and low variability (the REV) – similar to Fig. 4.21 – using the sketch below. Note that the horizontal axis is given as a vertical length scale (dz, across bedding) to make volume estimation easier.

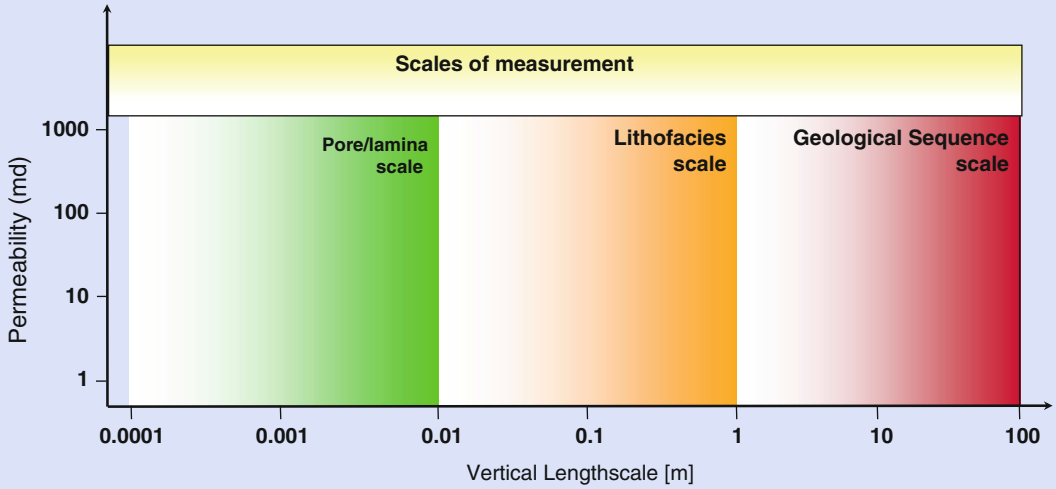

4.3.5 Construction of Geomodel and Simulator Grids

The choice of grid and grid-cell dimensions is clearly important. Upscaled permeability, the balance of fluid forces, and reservoir property variance are all intimately connected with the model length-scale. The construction of three dimensional geological models from seismic and well data remains a relatively time consuming task requiring considerable manual work both in construction of the structural framework and, not least, in construction of the grid for property modelling (Fig. 4.27).

Problems especially arise due to complex fault block geometries including reverse faults and Y-faults (Y-shaped intersections in the vertical plane). Difficulties relate partly to the mapping of horizons into the fault planes for construction of consistent fault throws across faults. Currently, most commercial gridding software is not capable of automatically producing adequate 3D grids for realistic fault architectures, and significant manual work is necessary. Upscaling procedures for regular Cartesian grids are well established, but the same operation in realistically complex grids is much more challenging.

The construction of 3D grids suitable for reservoir simulation is also non-trivial and requires significant manual editing. There are several reasons for this:

- The grid resolution in the geologic model and the simulation models are different, leading to missing cells or miss fitting cells in the simulation model. The consequences are overestimation of pore volumes, possibly wrong communication across faults, and difficult numerical calculations due to a number small or "artificial" grid cells.
- The handling of Y-shaped faults using corner point grid geometries (now widely used in black oil simulators) is difficult. Similarly, the use of vertically stair-stepped faults

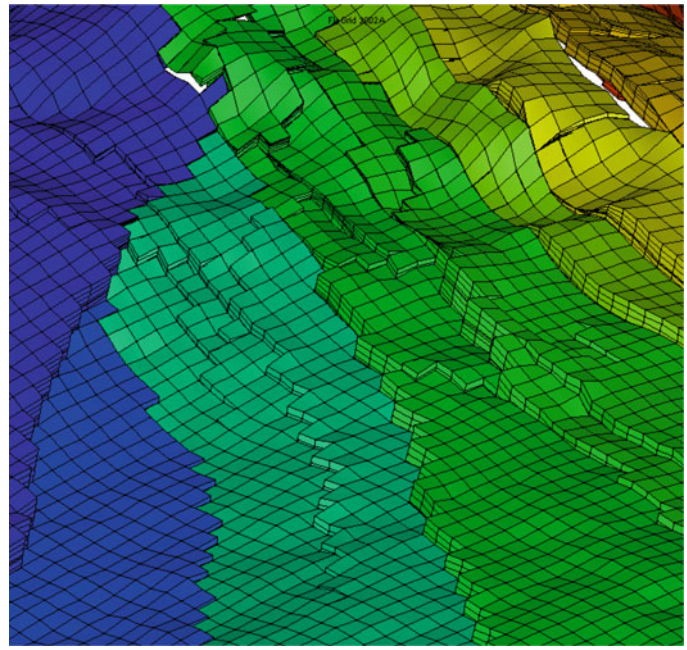

Fig. 4.27 Example reservoir model grid (Heidrun Field fault segments, colour coded by reservoir segment) (Statoil image archives, © Statoil ASA, reproduced with permission)

improves the grid quality and flexibility, but does not solve the whole problem. When using grids with stair-step faults special attention must be paid to estimation of fault seal and fault transmissibility. There is generally insufficient information in the grid itself for these calculations, and the calculation of fault transmissibility must be calculated based on information from the conceptual geological model.

- The handling of dipping reverse faults using stair-step geometry in a corner point grid requires a higher total number of layers than required for an un-faulted model.
- Regions with fault spacing smaller than the simulation grid spacing give problems for appropriate calculation of fault throw and zone to zone communication. Gridding implies that smaller-scale geomodel faults are merged and a cumulated fault throw is used in the simulation model. This is not generally possible with currently available gridding tools, and an effective fault transmissibility, including non-neighbour connections, must be calculated based on information from the geomodel, i.e. using the actual geometry containing all the merged faults.
- Flow simulation accuracy depends on the grid quality, and the commonly used numerical discretisation schemes in commercial simulators have acceptable accuracy only for 'near' orthogonal grids. Orthogonal grids do not comply easily with complex fault structures, and most often compromises are made between honouring geology and keeping "near orthogonal" grids.

Figure 4.28 illustrates how some of these problems have been addressed in oilfield studies (Ringrose et al. 2008). After detailed manual grid construction including stair-step faults to handle Y-faults, smaller faults are added directly into the flow simulation grid. However, some gridding problems cannot be fully resolved using the constraints of corner point simulation grids and optimal, consistent and automated grid generation based on realistic geomodels is a challenge. The use of unstructured grids reduces some of the gridding problems, but robust, reliable and cost efficient numerical flow solution methods for these unstructured grids are not generally available. Improved and consistent solutions for construction of structured grids and associated transmissibilities have been proposed (e.g. Manzocchi et al 2002; Tchelepi et al.

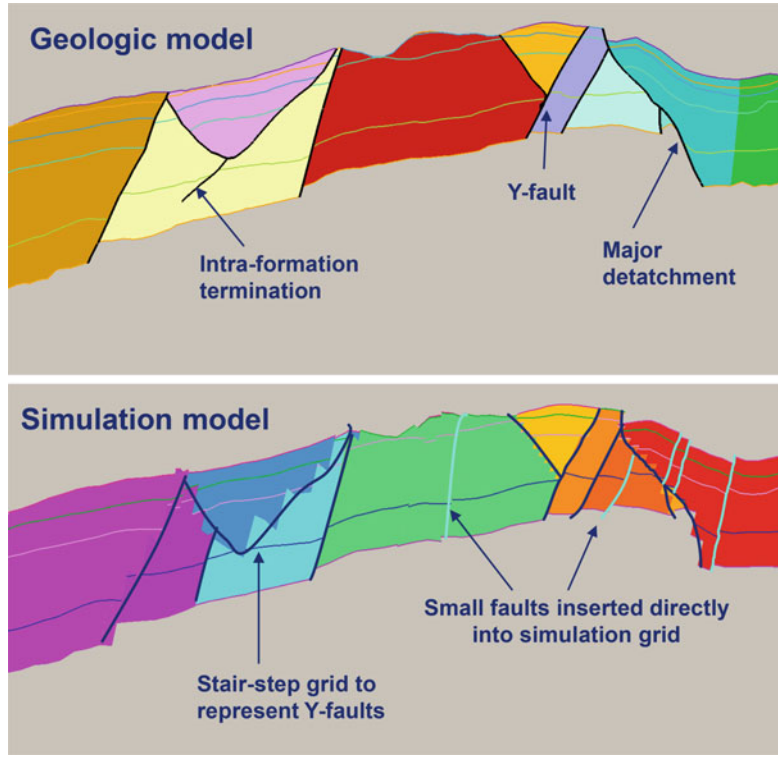

Fig. 4.28 Illustration of the transfer of a structural geological model to a reservoir simulation grid (Redrawn from Ringrose et al. 2008, The Geological Society, London, Special Publications 309 © Geological Society of London [2008])

2005) and flow simulation on faulted grids remains a challenge.

4.3.6 Which Heterogeneities Matter?

There are a number of published studies in which the importance of different multi-scale geological factors on reservoir performance have been assessed. Table 4.3 summarizes the findings of a selection of such studies in which a formalised experimental design with statistical analysis of significance has been employed. The table shows only the main factors identified in these studies (for full details refer to sources). What is clear from this work is that several scales of heterogeneity are important for each reservoir type. While one can conclude that stratigraphic sequence position is the most important factor in a shallow marine depositional setting or that vertical permeability is the most important factors in tidal deltaic setting, each case study shows that both larger and smaller-scale factors are generally significant. This is a clear argument in favour of explicit multi-scale reservoir modelling.

Furthermore, in the studies where the effects of structural heterogeneity were assessed, both structural and sedimentary features were found to be significant. That is to say, structural features and uncertainties cannot be neglected and are fully coupled with stratigraphic factors.

Another approach to this question is to consider how the fluid forces will interact with the heterogeneity in terms of the REV (Fig. 4.29). Pore and lamina-scale variations have the strongest effect on capillary-dominated fluid processes while the sequence stratigraphic (or facies association) scale most affects flow processes in the viscous-dominated regime. Gravity operates at all scales, but gravity-fluid effects are most important at the larger scales, where significant fluid segregation occurs. That is, when both capillary forces and applied pressure gradients fail to compete effectively against gravity stabilisation of the fluids involved.

Several projects have demonstrated the economic value of multi-scale modelling in the

Table 4.3 Summary of selected studies comparing multi-scale factors on petroleum reservoir performance

	Shallow Marine[a]	Faulted Shallow Marine[b]	Fluvial[c]	Tidal Deltaic[d]	Fault modelling[e]
Sequence model	V	V			V
Sand fraction	S	S	V	S	n/a
Sandbody geometry			S	S	n/a
Vertical permeability	S	S		V	n/a
Small-scale heterogeneity			S	S	n/a
Fault pattern	n/a	S	n/a	n/a	S
Fault seal	n/a	S	n/a	n/a	S

V Most significant factor, *S* Significant factor, *n/a* not assessed
[a]Kjønsvik et al. (1994)
[b]England and Townsend (1998)
[c]Jones et al. (1993)
[d]Brandsæter et al. (2001a)
[e]Lescoffit and Townsend (2005)

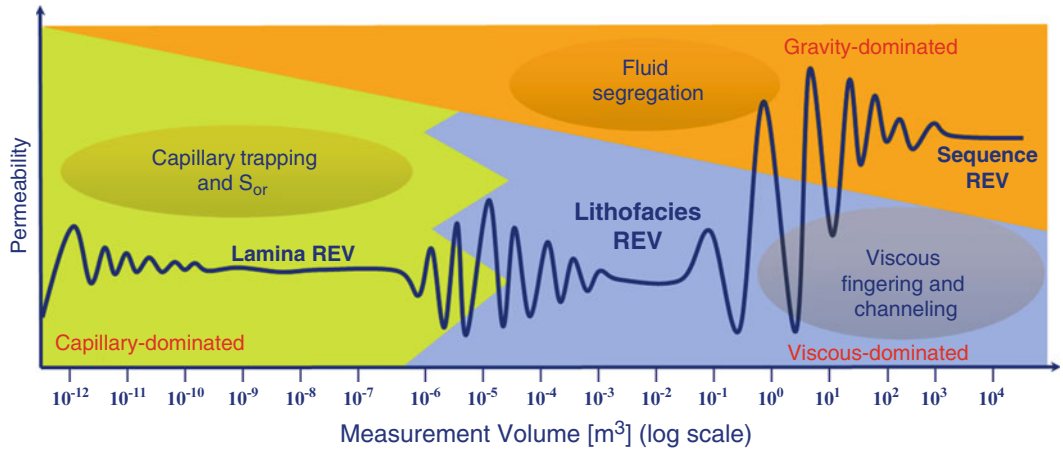

Fig. 4.29 Sketch illustrating the expected dominant fluid forces with respect to the important heterogeneity length-scales

context of oilfield developments. An ambitious study of the structurally complex Gullfaks field (Jacobsen et al 2000) demonstrated that 25 million-cell geological grid (incorporating structural and stratigraphic architecture) could be upscaled for flow simulation and resulted in a significantly improved history match. Both stratigraphic barriers and faults were key factors in achieving improved pressure matches to historic well data. This model was also used for assessment of IOR using CO_2 flooding.

Multi-scale upscaling has also been used to assess complex reservoir displacement processes, including gas injection in thin-bedded reservoirs (Fig. 4.30) (Pickup et al 2000; Brandsæter et al. 2001b, 2005), water-alternating-gas (WAG) injection on the Veslefrikk Field (Kløv et al 2003), and depressurization on the Statfjord field (Theting et al 2005). These studies typically show of the order of 10–20 % difference in oilfield recovery factors when advanced multi-scale effects are implemented, compared with conventional single-scale reservoir simulation studies. For example, Figure 4.31 shows the effect of one-step and two-step upscaling for the gas injection case study (illustrated in Fig. 4.30). The coarse-grid case without upscaling gives a forecasting error of over 10 % when compared to the fine-grid reference case, while the coarse-grid case with two-step upscaling gives a result very close to the fine-grid reference case.

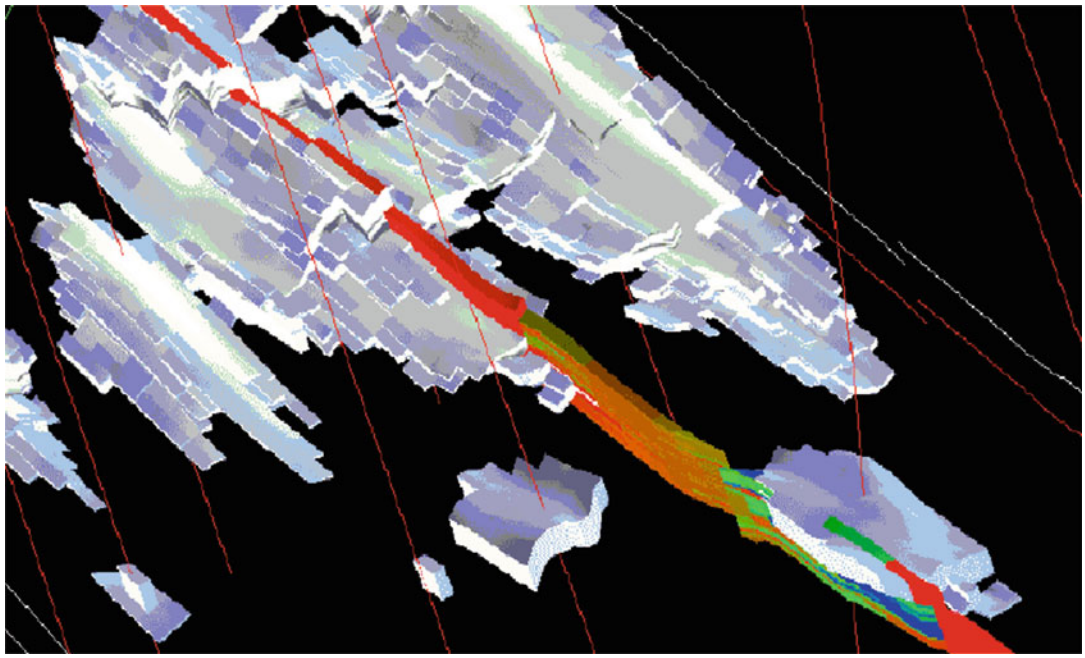

Fig. 4.30 Gas injection patterns in a thin-bedded tidal reservoir modelled using a multi-scale method and incorporating the effects of faults in the reservoir simulation model (From a study by Brandsæter et al 2001b)

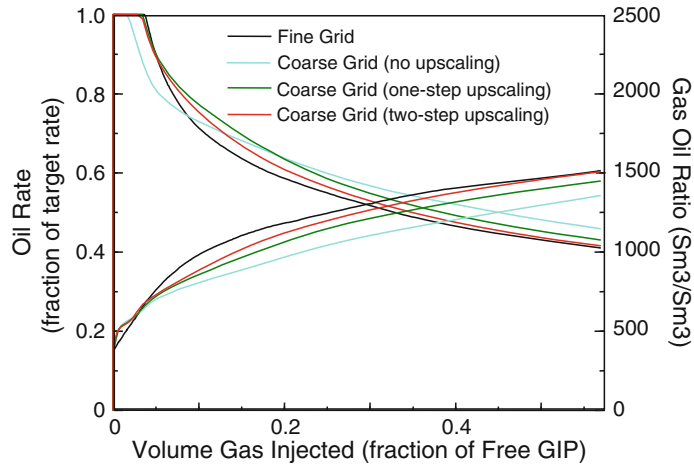

Fig. 4.31 Effect of multi-scale upscaling on estimates of oil rate and GOR for the gas injection case study shown in Fig. 4.30 (Redrawn from Pickup et al. 2000, ©2000, Society of Petroleum Engineers Inc., reproduced with permission of SPE. Further reproduction prohibited without permission)

4.4 The Way Forward

4.4.1 Potential and Pitfalls

Multi-scale reservoir modelling has moved from a conceptual phase, with method development on idealised problems, into a practical phase, with more routine implementation on real reservoir cases. The modelling methods have achieved sufficient speed and reliability for routine implementation (generally using steady-state methods on near-orthogonal corner-point grid systems). However, a number of challenges remain which require further developments of methods and modelling tools. In particular:

- Multi-scale modelling within a realistic structural geological grid is still a major challenge;

Handling Model Uncertainty

5

Abstract

The preceding chapters have highlighted a number of ways in which a reservoir model can go right or wrong.

Nothing, however, compares in magnitude with the mishandling of uncertainty. An incorrect saturation model, for example, can easily give a volumetric error of 10 % and perhaps even 50 %. A flawed geological concept could be much worse. Mishandling of uncertainty, however, can result in the whole modelling and simulation effort becoming worthless.

The cause of this is occasionally misuse of software, more commonly it is due to the limitations of our datasets, but primarily it is our behaviour and our design choices which are at fault.

Our aim is to place our models within a framework that can overcome data limitations and personal bias and give us a useful way of quantifying forecast uncertainty.

P. Ringrose and M. Bentley, *Reservoir Model Design*, DOI 10.1007/978-94-007-5497-3_5,

Did you expect to see the trees?

5.1 The Issue

5.1.1 Modelling for Comfort

In Chap. 1 we identified the tendency for modelling studies to become a panacea for decision making – modelling for comfort rather than analytical rigour. It is certainly often the case that reservoir modelling is used to hide uncertainty rather than illustrate it. We have a natural tendency to determine a best guess – the anchoring heuristic of Kahneman and Tverky (1974) – and the management process in many companies often inadvertently encourages the guesswork.

However, in a situation of dramatic undersampling the guess is often wrong and influenced unconsciously by behavioural biases of the individuals or teams involved (summarised in Kahneman 2011). Best-guess models therefore tend to be misleading and their role is reduced to one of providing comfort to support a business decision, one which has perhaps already been made. In this case we are indeed simply 'modelling for comfort', a low value activity, rather than taking the opportunity to use modelling to identify a significant business risk.

5.1.2 Modelling to Illustrate Uncertainty

Useful modelling can be expressed as 'reasonable forecasting.' A convenient metaphor for this is our ability to predict the image on a picture from a small number of sample points.

We illustrate this, graphically, using sampled selections (Fig. 5.1) from a landscape photograph (the chapter cover image). A routine modelling workflow would lead us to analyse and characterise each sample point: the process of reservoir characterisation. Data-led modelling with no underlying concept and no application of trends

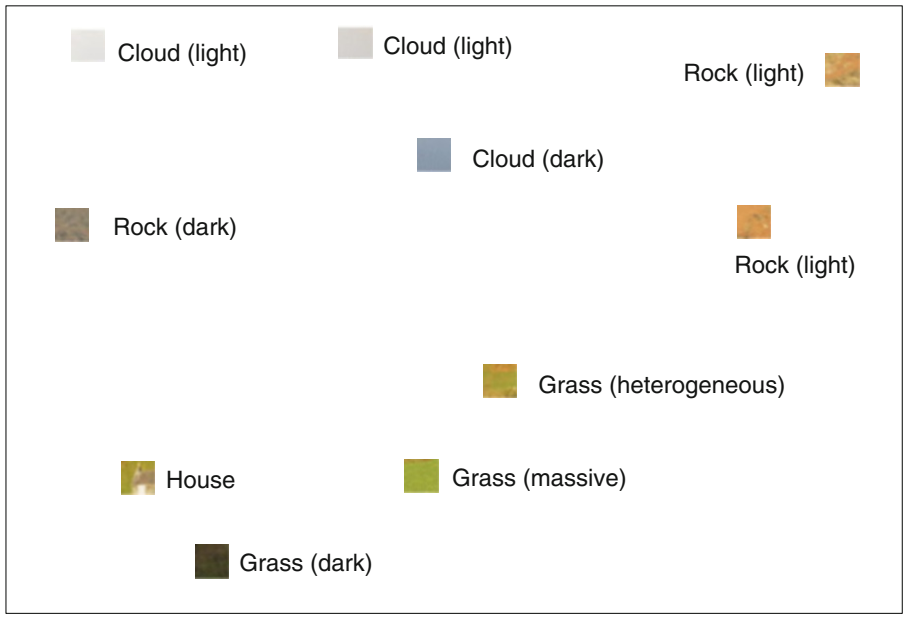

Fig. 5.1 An undersampled picture – our task is to determine the image

could produce the stochastic result shown in Fig. 5.2. This representation is statistically consistent with the underlying data, and would pass a simple QC test comparing frequency of occurrences in the data and in the model, yet the result is clearly meaningless.

Application of logical deterministic trends to the modelling process, as described in Chap. 2, would make a better representation, one which would at least fit an underlying landscape concept: the sky is more likely to be at the top, the grass at the bottom (Fig. 5.3). Furthermore, there is an anisotropy ratio we can use so that we can predict better spatial correlation laterally (the sky is more likely to extend across much of the image, rather than up and down). If the texture from this trend-based approach is deemed unrepresentative of landscapes, an object-based alternative may be preferred (Fig. 5.4). Grass is accordingly arranged in clusters, broadly elliptical, as are sky colours (clouds) and the rocky areas are arranged into 'hills', anchored around the data points they were observed in. A rough representation is beginning to take shape.

The model representations in Figs. 5.2, 5.3, and 5.4 each adhere to the same element proportions, and in this sense all 'match' the data, although with strongly contrasting textures. Assuming we then proceeded to add "colours" for petrophysical properties (Chap. 3) and rescale the image for flow simulation (Chap. 4), these images would produce strongly contrasting fluid-flow forecasts.

Using these different images as possible alternative realisations could be one way of exploring uncertainty, but we argue this would be a poor route to follow. Reference to the actual image (Fig. 5.5) reveals a familiar theme:

$$data \neq model \neq truth$$

Even though most aspects of the image were sampled, and the applied deterministic trends were reasonable, there are significant errors in the representation – object modelling of the sky was inappropriate, hierarchical organisation was missed, and even some aspects of the characterisation (grass vs. rocks) were oversimplified. There are also some modelling elements missing, most noticeably: *there were no trees*. Rearranging the data and detailed analysis of the original samples does not reveal the

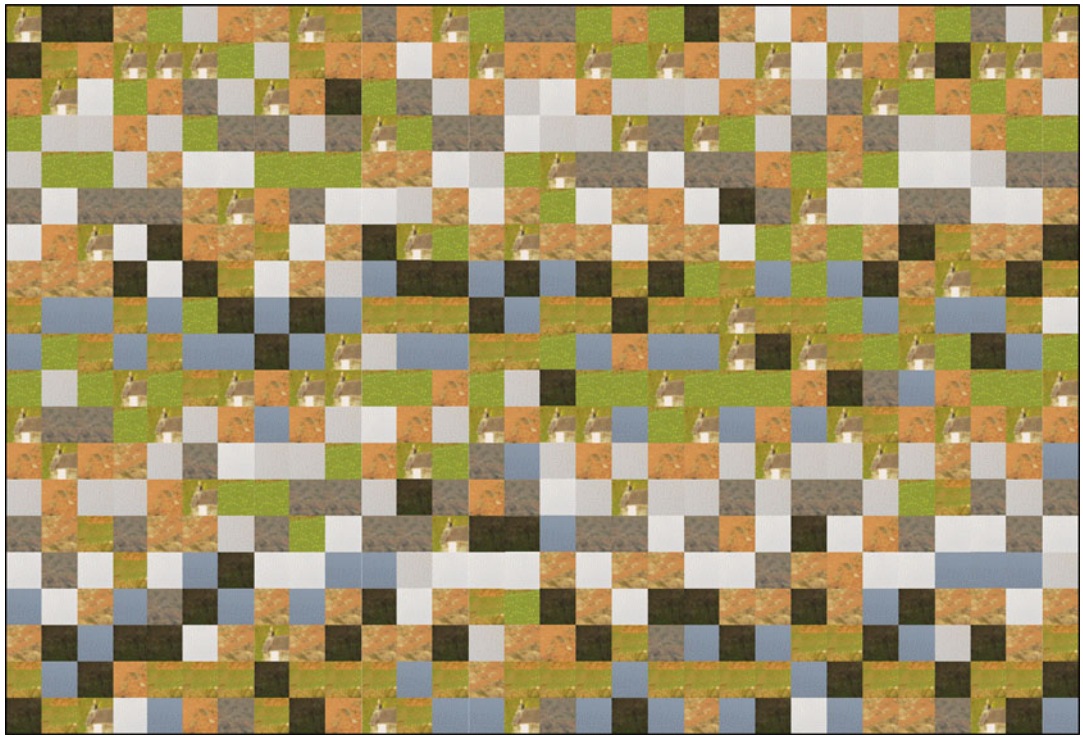

Fig. 5.2 Stochastic model representation of the data in Fig. 5.1, assuming stationarity

Fig. 5.3 Overlay of deterministic trends on the stochastic model in Fig. 5.2, overcoming stationarity

Fig. 5.4 Object model alternative to Fig. 5.3, maintaining deterministic trends and embracing a loose alignment of lozenge shapes

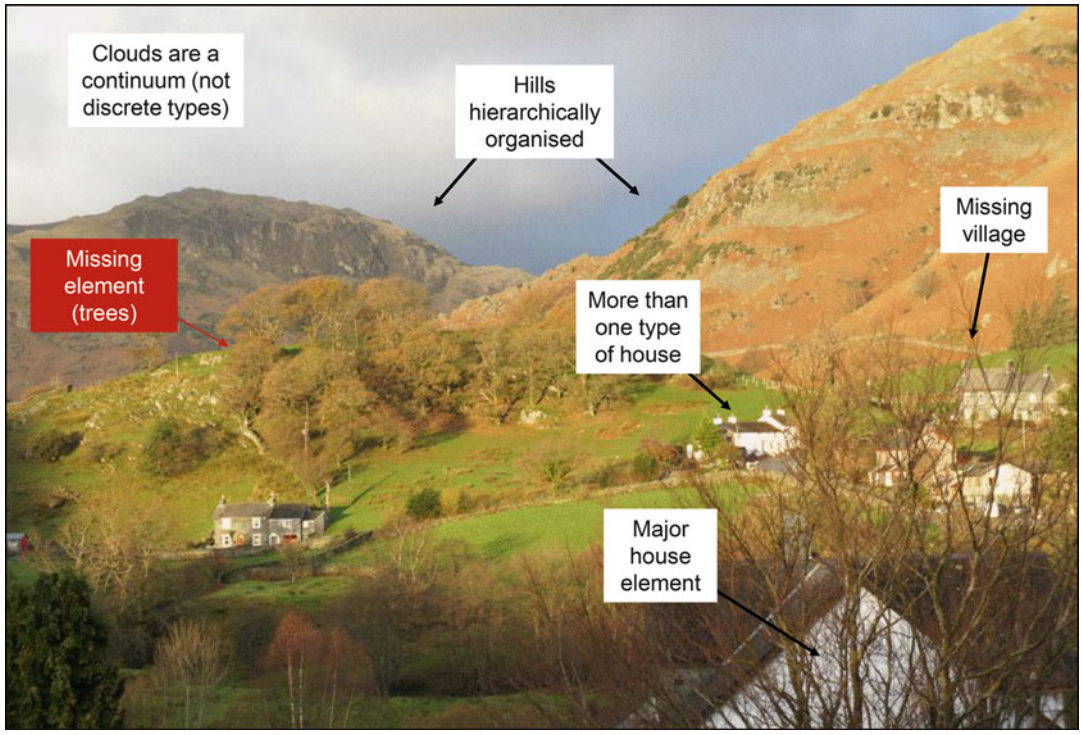

Fig. 5.5 Reality: the data set was unable to detect key missing elements, therefore these elements are also absent from the simple probabilistic model, even with a useful deterministic trend imposed

missing elements. On reflection, we can see that the aim of reproducing the statistical content of the sample dataset brings with it a major flaw in all the models.

Could the missing elements in Fig. 5.5 have been foreseen, given that they were absent in the data sample? We would argue yes, to a large extent. From the data set it is possible to establish a concept of hilly countryside in a temperate climate – the 'expert judgement' of Kahneman and Klein (2009). Having established this, there are in fact certain aspects which are consistent with the concept but not actually seen by the sample data. However, these can be anticipated. Ask yourself:

- Could there be more than one type of house? *Yes*.
- Could there be a small village? *Yes*.
- Is there a structure to the clouds? *Yes*.
- Are the hills logically arranged, ones with greater contrast in the foreground? *Yes*
- Could there be trees?

Taking the issue of trees specifically, these are highly likely to be present, given the underlying concept (grass and hills in a temperate climate). They are also likely to be under-sampled.

The parallels with reservoir modelling are hopefully clear: we need to use concepts to honour the data but work beyond it to include missing elements. If these elements are important to the field development (e.g. open natural fractures, discontinuous but high permeability layers, cemented areas, sealing sub-seismic faults, thin shales) then the presence or absence of these features becomes the important uncertainty. We should always ask ourselves: "could there be trees?"

5.2 Differing Approaches

Abandoning the route of modelling for comfort and embarking on the harder but more interesting and ultimately more useful route of modelling to illustrate uncertainty, we need a workflow (see Caers 2011, for a summary of statistical methodologies). This chapter will review alternative approaches to uncertainty handling, and lead to a general recommendation for scenario-based approaches, along the way also distinguishing different flavours of 'scenario'.

Scenario-based modelling became a popular means of managing sub-surface uncertainty during the 1990s, although opinions differ widely on the nature of the 'scenarios' – particularly with reference to the relative roles of determinism and probability. In the context of reservoir modelling, a scenario is defined here as *a possible real-world outcome* and is one of several possible outcomes (Bentley and Smith 2008).

The idea of alternative, discrete scenarios followed on logically from the emergence of integrated reservoir modelling tools (e.g. Cosentino 2001; Towler 2002), which emphasised the use of 3D static reservoir modelling, ideally fed from 3D seismic data and leading to 3D dynamic reservoir simulation, generally on a full-field scale.

Appreciating the numerous uncertainties involved in constructing such field models, the desire for multiple modelling naturally arises. Although not universal (see discussion in Dubrule and Damsleth 2001), the application of multiple stochastic modelling techniques is now widespread, with the alternative models described variously as 'runs', 'cases', 'realisations' or 'scenarios'.

The different terminologies are more than semantic. The notion of multiple modelling has been explored differently by different workers, the essential variable being the balance between deterministic and probabilistic inputs. Using "multiple realisations" may sound more routed in statistical theory than using some alternative "model runs" – but is it? These concepts are best related to differing approaches to the application of geostatistical algorithms, and to differing ideas on the role of the probabilistic component (Fig. 5.6).

The contrasting approaches to uncertainty handling broadly fall into three groups:

Rationalist approaches, in which a preferred model is chosen as a base case (Fig. 5.7). The model is either run as a technical best guess, or with a range of uncertainty added

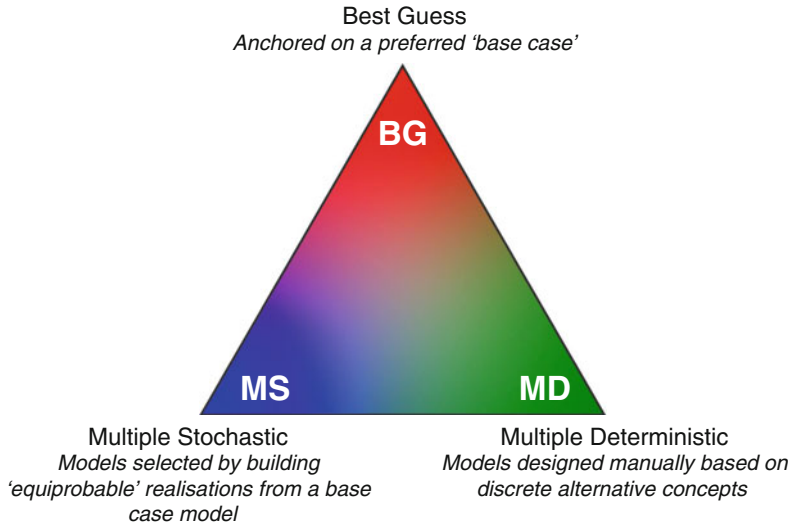

Fig. 5.6 Alternative approaches to uncertainty handling

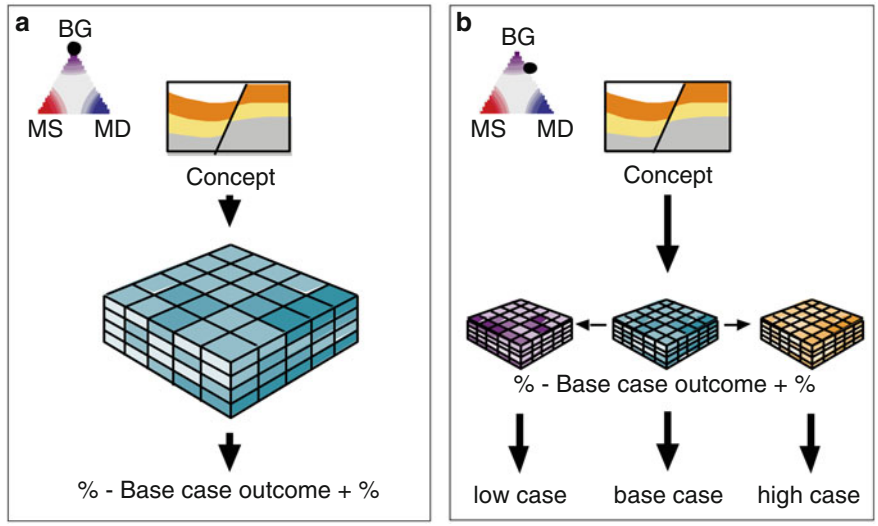

Fig. 5.7 Base case–dominated, rationalist approaches (Redrawn from Bentley and Smith 2008, The Geological Society, London, Special Publications 309 © Geological Society of London [2008])

to that guess. This may be either a percentage factor in terms of the model output (e.g. ±20 % of the base case volumes in-place) or separate low and high cases flanking the base case. This approach can be viewed as 'traditional' determinism.

Multiple stochastic approaches, in which a large number of models are probabilistically generated by geostatistical simulation (Fig. 5.8). The deterministic input lies in the choice of the boundary conditions for the simulations, such as assumed correlation lengths. Yarus and Chambers (1994) give several examples of this approach, and the options and choices are reviewed by Caers (2011).

Multiple deterministic approaches, which avoid making a single best-guess or choosing a preferred base-case model (Fig. 5.9). In this approach a smaller number of models

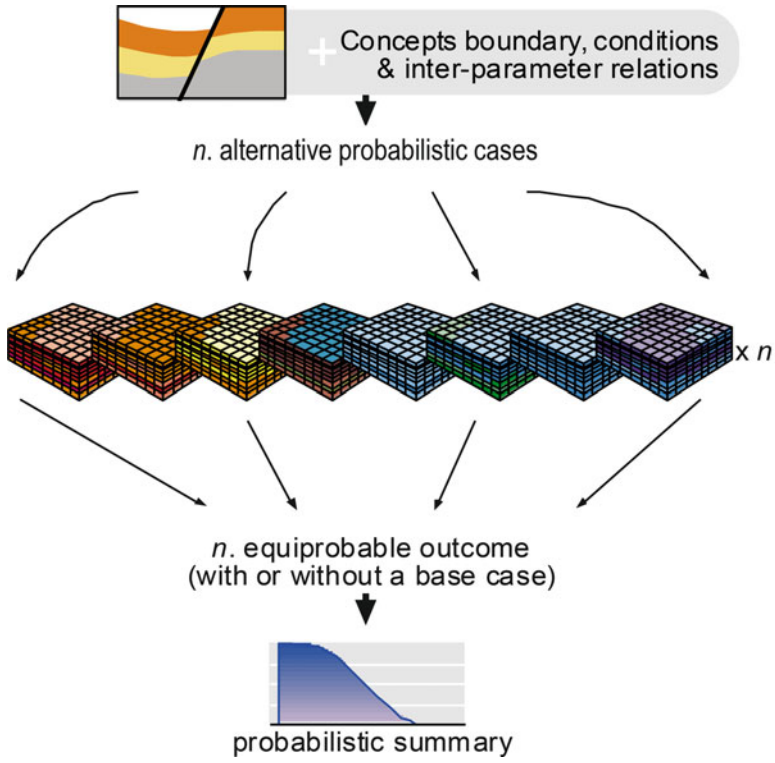

Fig. 5.8 Multiple stochastic approaches (Redrawn from Bentley and Smith 2008, The Geological Society, London, Special Publications 309 © Geological Society of London [2008])

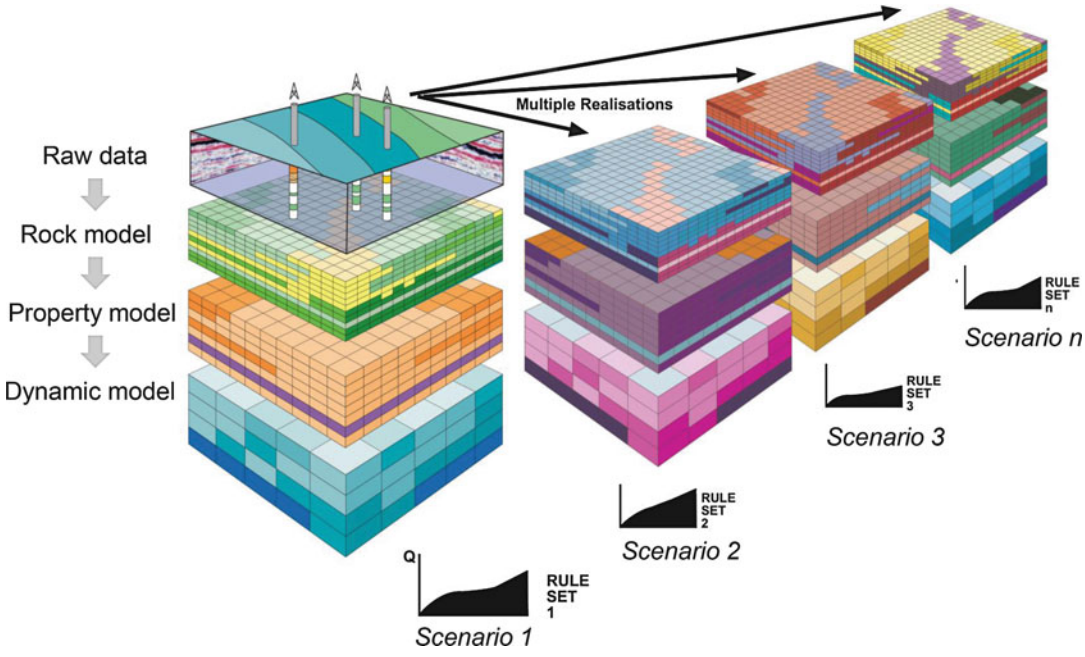

Fig. 5.9 Multiple-deterministic, 'scenario-based' approach

are built, each one reflecting a complete real-world outcome following an explicitly-defined reservoir concept. Geostatistical simulation may be applied in the building of the 3D model but the *selection* of the model realisations is made manually (or mathematically) rather than by statistical simulation (e.g. van de Leemput et al. 1996).

Each of the above approaches have been referred to as 'scenario modelling' by different reservoir modellers. The argument we develop here is that although all three approaches have some application in subsurface modelling, multiple-deterministic scenario-building is the preferred route in most circumstances.

In order to make this case, we need to recall the underlying philosophy of uncertainty handling and give a definition for 'scenario modelling'.

5.3 Anchoring

5.3.1 The Limits of Rationalism

The rationalist approach, described above as the 'best-guess' method, is effectively simple forecasting – and puts faith in the ability of an individual or team to make a reasonably precise judgement. If presented as the best judgement of a group of professional experts then this appears reasonable. The weak point is that the best guess is only reliable when the system being described is well ordered and well understood, to the point of being highly predictable (Mintzberg 1990). It must be assumed that enough data is available from past activities to predict a future outcome with confidence, and this applies equally to production forecasting, exploration risking, volumetrics or well prognoses. Although this is rarely the case in the subsurface, except perhaps for fields with a large (100+) number of regularly spaced wells, there is a strong tendency for individuals or teams (or managers) to desire a best guess, and to subsequently place too much confidence in that guess (Baddeley et al. 2004).

It is often stated that for mature fields, a simple, rationalist approach may suffice because uncertainty has reduced through the field life cycle. This is a fallacy. Although, the *magnitude* of the initial development uncertainties tends to decrease with time, we generally find that as the field life cycle progresses new, more subtle, uncertainties arise and these now drive the decision making. For example, in the landscape image in Fig. 5.5, 100 samples would significantly improve the ability to describe the image, but this is still insufficient to specify the location of an unsampled house. The impact of uncertainties in terms of their ability to erode value may, in fact, be as great near the end of the field life as at the beginning.

Despite this, rationalist, base-case modelling remains common across the industry. In a review of 90 modelling studies conducted by the authors and colleagues across many companies, field modelling was based on a single, best-guess model in 36 % of the cases (Smith et al. 2005). This was the case, despite a bias in the sampling from the authors' own studies, which tended to be scenario-based. Excluding the cases where the model design was made by the authors, the proportion of base case-only models rose to 60 %.

5.3.2 Anchoring and the Limits of Geostatistics

The process of selecting a best guess in spite of wide uncertainty is referred to as 'anchoring', and is a well-understood cognitive behaviour (Kahneman and Tverky 1974). Once anchored, the adjustment away from the initial best guess is too limited as the outcome is overly influenced by the anchor point.

This often also occurs in statistical approaches to uncertainty handling, as these tend to be anchored in the available data and may therefore make the same rational starting assumption as the simple forecast, although adding ranges around a 'most probable' prediction (see examples in Chellingsworth et al. 2011).

Geostatistical simulation allows definition of ranges for variables, followed by rigorous

sampling and combination of parameters to yield a range of results, which can be interpreted probabilistically. If the input data can be specified accurately, and if the combination process maintains a realistic relationship between all variables, the outcome may be reasonable. In practice, however, input data is imperfectly defined and the 'reasonableness' of the automated combination of variables is hard to verify. Statistical rigour is applied to data sets which are not necessarily statistically significant and an apparently exhaustive analysis may have been conducted on insufficient data.

The validity of the outcome may also be weakened by centre-weighting of the input data to variable-by-variable best-guesses, which creates an inevitability that the 'most likely' probabilistic outcome will be close to the initial best guess (Wynn and Stephens 2013). The geostatistical simulation itself is thus 'anchored'.

It is therefore argued that the application of geostatistical simulation does not in itself compensate for a natural tendency towards a rationalist best guess – it often tends to simply reflect it. The crucial step is to select a workflow which removes the opportunity for anchoring on a best guess; and this is what scenario modelling, as defined here, attempts to achieve.

5.4 Scenarios Defined

The definition of 'scenario' adopted here follows that described by van der Heijden (1996), who discussed the use of scenarios in the context of corporate strategic planning and defined scenarios as *a set of reasonably plausible, but structurally different futures*.

Alternative scenarios are not incrementally different models based on slight changes in continuous input data (as with multiple probabilistic models), but models which are *structurally* distinct based on some defined design criteria. Translated to oil and gas field development, a 'scenario' is therefore a plausible development outcome, and the 'scenario-based approach' to reservoir modelling is defined as:

> *the building of multiple, deterministically-driven models of plausible development outcomes*

Each scenario is a complete and internally consistent static/dynamic subsurface realisation with an associated plan tailored to optimise its development. In an individual subsurface scenario, there is clear linkage between technical detail in a model, and an ultimate commercial outcome; a change in any element of the model prompts a quantitative change in the outcome and the dependency between *all* parameters in the chain (between the changed element and the outcome) is unbroken.

This contrasts with many probabilistic simulations, in which model design parameters are statistically sampled and cross-multiplied, and in which dependencies between variables are either lost, or collapsed into correlation coefficients.

The scenario approach therefore places a strong emphasis on deterministic representation of a subsurface concept: geological, geophysical, petrophysical and dynamic. Without a clearly defined concept of the subsurface – clear in the sense that a geoscientist could represent it as a simple sketch – the modelling cannot progress meaningfully. We have used the mantra: *if you can sketch it, you can model it*. Geostatistical simulation may be a key tool required to build an individual scenario but the design of the scenarios is determined directly by the modeller. Multiple models are based on multiple, deterministic designs. This distinguishes the workflows for scenario modelling, as defined here, from multiple stochastic modelling which tends to be based on statistical sampling from a single initial design. Note that multiple stochastic modelling is a powerful tool for understanding reservoir model ranges and outcomes; it is simply not sufficient to fully explore subsurface uncertainties from poorly sampled reservoirs.

Scenario-based approaches place an emphasis on listing and ranking of uncertainties, from which a suite of scenarios will be built, with no attempt being made to select a best guess case up-front.

5.5 The Uncertainty List

The key to success in scenario modelling lies in deriving an appropriate list of key uncertainties, a matter of experience and judgement. However, there is a strong tendency to conceptualise key uncertainties for at least the static reservoir models in terms of the parameters of the STOIIP equation, *i.e.* when asked to define the key uncertainties in the field, modellers will often quote parameters such as 'porosity' or 'net sand' as key factors. If the model-build progresses with these as the key uncertainties to alter, this will most likely be represented as a range for a continuous variable, anchored around a best guess.

A better approach is to question why 'porosity' or 'net sand count' are considered significant uncertainties. It will either emerge that the uncertainty is not that significant or, if it is, then it relates to some underlying root cause, such as heterogeneous diagenesis, or some local facies control which has not been extracted from the data analysis.

For example, in Fig. 5.10 a PDF of net-to-gross is shown. A superficial approach to model uncertainty would involve taking the PDF, inputting it to a geostatistical algorithm and allowing sampling of the spread to account for the uncertainty. As the data in the figure illustrates, this would be misleading, because the range is reflecting mixed geological concepts. The real need is to understand the facies distribution, and isolate the facies-based factors (in this case the proportion of different channel types), and then establish whether this ratio is known within reasonable bounds. If not known, the uncertainty can be represented by building contrasting, but realistic, depositional models (the basis for two scenarios) in which these elements are specifically contrasted. The uncertainty in the net-to-gross parameter within each scenario is a second-order issue to the geological uncertainty.

In defining key uncertainties, the need is therefore to chase the source of the uncertainty to the underlying causative factor – 'root cause analysis' – and model the conceptual range of uncertainty of that factor with discrete cases, rather than simply input a data distribution for a higher level parameter such as net-to-gross.

5.6 Applications

5.6.1 Greenfield Case

The application of scenario modelling has been most successfully reported for cases involving new or 'greenfield' reservoir studies.

One of the first published examples was that of van de Leemput et al. (1996), who described an application of scenario-based modelling in the context of an LNG field development. Once sufficient proven volumes were established to support the scheme, the commercial structure of the project focussed attention on the issue of the associated capital expenditure (CAPEX). CAPEX therefore became the prime quantitative outcome of the modelling exercise, driven largely by well numbers and the requirements for, and timing of, gas compression facilities.

The model scenarios were driven by a selection of principal uncertainties, summarised in Fig. 5.11. Six static and five dynamic uncertainties were drawn up, based on the judgement of the project team and input from peers. Maintaining the uncertainty list became a continuing process, iterating with new well data from appraisal drilling, and the changing views of the group.

For the field development plan itself, the uncertainty list generated 22 discrete scenarios, each of which was matched to the small amount of production data, then individually tailored to optimise the development outcome over the life of the LNG scheme. The outcomes, in term of impact on project cost (CAPEX), are shown in Fig. 5.11.

A key learning outcome from this exercise was that a list of 11 uncertainties was unnecessarily long to generate the ultimate result, although convenient for satisfying concerns of stakeholders. The effect of statistical dominance meant that the range was not driven by all

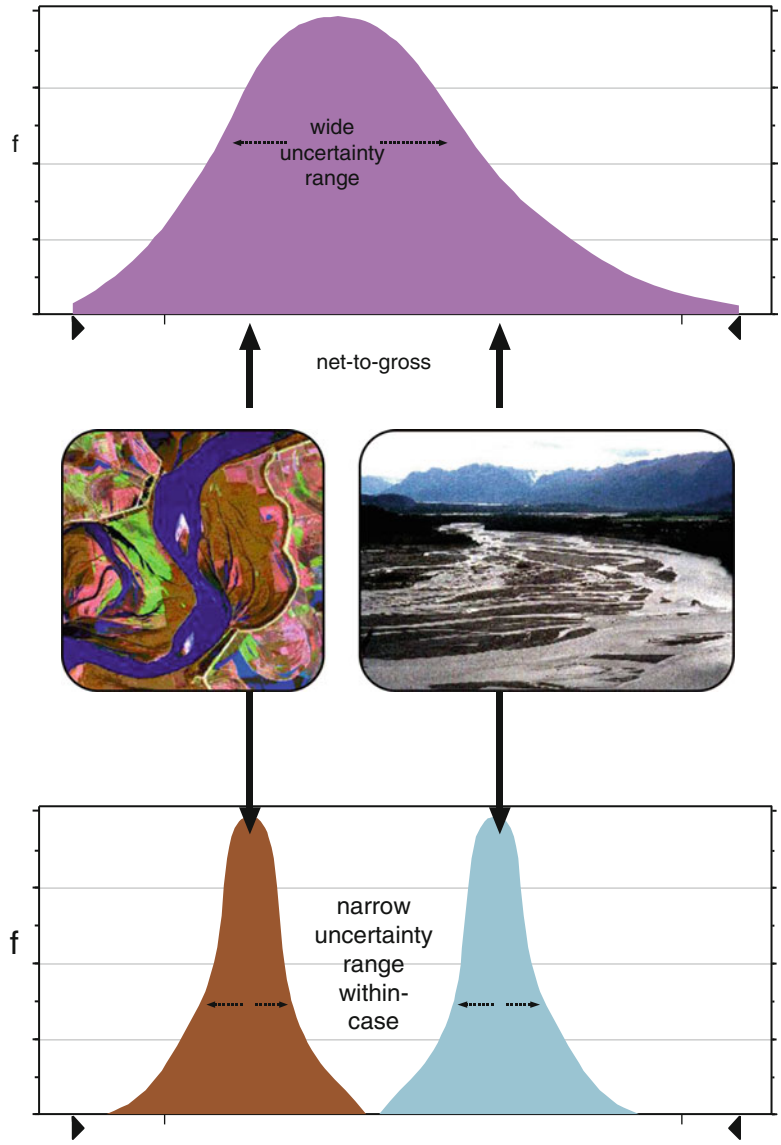

Fig. 5.10 Root-cause analysis: defining the underlying causative uncertainty (Redrawn from Bentley and Smith 2008, The Geological Society, London, Special Publications 309 © Geological Society of London [2008])

11 uncertainties, but by 2 or 3 key uncertainties to which the scheme was particularly sensitive.

Contrary to the expectations of geoscientists, gross rock volume on the structures was not a key development issue, even though the fields were large and each had only two or three well penetrations at the time of the field development plan (FDP) submission. The key issue was the potential enhancements of well deliverability offered by massive hydraulic fracturing – not a factor typically at the heart of reservoir modelling studies. The majority of the issues normally addressed by modelling: sand body geometries, relative permeabilities, aquifer size *etc*., were certainly poorly understood, but could be shown to have no significant impact on the field development decision. In hindsight, the dominant issues were foreseeable without modelling.

In the light of the above, continued post-FDP modelling became more focussed, with a smaller number of scenarios fleshing out the dominant issues only. Tertiary issues were effectively treated as constants.

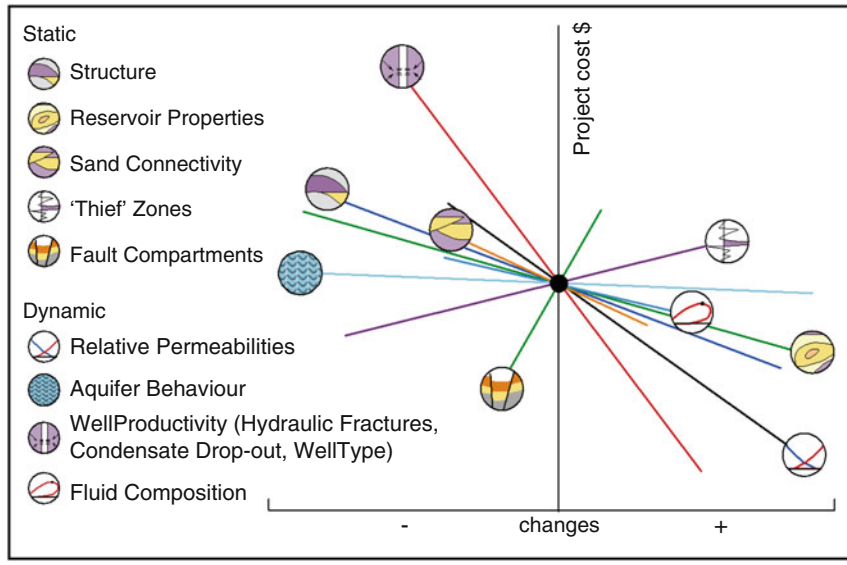

Fig. 5.11 Application of deterministic scenarios to a green field case: forecasting costs (Redrawn from Bentley and Smith 2008, The Geological Society, London, Special Publications 309 © Geological Society of London [2008])

The above example was conducted without selecting a 'base case' model. A development scheme was ultimately selected, but this was based on a range of outcomes defined by the subsurface team.

Scenario modelling for greenfields has been conducted many times since the publication of this example. In the experience of the authors, the early learnings described in the case above have held true, notably:

- Large numbers of scenarios are not required to capture the range of uncertainty;
- The main uncertainties can generally be drawn up through cross-discipline discussion prior to modelling – if not these can be established by running quick sensitivities;
- This list should be checked and iterated as the modelling progresses;
- The dominant uncertainties on a development project do not always include the issue of seismically driven gross rock volume, even at the pre-development phase;
- It is not necessary to select a base case model.

5.6.2 Brownfield Case

Two published examples are summarised here which illustrate the extension of scenario modelling to mature, or 'brownfield', reservoir cases.

The first concerns the case of the Sirikit Field in Thailand (Bentley and Woodhead 1998). The requirement was to review the field mid-life and evaluate the potential benefit of introducing water injection to the field. At that point the field had been on production for 15 years, with 80 wells producing from a stacked interval of partially-connected sands. The required outcome was a quantification of the economic benefit of water injection, to which a scenario–based approach was to be applied.

The uncertainty list is summarised in Fig. 5.12. The static uncertainties were used to generate the suite of static reservoir models for input to simulation. In contrast to the greenfield cases, where production data is limited, the dynamic uncertainties were used as the history

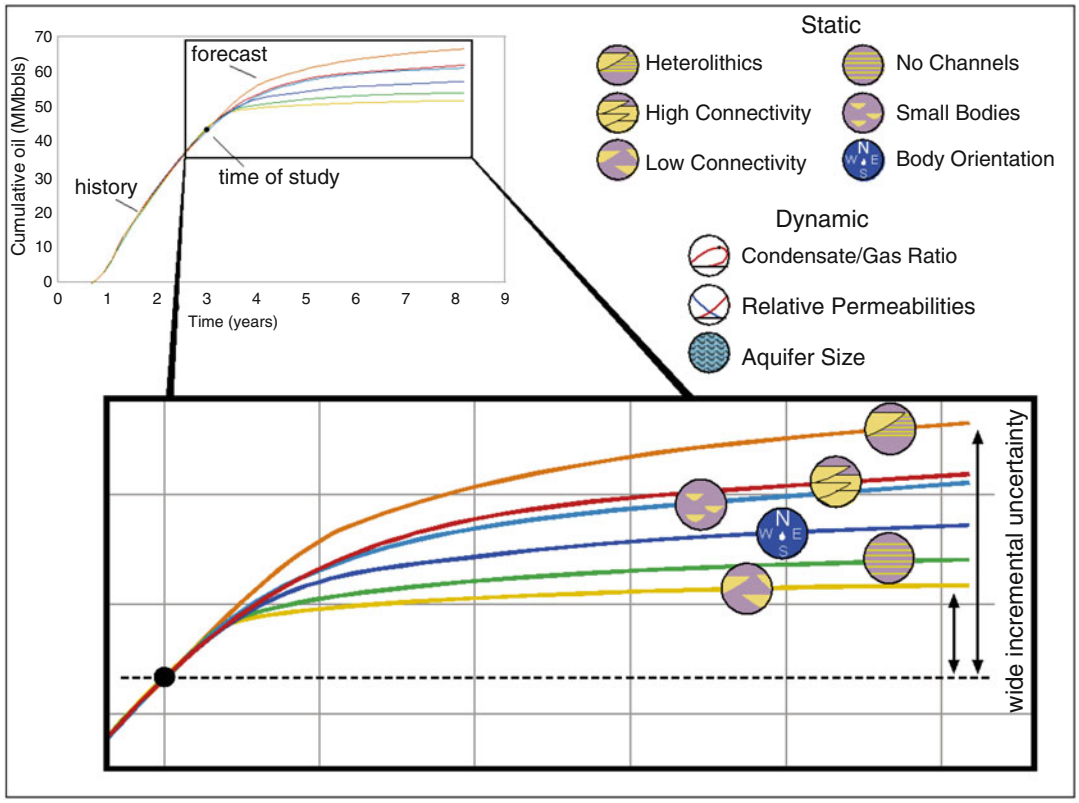

Fig. 5.12 Application of deterministic scenarios to a brownfield case: forecasting production (Redrawn from Bentley and Smith 2008, The Geological Society, London, Special Publications 309 © Geological Society of London [2008])

matching tools – the permissible parameter ranges for those uncertainties being established *before* the matching began.

A compiled production forecast for the 'no further drilling case' is shown in Fig. 5.12. The difference between that spread of outcomes and the spread from a parallel set of outcomes which included water injection, was used to quantify the value of the injection decision. Of interest here is the nature of that spread. Although all models gave reasonable matches to history, the incremental difference between the forecasts was larger than that expected by the team. It was hoped that some of the static uncertainties would simply be ruled out by the matching process. Ultimately none were, despite 80 wells and 15 years of production history.

The outlier cases were reasonable model representations of the subsurface, none of the scenarios was strongly preferred over any other, and all were plausible. A base case was not chosen.

The outcome makes a strong statement about the non-uniqueness of simulation model matches. If a base case model had been rationalised based on preferred guesses, any of the seven scenarios could feasibly have been chosen – only by chance would the eventual median model have been selected.

The Sirikit case also confirmed that multiple deterministic modelling was achievable in reasonable study times – scaled sector models were used to ease the handling of production data (see Bentley and Woodhead 1998). The workflow yielded a surprisingly wide range of model forecasts.

Fig. 5.13 summarises an application of scenario modelling to a producing field with 4D seismic, which generated additional insights into the use of scenarios. The case is from the

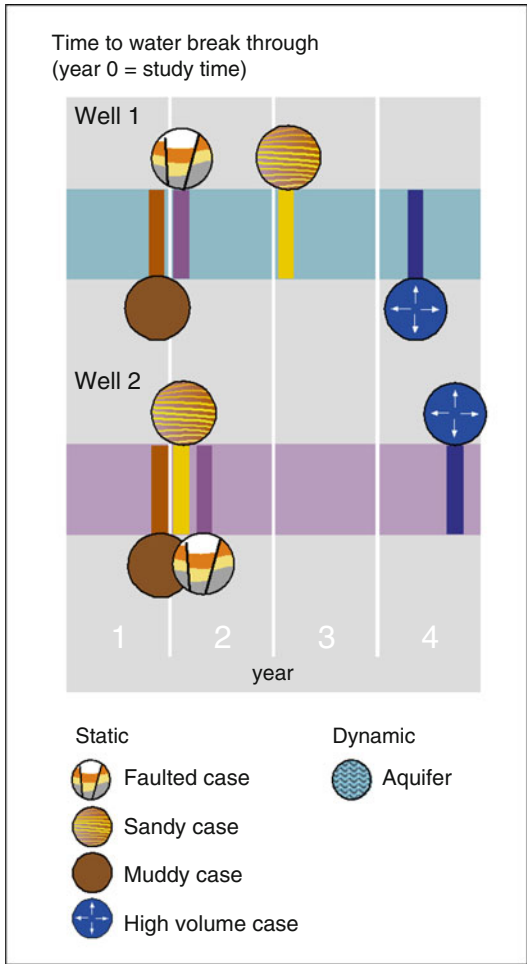

Fig. 5.13 Application of deterministic scenarios to a brownfield case: forecasting water breakthrough (Redrawn from Bentley and Smith 2008, The Geological Society, London, Special Publications 309 © Geological Society of London [2008])

Gannet B Field in the Central North Sea (Bentley and Hartung 2001; Kloosterman et al. 2003).

The issue to model in the Gannet B case was the risk and timing of potential water breakthrough in one of the field's two gas producers, and placing value on the possible contingent activities post-breakthrough. As with the cases above, the study started with a listing and qualitative ranking of principal uncertainties in a cross-discipline forum. Unlike the previous cases, it proved not to be possible to match all static reservoir models with history. The lowest volume realisation would not match. The model outcome – a range of water-cut breakthrough times – is illustrated in Fig. 5.13.

The Gannet B study offered some additional insights into mature field scenario modelling:

- Although the truism is offered that multiple models can match production data (there is no uniqueness to history matches), the converse is not necessarily true – everything cannot always be matched;
- The above is more likely to be true in smaller fields, where physical field limitations constrain possible scenarios;
- In the specific case of Gannet B, the principal matching tool was 4D seismic data (not well production data), and it was the seismic which was the matching target for the multiple model scenarios;
- A base case selection from the quantified range in water breakthrough times would have been highly misleading; "between 9 months and 4 years" was the answer to the question based on the available data. Making a median guess would have simply hidden the risk.

5.7 Scenario Modelling – Benefits

The scenario-based approach as defined here offers specific advantages over base case modelling and multiple probabilistic modelling:

Determinism: the dominance of the underlying conceptual reservoir model, which is deterministically applied via the model design. Although the models may use any required level of geostatistical simulation to re-create the desired reservoir concept, the geostatistical algorithms are not used to select the cases to be run, nor to quantify the uncertainty ranges in the model outcomes.

Lack of anchoring: the approach is not built on the selection of a base case, or best guess. Qualitatively, the natural tendency to underestimate uncertainties is less prone to occur if a best guess is not required – the focus lies instead on an exploration of the range.

Dependence: direct dependence between parameters is maintained through the modelling process; a contrast between two model

realisations is fed through directly to two quantitative scenarios, which allow the significance of the uncertainty to be evaluated.

Transparency: although the models may be internally complex, the workflow is simple, and feeds directly off the uncertainty list, which may be no more complex than a short list of the key issues which drive the decision at hand. If the key issues which could cause a project to fail are identified on that list, the model process will evaluate the outcome in the result range. The focus is therefore not on the intricacies of the model build (which can be reviewed by an expert, as required), but on the uncertainty list, which is transparent to all interested parties.

5.8 Multiple Model Handling

It is generally assumed that more effort will be required to manage multiple models than a single model, particularly when brownfield sites require multiple history matching. However, this is not necessarily the case – it all comes down to a choice of workflow.

Multiple model handling in greenfield sites is not necessarily a time-consuming process. Figure 5.14a illustrates results from a study involving discrete development scenarios. These were manually constructed from permutations of 6 underlying static models and dynamic uncertainties in fluid distribution and composition. This was an exhaustive approach in which all combinations of key uncertainties were assessed. The final result could have been achieved with a smaller number of scenarios, but the full set was run simply because it was not particularly time-consuming (the whole study ran over roughly 5 man weeks, including static and dynamic modelling). The case illustrates the efficacy of multiple static/dynamic modelling in greenfields, even when the compilation of runs is manual. Figure 5.14b shows the results of a more recent study (Chellingsworth, et al. 2011) in which 124 STOIIP-related cases were efficiently analysed using a workflow-manager algorithm.

This issue is more pressing for brownfield sites, although the cases described above from the Sirikit and Gannet fields illustrate that workflows for multiple model handling in mature fields can be practical. This challenge is also being improved further by the emergence of a new breed of automatic history matching tools which achieve model results according to input guidelines which can be deterministically controlled.

It is thus suggested that the running of multiple models is not a barrier to scenario modelling, even in fields with long production histories. Once the conceptual scenarios have been clearly defined, it often emerges that complex models are not required. Fit-for-purpose models also come with a significant time-saving.

Cross-company reviews by the authors indicate that model-building exercises which are particularly lengthy are typically those where a very large, detailed, base-case model is under construction. History matching is often pursued to a level of precision disproportionate to the accuracy of the static reservoir model it is based on. By contrast, multiple modelling

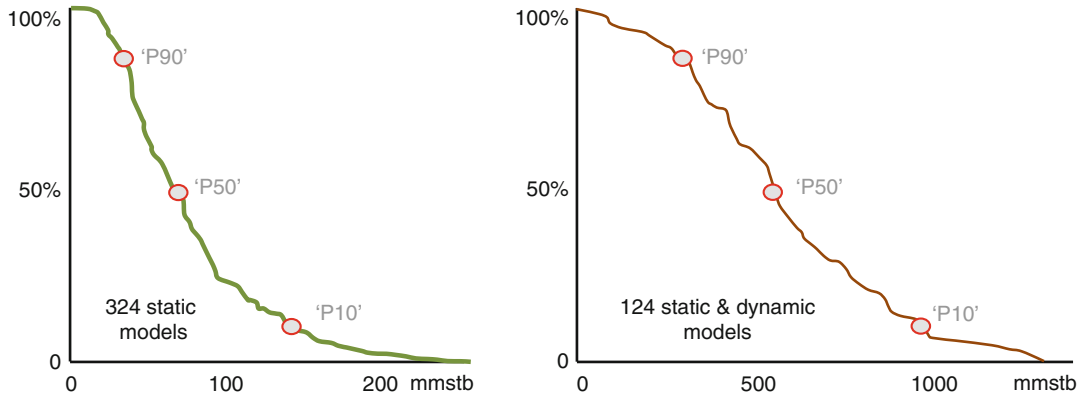

Fig. 5.14 Multiple deterministic cases for STOIIP (*left*) and ultimate recovery (*right*)

exercises tend to be more focussed and, paradoxically, tend to be quicker to execute than the very large, very detailed base-case model builds.

5.9 Linking Deterministic Models with Probabilistic Reporting

The next question is how to link multiple-deterministic scenarios with a probabilistic framework? Ultimately we wish to know how likely an outcome is. In reservoir modelling, probability is most commonly summarised as the percentiles of the cumulative probability distribution – P90, P50, and P10, where P90 is the value (e.g. reserves) which has a 90 % probability of being exceeded, and P50 is the median of the distribution. With multiple-deterministic scenarios, as each scenario is qualitatively defined, the link to statistical descriptions of the model outcome (*e.g.* P90, P50 and P10) can be qualitative (e.g. a visual ranking of outcomes) or formalised in a more quantitative manner.

An important development has been the merging of deterministically-defined scenario models with probabilistic reporting using a collection of approaches broadly described as 'experimental design'. This methodology offers a way of generating probabilistic distributions of hydrocarbons in place or reserves from a limited number of deterministic scenarios, and of relating individual scenarios to specific positions on the cumulative probability function (or 'S' curve). In turn, this provides a rationale for selecting specific models for screening development options.

Experimental design is a well-established technique in the physical and engineering sciences where it has been used for several decades (*e.g.* Box and Hunter 1957). It has more recently become popular in reservoir modelling and simulation (*e.g.* Egeland et al. 1992; Yeten et al. 2005; Li and Friedman 2005) and offers a methodology for planning experiments so as to extract the maximum amount of information about a system using the minimum number of experimental runs. In subsurface modelling, this can be achieved by making a series of reservoir models which combine uncertainties in ways specified by a theoretical template or design.

The type of design depends on the purpose of the study and on the degree of interaction between the variables. A simple approach is the Plackett-Burmann formulation. This design assumes that there are no interactions between the variables and that a relatively small number of experiments are sufficient to approximate the behaviour of the system. More elaborate designs, for example D-optimal or Box-Behnken (e.g. Alessio et al. 2005; Cheong and Gupta 2005; Peng and Gupta 2005), attempt to analyse different orders of interaction between the uncertainties and require a significantly greater number of experiments. The value of elaboration in the design needs to be assessed – *more is not always better* – and depends on the model purpose, but the principles described below apply generally.

A key aspect of experimental design is that the uncertainties can be expressed as end-members. The emphasis on making a base case or a best guess for any variable is reduced, and can be removed.

The combination of Plackett-Burmann experimental design with the scenario-based approach is illustrated by the case below from a mature field re-development plan involving multiple-deterministic scenario-based reservoir modelling and simulation (Bentley and Smith 2008). The purpose of the modelling was to build a series of history-matched models that could be used as screening tools for a field development.

As with all scenario-based approaches, the workflow started with a listing of the uncertainties (Fig. 5.15), presumed in this case to be:

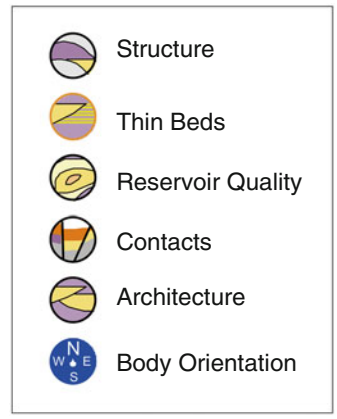

Fig. 5.15 Experimental design case: uncertainty list

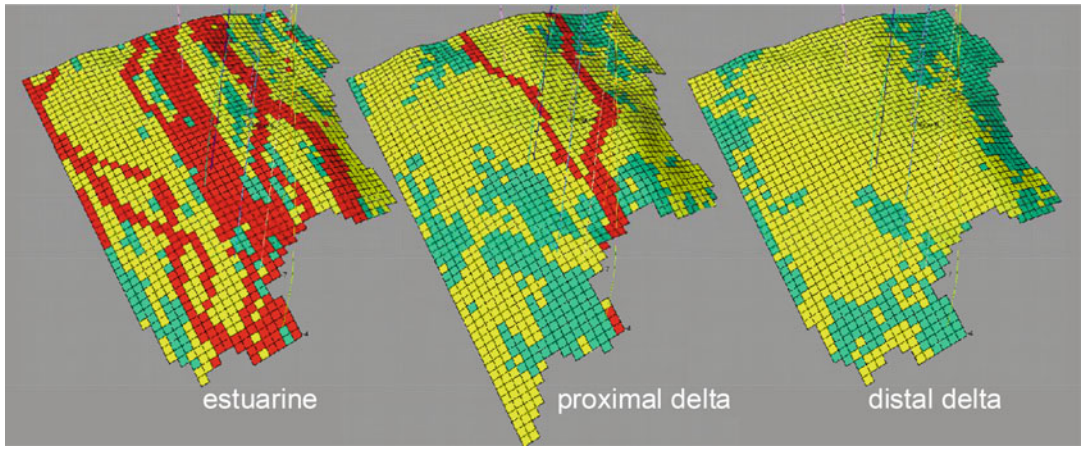

Fig. 5.16 Alternative reservoir architectures (Images courtesy of Simon Smith) (Redrawn from Bentley and Smith 2008, The Geological Society, London, Special Publications 309 © Geological Society of London [2008])

Realisation	Structure	Quality	Contacts	Architecture	Thin beds	Orientation	Response
1	-1	1	1	1	-1	1	1178
2	-1	-1	1	1	1	-1	380
3	-1	-1	-1	-1	-1	-1	109
4	1	-1	1	1	-1	1	1105
5	-1	-1	-1	1	1	1	402
6	1	-1	1	-1	-1	-1	1078
7	1	1	-1	1	1	-1	1176
8	1	-1	-1	-1	1	1	1090
9	-1	1	-1	-1	-1	1	870
0	-1	1	1	-1	1	-1	932
11	1	1	-1	1	-1	-1	1201
12	1	1	1	-1	1	1	1245
13	0	0	0	0	0	0	956
14	1	1	1	1	1	1	1656

Fig. 5.17 Plackett-Burmann matrix showing high/low combinations of model uncertainties and the resulting response (resource volumes in Bscf)

1. *Top reservoir structure;* caused by poor quality seismic and ambiguous depth conversion. This was modelled using alternative structural cases capturing plausible end-members.
2. *Thin-beds;* the contribution of intervals of thin-bedded heterolithics was uncertain as these intervals had not been produced or tested in isolation. This uncertainty was modelled by generating alternative net-to-gross logs.
3. *Reservoir architecture;* uncertainty in the interpretation of the depositional model was expressed using three conceptual models: tidal estuarine, proximal tidal-influenced delta and distal tidal-influenced delta models (Fig. 5.16). A model was built for each, with no preferred case.
4. *Sand quality;* this is an uncertainty simply because of the limited number of wells and was handled by defining alternative cases for facies proportions, the range guided by the best and worst sand quality seen in wells.
5. *Reservoir orientation;* modelled using alternative orientations of the palaeodip.
6. *Fluid contacts;* modelled using plausible end-members for fluid contacts.

These six uncertainties were combined using a 12-run Plackett-Burmann design. The way in which the uncertainties were combined is shown

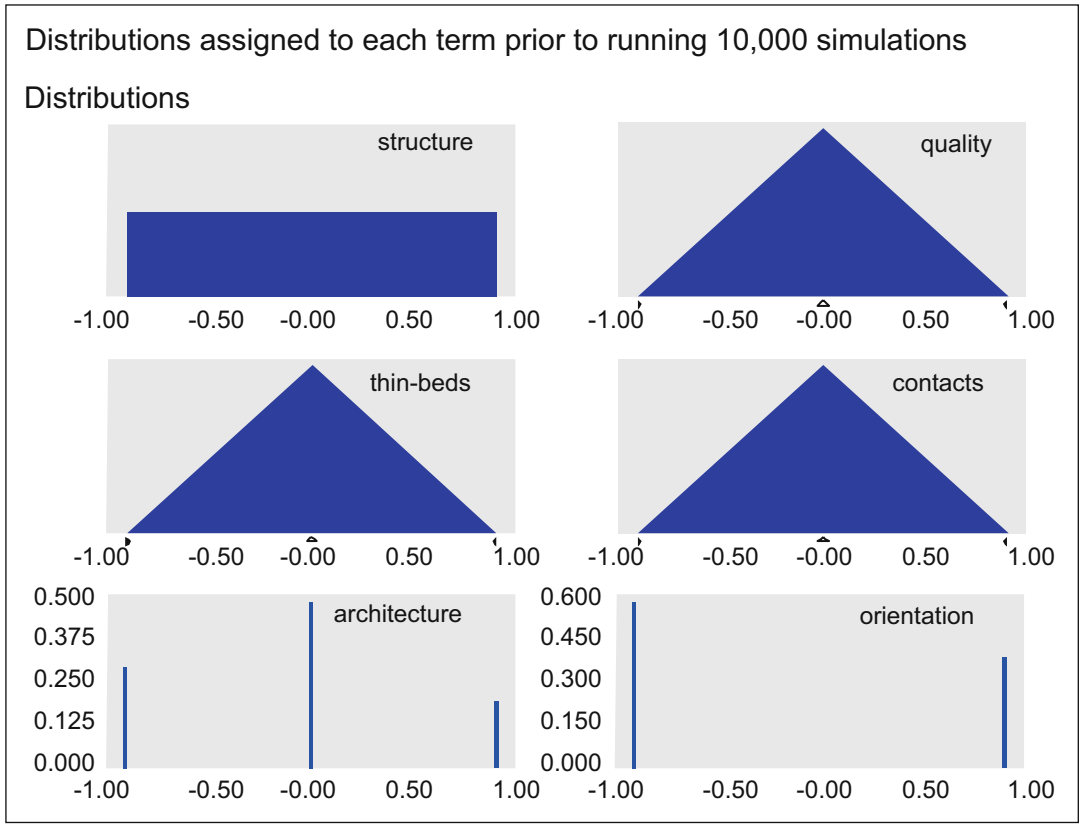

Fig. 5.18 Parameter ranges and distribution shapes for each uncertainty

in the matrix in Fig. 5.17, in which the high case scenario is represented by +1, the low case by −1 and a mid case by 0. In this case two additional runs were added, one using all the mid points and one using all the low values. Neither of these two cases is strictly necessary but can be useful to help understand the relationship between the uncertainties and the ultimate modelled outcome.

The 14 models were built and the resource volume (the 'response') determined for each reservoir. A linear least-squares function was derived from the results, capturing the relationship between the response and the individual uncertainties. The relative impact of the individual uncertainties on the resource volumes is captured by a co-efficient specific to the impact of each uncertainty.

The next step in the workflow is to consider the likelihood of each uncertainty occurring in between the defined end-member cases, that is, in between the '1' and the '−1'. This relates back to the underlying conceptual model, and requires the definition of a parameter distribution function (e.g. uniform, Gaussian, triangular). The distribution shapes selected for each uncertainty in this case are shown in Fig. 5.18. For variables where the value can be anywhere between the 1 and −1 end members, a uniform distribution is appropriate, for those with a central tendency a normal distribution is preferred (simplified as a triangular distribution) and for some variables only discrete alternative possibilities were chosen.

Once the design is set up, and assuming the independence of the chosen variables is still valid, the distributions can then be sampled by standard Monte-Carlo analysis to generate a probabilistic distribution. The existing suite of models can then be mapped onto a probabilistic, or S-curve, distribution (Fig. 5.19).

There are three distinct advantages to using this workflow. Firstly, it makes a link between

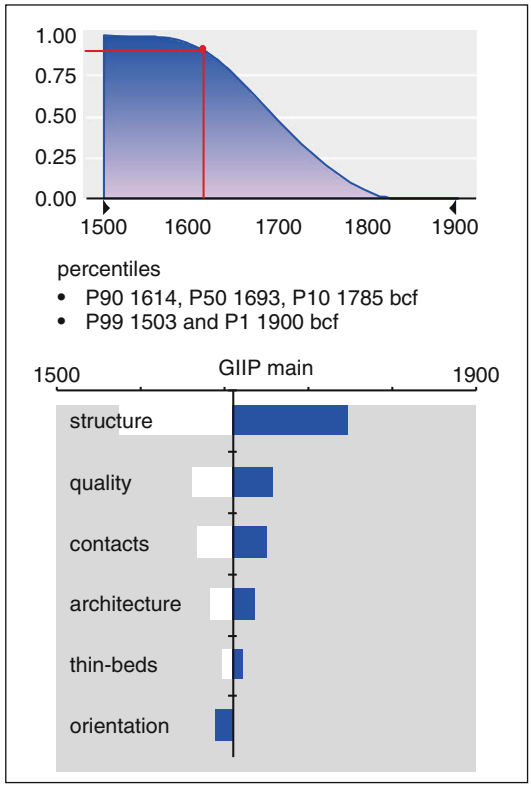

Fig. 5.19 Probabilistic volumes from Monte Carlo simulation of the experimental design formulation

probabilistic reporting and discrete multiple-deterministic models. This can be used to provide a rationale for selecting models for simulation. For example, P90, P50 and P10 models can be identified from this analysis and it may emerge that models reasonably close to these probability thresholds were built as part of the initial experimental design. Alternatively, the comparison may show that new models need to be built. This is easier to do now that the impact of the different uncertainties has been quantified, and is an improvement on an arbitrary assumption that a high case model, for example, represents the P10 case. Secondly, the workflow focuses on the end-members and on capturing the range of input variables, avoiding the need to anchor erroneously on a best guess. Finally, the approach provides a way of quantifying the impact of the different uncertainties via tornado diagrams or simple spider plots, which can in turn be used to steer further data gathering in a field.

Moreover, having conducted an experimental design, it may emerge that the P50 outcome is significantly different from the previously assumed initial 'best guess.' That is, this uncertainty modelling approach can help compensate for the biases that the user, or subsurface team, started with.

5.10 Scenarios and Uncertainty-Handling

Scenario-based approaches offer an improvement over base-case modelling, as results from the latter are anchored around best guess assumptions. Best guesses are invariably misleading because data from the subsurface is generally insufficient to be directly predictive. Scenarios are defined here as 'multiple, deterministically-driven models of plausible development outcomes', and are preferred to multiple stochastic modelling alone, the application of which is limited by the same data insufficiency which limits base case modelling. Each scenario is a plausible development future based on a specific concept of the subsurface, the development planning response to which can be optimised.

The application of geostatistical techniques, and conditional simulation algorithms in particular, is wholly supported as a means of completing a realistic subsurface model – usually by infilling a strongly deterministic model framework. Multiple stochastic modelling can also be useful to explore sensitivities around an individual deterministic scenario. Deterministic design of each over-arching scenario, however, is preferred because of transparency, relative simplicity and because each scenario can be validated as a realistic subsurface outcome.

Scenario-based modelling is readily applicable to greenfield sites but, as the examples shown here confirm, is also practical for mature, brownfield sites, where multiple history matching may be required at the simulation stage.

The key to success is the formulation of the uncertainty list. If the issues which could cause the business decision to fail are identified, then the modelling workflow will capture this and the decision risk can be mitigated. If the issue is

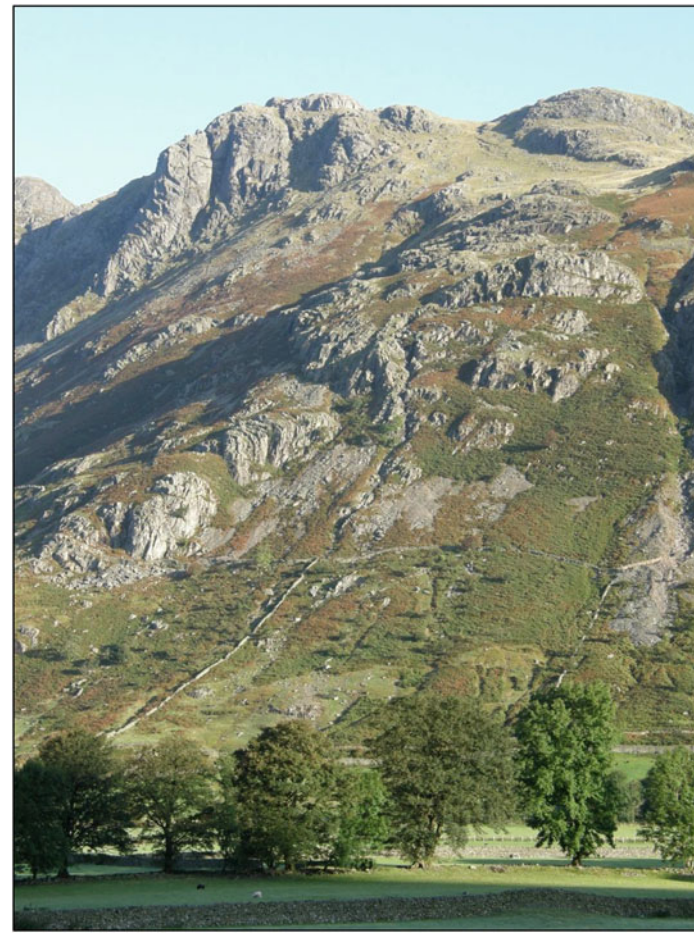

Fig. 5.20 Did you anticipate the trees?

missed, no amount of modelling of any kind can compensate. The list is therefore central, including the identification of issues not explicit in the current data set, but which can be anticipated with thought. Remember, there may be trees (Fig. 5.20).

References

Alessio L, Bourdon L, Coca S (2005) Experimental design as a framework for multiple realisation history matching: F6 further development studies. SPE 93164 presented at SPE Asia Pacific Oil and Gas conference and exhibition, Jakarta, 5–7 Apr 2005

Baddeley MC, Curtis A, Wood R (2004) An introduction to prior information derived from probabilistic judgements: elicitation of knowledge, cognitive bias and herding. In: Curtis A, Wood R (eds) Geological prior information. Informing science and engineering, The Geological Society special publications, 239. The Geological Society, London, pp 15–27

Bentley MR, Hartung M (2001) A 4D surprise at Gannet B. EAGE annual technical conference, Amsterdam (extended abstract)

Bentley M, Smith S (2008) Scenario-based reservoir modelling: the need for more determinism and less anchoring. In: Robinson A et al (eds) The future of geological modelling in hydrocarbon development, The Geological Society special publications, 309. The Geological Society, London, pp 145–159

Bentley MR, Woodhead TJ (1998) Uncertainty handling through scenario-based reservoir modelling. SPE paper 39717 presented at the SPE Asia Pacific conference on Integrated Modelling for Asset Management, 23–24 Mar 1998, Kuala Lumpur

Box GEP, Hunter JS (1957) Multifactor experimental designs for exploring response surfaces. Ann Math Stat 28:195–241

Caers J (2011) Modeling uncertainty in the earth sciences. Wiley (published online)

Chellingsworth L, Kane P (2013) Expectation analysis in the assessment of volume ranges in appraisal and development – a case study (abstract). Presented at the Geological Society conference on Capturing Uncertainty in Geomodels – Best Practices and Pitfalls, Aberdeen, 11–12 Dec 2013. The Geological Society, London

Chellingsworth L, Bentley M, Kane P, Milne K, Rowbotham P (2011) Human limitations on hydrocarbon resource estimates – why we make mistakes in data rooms. First Break 29(4):49–57

Cheong YP, Gupta R (2005) Experimental design and analysis methods for assessing volumetric uncertainties. SPE J 10(3):324–335

Cosentino L (2001) Integrated reservoir studies. Editions Technip, Paris, 310 p

Dubrule O, Damsleth E (2001) Achievements and challenges in petroleum geostatistics. Petroleum Geosci 7:S53–S64

Egeland T, Hatlebakk E, Holden L, Larsen EA (1992) Designing better decisions. SPE paper 24275 presented at SPE European Petroleum Computer conference, Stavanger, 25–27 May 1992.

Kahneman D (2011) Thinking fast and slow. Farrar, Straus and Giroux, New York, 499 p

Kahneman D, Klein G (2009) Conditions for intuitive expertise: a failure to disagree. Am Psycol 64:515–526

Kahneman D, Tverky A (1974) Judgement under uncertainty: heuristics and biases. Science 185:1124–1131

Kloosterman HJ, Kelly RS, Stammeijer J, Hartung M, van Waarde J, Chajecki C (2003) Successful application of time-lapse seismic data in Shell Expro's Gannet Fields, Central North Sea, UKCS. Petroleum Geosci 9:25–34

Li B, Friedman F (2005) Novel multiple resolutions design of experiment/response surface methodology for uncertainty analysis of reservoir simulation forecasts. SPE paper 92853, SPE Reservoir Simulation symposium, 31 Jan–2 Feb, The Woodlands, 2005

Mintzberg H (1990) The design school, reconsidering the basic premises of strategic management. Strateg Manage J 6:171–195

Peng CY, Gupta R (2005) Experimental design and analysis methods in multiple deterministic modelling for quantifying hydrocarbon in place probability distribution curve. SPE paper 87002 presented at SPE Asia Pacific conference on Integrated Modelling for Asset Management, Kuala Lumpur, 29–30 Mar 2004

Smith S, Bentley MR, Southwood DA, Wynn TJ, Spence A (2005) Why reservoir models so often disappoint – some lessons learned. Petroleum Studies Group meeting, Geological Society, London. Abstract.

Towler BF (2002) Fundamental principles of reservoir engineering, vol 8, SPE textbook series. Henry L. Doherty Memorial Fund of AIME, Society of Petroleum Engineers, Richardson

van de Leemput LEC, Bertram D, Bentley MR, Gelling R (1996) Full-field reservoir modeling of Central Oman gas/condensate fields. SPE Reservoir Eng 11(4):252–259

van der Heijden K (1996) Scenarios: the art of strategic conversation. Wiley, New York, 305pp

Wynn T, Stephens E (2013) Data constraints on reservoir concepts and model design (abstract). Presented at the Geological Society conference on Capturing Uncertainty in Geomodels – Best Practices and Pitfalls, Aberdeen, 11–12 Dec 2013

Yarus JM, Chambers RL (1994) Stochastic modeling and geostatistics principals, methods, and case studies. AAPG Comput Appl Geol 3:379

Yeten B, Castellini A, Guyaguler B, Chen WH (2005) A comparison study on experimental design and response surface methodologies. SPE 93347, SPE Reservoir Simulation symposium, The Woodlands, 31 Jan–2 Feb 2005